MASTER OF SCIENCE THESIS

Utilization of Rice husk ash in GeoTechnology

Applicability and effect of the burning conditions

Vinh Pham

Faculty of Civil Engineering and GeoScience

July 2012

Utilization of Rice husk ash in GeoTechnology

Applicability and effect of the burning conditions

MASTER OF SCIENCE THESIS
Delft University of Technology, faculty of Civil Engineering and Geosciences
Master Civil Engineering, Track Geo-Engineering

Student:
Pham Phu Vinh
4117883
p2v961@gmail.com

Committee:
Prof. Ir. A.F. van Tol (TU Delft, CiTG – Geo-engineering)
Dr. Ir. L.A. van Paassen (TU Delft, CiTG – Geo-engineering)
Dr. G. Ye (TU Delft, CiTG – Materials and Environment)
Dr. Ir. W. van der Star (Deltares)

Summary

Rice husk ash is an attractive pozzolan. Due to its low cost and high activity it has a promising perspective in sustainable construction. In combination with lime, its effect in soil improvement can be equal to cement treatment but its production process consumes much less energy.

The main component of the rice husk ash is silica, which is the element that governs the reactivity of the ash. A delicate burning process is required to eliminate the organic components in the rice husk but keep the silica to be amorphous so that a highly reactive rice husk ash can be obtained. A too high temperature would transform amorphous silica to crystalline silica, which would reduce the reactivity. The suggested burning process in literature is 2 hours at 500°C. However, due to the exothermic property of the burning rice husk it is difficult to control the exact burning temperature, hence there is still a possibility that the carbon and the crystallized silica are present and hinder the activity of the rice husk ash. Based on the silica state and the carbon content, the rice husk ash is classified in three types: C-RHA which is collected from a quick and open-air burning and contains a large amount of carbon; Cr-RHA which is collected form slow burning at above 600°C and contains a large amount of crystallized silica; and A-RHA which is collected from the suggested burning process which is 500°C in 2 hours and is considered to be the most active.

The activity of these three types of rice husk ash and their effect in soil improvement were tested. As expected, the higher reactivity of the A-RHA compared with the Cr-RHA confirmed the capability of these burning conditions. Surprisingly, the C-RHA appeared to be the most reactive and its effect to the soil was also the most positive despite of the large carbon content and the detected crystalline silica. The high reactivity of the C-RHA derives that there is a hierarchy of the solubility depending on the burning duration so that although all the three types of ash were mainly amorphous, the C-RHA is the most soluble. From the experiments, the role of the carbon was seen in only the term of quantity as it reduce the proportion of the silica, but might it have any support to the reactivity of the material in those experiments then it needs more investigation.

The results of the treated soil showed that the rice husk ash need the lime to be activated, but then it helped to enlarge the possitive effect of the lime. The immediate effect of the additives to the plasiticity of the soil were seen to be the results of the lime only, but the long-term effect of the strength and the compression of the soil were seen to be the results of the combination between rice husk ash and lime. Especially in the case of C-RHA, it can reduce half the amount of lime in the case of 6% lime mixing to give similar undrained shear strength which was about 410 kPa. Because the carbon is not a serious harmful factor in the soil, and the soil can also take the advantage of the firmness of the quartz, so between the two cases, the rice husk ash with large carbon content and also considerable amount of quartz but higher reactivity, and the rice husk ash which is almost purely amorphous silica but less reactive, the former is the preferred for the soil improvement purpose.

Acknowledgements

This research is a part of the master program that I have attended at the Delft University of Technology, and together with the study at the university, this research has brought to me many new experiences. There were some experiments that I never thought I could do, and also there were some small accidents to remind me to be careful. I would like to say thank Dr. Ir. L.A. van Paassen and Dr. Ir. W. van der Star very much that gave me the chances to experience all of these. And also their detailed support and trust for me, I am deeply indebted to them.

And my grateful thank to Prof. Ir. A.F. van Tol and Dr. G. Ye for their valuable comments and also the time. Without this support this research might lack some important matters.

Because this research was executed in the collaboration of the university and Deltares, I had the chance to cooperate with the friendly technicians of both the university and Deltares. Many thanks to them that helped me to complete the experiments.

And surely I could not completely enjoy my study here without the love and trust from my family, especially from my father with his inspiration to me. I am permanently indebted to them.

My study of the master program at Delft University of Technology has been sponsored by the Agricultural Science and Technology Project belonging to the Ministry of Agriculture and Rural Development of Vietnam. I have a deep gratitude to them because without this grant I could hardly be here.

And to all my friends, grateful thank from me that have been making my stay here in the Netherlands joyful and unforgettable. I am very grateful about our friendships, and hope we will meet again, soon and often, here in the Netherlands or there in Vietnam or may be somewhere else in the world.

Contents

Figures

Tables

1. Introduction

1.1. Soft soil conditions and stabilization methods

Soft soil conditions are characterized by low strength and show a large deformation upon loading so that they do not satisfy the designed engineering properties and hence, require reinforcement treatments. One of the indications for the soft soil is an undrained shear strength smaller than 40 kPa [1]. According to the classification in NEN 6740 the soil types which satisfy this indication and considered to be weak are mainly peat and clay [2].

Most soft soils originate from the Holocene, the most recent epoch which started about twelve thousand years ago after the end of the last glacial period[3]. The Holocene marks the formation and development of the human civilization. This process began with stable agriculture, which was normally located in the delta areas where river and marine sediments were providing fertile grounds for growing crops. This leads to the large occurrence of soft soils in the crowed areas nowadays. The delta areas of the Red river system and the Mekong system in South East Asia are examples. In Vietnam, the area of these river basins accounts for 16% of the land area but accommodates almost half the country's population[4].

The Holocene deposits are normally sand, clay and peat, but the proportion can vary largely depending on the geological history. In the Netherlands peat accounts for a large part of the Dutch basement as the low elevation level - the country is known to be the unique one lying below the sea level - and high level of groundwater leads to the development of swamps [5]. This happened similarly in the Southern delta of Vietnam where the land level is approximately equal to the sea level [6], causing a very thick layer of peat and clayey peat. The Red river delta in the North of the country, where the capital is located, is higher than the South and is less vulnerable to the sea level. As shown in Figure 1 [7], the proportion of organic clay and peat is less than that of clay.

The soils in delta areas are often humid because of high water level compared to the surface level. The range of the water content can vary from 100% to 500% for peat. For clay, the most common state is liquidly plastic and the Liquidity Index is close to one. According to an overall site investigation of Hanoi, Vietnam [7], the Liquidity Index of the clay here is above 0.75. In Ariake, Japan, the marine clay shows even a higher liquidity, as the water content varies from 80% to 160% and excesses its Liquid Limit [8]. This type of soil is normally very weak and can show large deformation upon loading. As these areas are highly populated, much effort has been taken to improve the soil properties for construction purposes.

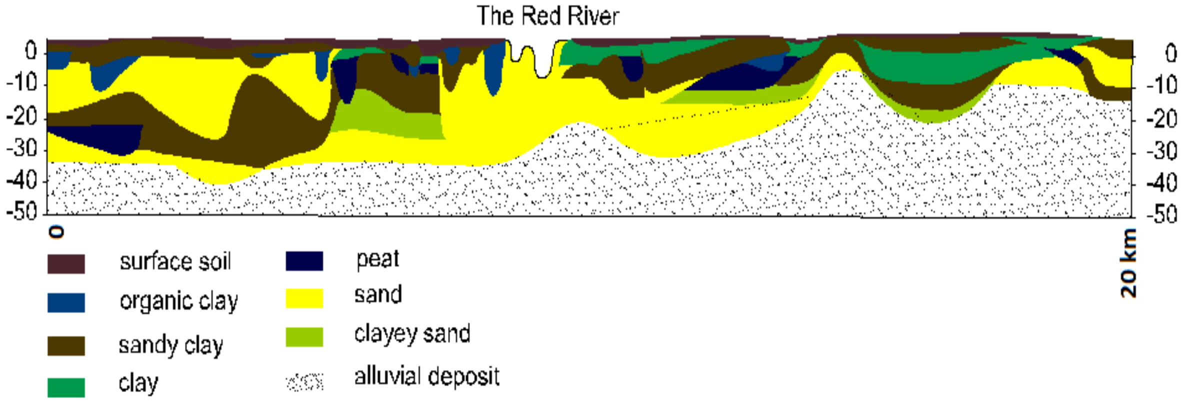

Figure 1. The thick Holocene deposits in the delta of the Red river, north of Vietnam

The ground improvement methods for the soft soil can be categorized according to the manner of treating the soil [9]. Mass improvement is the method that is able to improve the soil by modifying either its physical or chemical properties, or both of them in such a way that the soil becomes consistent, hence the strength is increased and deformability and permeability are reduced. This can be done by compaction or consolidation acceleration methods, or by stabilizing reagents. The most popular chemical binders are lime and cement, and their role is to bind the particles and aggregate them together, consequently improve the soil structure and properties. While the compactions and consolidation methods take rather a long time for the soil to consolidate (months to years) especially with the cohesive soil [10], the stabilizing reagents effect can be seen immediately [11] and approximately after 1 week the construction site can be ready. This is one of the reasons that make this method mainly be used in infrastructure projects [9].

In case the soft soil is not possible to be improved then replacement methods are considered, and normally this is the case of highly organic soil. However the replacement is not adaptable in a large construction site with a thick layer of peat, then installing stiff elements into the soil can be effective. Beside compound wooden and stone columns, methods with cementitious materials is very popular because it can work with almost all types of soil by various manners including deep mixing and grouting.

In the global trend of long-term development, there are various sources of silica which is able to partly replace the cement or cooperate with lime to produce pozzolanic cement [12]. The firstly used source is the natural pozzolanas, which is volcanic ash, and its product with lime is discovered to appear from the 2nd century AD in Roman catacombs [13]. In present, the typical binders are blast furnace slag from metal industry and fly ash from coal used for electric production. Rice husk ash is another source which is relatively new although research about it has been seen from 1924 in literature cites [12].

1.2. Rice husk and rice husk ash: characteristics and applications

Thanks to the relationship between the agriculture and the civilization, delta areas are the granaries for the world population. According to the statistic database of Food and Agriculture Organization of the United Nations, half of the world population has rice as the main source of staple and the rice consumption has exceeded the production since 2000 [14]. Data of rice and other cereal[1] production in the last xdr20 years [15] was plotted in Figure 2 and it shows that rice has occupied almost a third of cereal production of the world. In this period, rice production increased by about 170 million tons from 520 MT to 690 MT in 2009. As seen in Table 1, the rice mainly comes from the developing countries [15] locating in large delta areas such as Yangtze river delta (China), the Ganges delta (India and Bangladesh) or Mekong delta (China, Thailand, Vietnam).

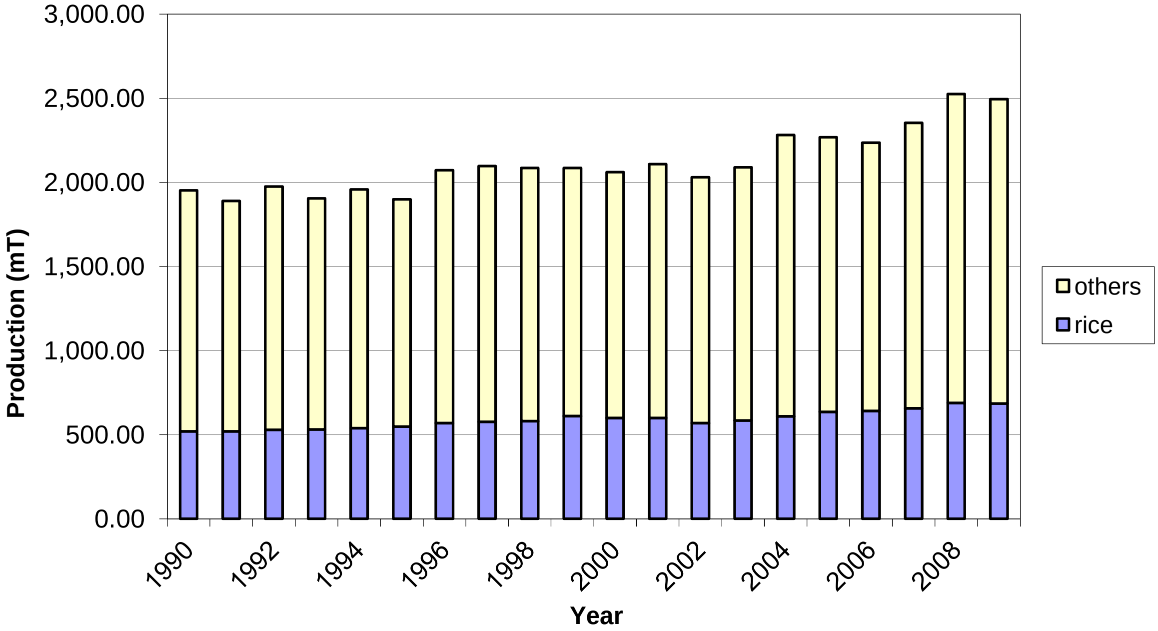

Figure 2. Cereal production in the last 20 years

Together with the function of food supplier, this production also creates large amount of rice husk, which causes problems of space and environment if it is not well utilized. This is the consequence of bulk characteristic of the husk with an average bulk density of about 110 kg/m^3 and compacting this material is difficult [13]. Amount of husk from rice milling counts for about 20% of the rice by weight; accordingly, approximately 130 MT of husk was created in 2009 and it needed a space of 1.25 km^3 which is equivalent to

---

[1] Cereal are the staple crops, including rice, maize, wheat, bean and millet.

capacity of a reservoir for a 45 MW hydro power station (this is the parameter of Seminoe Reservoir in the United States).

However, in almost all rice-producing households, rice husk is considered exclusively a waste and used mainly for heat by burning while it is a potential industrial material. In an estimation of Pörner Group, a Germany contractor working on rice husk technologies, only 30% of rice husk is commercially used. If the entire husk can be fully used in industrial fields then it can bring much benefit to the rice-producing countries.

Table 1. Top rice-producing countries in 2009 (FAO statistic)

Rank	**Country**	**Yield (kg/Ha)**	**Production (tonnes)**
1	China	6582	196 681 170
2	India	3195	133 700 000
3	Indonesia	4998	64 398 900
4	Bangladesh	4203	47 724 000
5	Vietnam	5228	38 895 500
6	Myanmar	4085	32 682 000
7	Thailand	2870	31 462 900
8	Philippines	3589	16 266 400
9	Brazil	4405	12 651 800
10	Japan	6523	10 592 500

Rice husk ash (RHA) is a poor nutrition material and it is rarely used for agricultural purposes such as animal food or fertilizer. The feature property of the rice husk is that its combustion heat is approximately 13.4 MJ/kg, which is a high average calorific value [16]. The inorganic component lying in the collected ash after burning is dominated by silica. The ash is about 20% of weight of the rice husk, and silica amount can reach to 96% of the ash by appropriate burning condition. Consequently, the main perspectives of utilizing rice husk are for energy purpose and silica resource.

In terms of energy, comparison to coal whose combustion heat is about 30 MJ/kg [17] shows that a ton of rice husk is equivalent to 0.4 ton of coal. Besides, being plants means that this source of energy is CO_2 neutral as CO_2 released from pyro-processing is equal to the consumed amount during its life [18]. This is the important point that makes rice husk attractive for sustainable energy. As rice husk is agricultural waste, utilizing it does not conflict with food production like other plants in the group of the 1st generation biofuels such as maize or sugar cane. So in the field of biofuels, rice husk is gathered with other agricultural residues to be the 2nd generation biofuels. On the rise of biofuels consumption in the last 20 years, the European Commission has set a target of 10%

biofuels share in the fuel for transport by 2020 [19]. whether this target is achievable, but statement in the report of the REFUEL project showed that this target is attainable, and combination of the 1st and the 2nd generation biofuels order the most cost-effective solution [20].

About silica industry, silica has a wide range of industrial applications, such as rubber reinforcement, solar panels, catalyst and coating, or detergent and soaps. Another product from this material is liquid sodium silicates and it can also be used for ceramics and binders or in water treatment and textile processing [21]. These various applications make the rice husk ash become attractive and the technique to collect pure amorphous silica from rice husk has been being investigated. In construction field, the most attractive property of silica is its pozzolanic reaction with calcium hydrate to produce calcium silicate hydrate which is the main source of strength of cement and concrete. Besides, the production of silica from rice husk for this purpose is not as complex as the processes for the industrial purposes, so it has been utilized in this area the most at the present.

Replacement of Portland cement is a promising application not only in the field of concrete but also in the field of soil improvement, and effect of calcium silicate hydrate is expected to be similar within soil grains. Research on this application of rice husk ash has been carried out more often recently and all of them share the same observation that in cooperation with lime, the mixture can help to considerably improve the strength, permeability, durability and volume stability of different types of soft soil. The main advantage of the lime-rice husk ash cement compared with the Portland cement is that it can save much energy. Detail calculation of comparison between the two systems by a simple Life cycle inventory analysis in the Appendix 1 shows that the electricity used by the system of lime and rice husk ash is only one fifteenth of the amount of the case of Portland cement.

The common sense for rice husk ash producing is the more active ash the more efficient reaction, so almost all the experiments for soil improvement were implemented with the ash which is supposed to be active by burning at an appropriate temperature and duration. However, exothermic property of the burning rice husk makes the inner temperature of the burning mass uncontrollable. Consequently the quality of the rice husk ash can be largely various even the burning condition is set up at the optimum, accordingly the overall positive effect of the additives might come not only from the good quality of the ash. There was also research about soil improvement effect with uncontrolled burnt ash and it also showed a good result.

A vertical system where rice husk ash from pyro-processing for heat production is collected for other applications of silica as mentioned above is an ideal manner for rice utilization. However, quality of silica highly depends on the pyro-processing condition, and the process which can produce the good quality ash is not compatible with an energy extraction system [22]. In addition, it is this dependence that hinders the application of rice husk ash in industrial scale.

1.3. Research questions and approach

Expectations of the active rice husk ash burnt under a strictly pyroprocessing is high, but there is also promising usage of the ash burnt in a less strict condition. Indeed almost all the done research about the utilization of rice husk ash in soil improvement did not pay much attention on the rice husk ash but mainly its effect to the soil while the activity of the ash is the govern factor and it is sensitive to the burning process.

So this research will focus on the question: How the burning conditions affect to the rice husk ash applications in Geo engineering.

Two matters will be dealt with to establish the above subject:

- Identifying burning conditions to produce the rice husk ash and characterizing the rice husk ash activity;
- Estimating soil improvement ability of these rice husk ash.

Background of the two matters will be presented in the next section of the thesis. This section will introduce the overview of the soil stabilization methods using different reagents among which the rice husk ash has performed to be effectively. It will also present the basis of rice husk ash characterizing together with a short introduction about the common methods in evaluating the rice husk ash activity. The different types of rice husk ash burnt from different conditions were investigated based on these contents and the results as well as the implemented processes will be presented in the following section which is section 3. Their effectiveness in soil improvement was tested and will be presented in the section 4. The last section which is section 5 will generalize all the results so that conclusions about the efficiency of the different burning processes to the reactivity of the rice husk ash and its effectiveness in soil improvement will be raised.

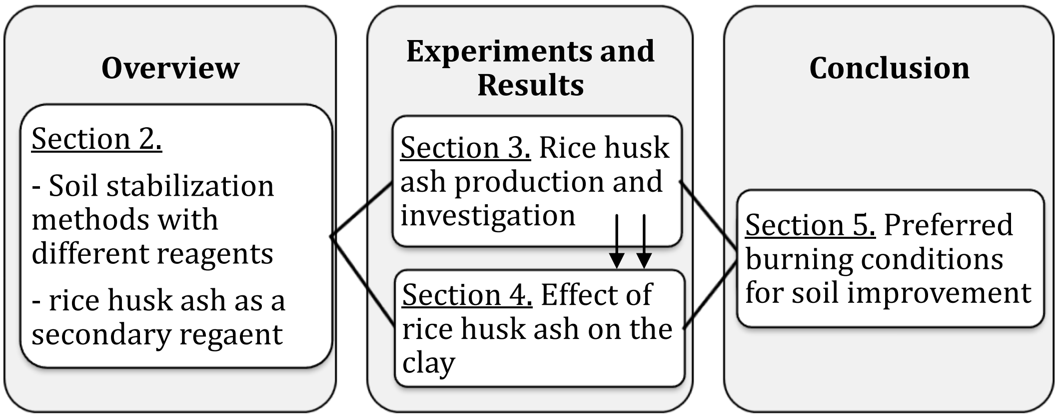

Figure 3. Outline of the thesis

The promising effect of an active ash strongly depends on the added amount and the mixing ratio of lime and rice husk ash, and this mixing parameter is regional and varies through every individual case. However, this research does not focus on a specific regional soil but the influence of the burning condition to the rice husk ash application, so the mixing ratio between lime and rice husk ash will be fixed to be one, and amount of rice husk ash will be varied as seen in the following chart.

RHA \ Lime	0%	1%	2%	3%	6%
0%		×	×	×	×
1%		×			
2%			×		
3%				×	
6%	×				

For the purpose of clarifying the influence of different additives, river clay in the Netherlands is chosen for the observation of improvement process. The highly isotropy and homogeneous properties of this inorganic clay can be useful in making the soil to be “transparent” to the effect of the additives, so that the difference in the possible result can be mainly caused by the different additives with the least interference. Because of the large distribution of liquid clay in the delta areas, the clay will be soaked to a higher liquidity index for practical reason.

2. Background of soil stabilization with different reagents including the rice husk ash

Soil stabilization using rice husk ash and lime has been more attractive recently due to its promising results compared to other siliceous sources. Overview about the methods and the basis of the rice husk ash utilization in this application will be presented in this section. The common criteria and methods to evaluate the activity of the rice husk ash will also be introduced and these will be the basis for the evaluation of the rice husk ash in the next section.

2.1. Available reagents for soil stabilization

Soil stabilization mentioned in the overview of Sherwood [11] is the alteration of the current properties of the soil to meet the specified engineering requirements, and using chemical reagents is one of the main techniques. The mechanism which helps to stabilize the soil is that the reagents create a matrix within the soil mass, hence particles are bonded together and the overall strength is increased while water absorption is reduced.

The matrix can be created by physical or chemical reactions. The most common method of physical reaction for soil stabilization is bitumen in road construction. The bitumen is made to be more fluid before operation, and it will come back to the viscous semi-solid state inside the soil mass by temperature reduction and evaporation. By this way, the soil particles are fixed in the bitumen matrix, nevertheless the bonding is relatively weak.

Chemical reactions for soil stabilization can be either the reactions between different reagents so that the matrix will cover the soil particles or the reactions between the reagents with the soil. The precipitation of calcium silicate from sodium silicate and calcium chloride is an example for the case which the soil does not join into the reaction but sinks into the product of the reaction.

When the soil joins into the reaction, hydrated lime is the typical reagent for this case because of its intermediate affect in drying the soil and the pozzolanic reaction with some clay minerals for long-term strength development of the soil mass. Portland cement can also categorized into this group because beside the calcium silicate hydrate formed from the hydration of the clinkers, other products including calcium hydrate can also cooperate with some components of the soil.

Available reagents for soil stabilization are categorized into two groups. The primary stabilizing reagents are the ones which they themselves can stabilize the soil. So the reagents mentioned above, which are bitumen, the lime or Portland cement are in this group. The secondary stabilizing reagents need the lime or cement to be activated, and these are the blast furnace slag or the pozzolanas such as fly ash or rice husk ash.

2.1.1. Cement and lime to be the primary reagent

The primary stabilizing reagents which are cement and lime are very well known because they can work with wide range types of soil in various foundation conditions. The main effect of the additives is modifying both the physical and chemical properties of the soil in such a way that the strength, volume stability, durability and permeability are improved.

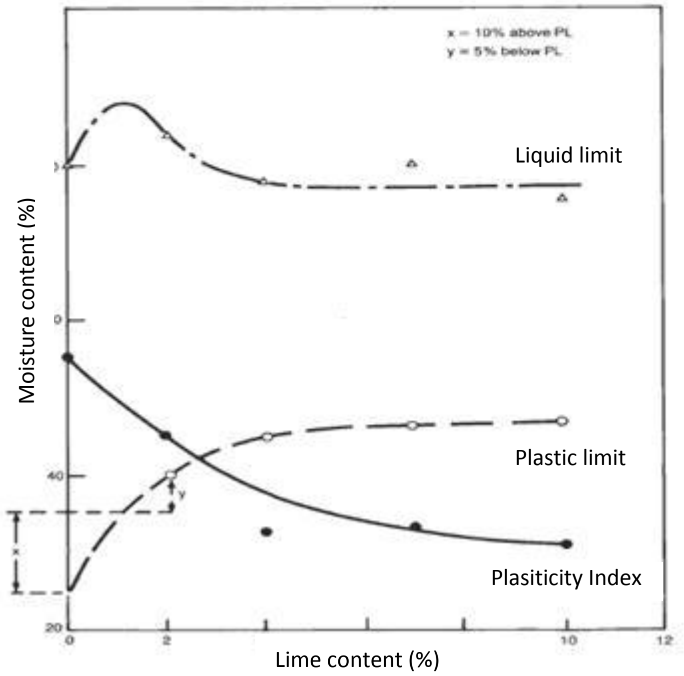

Figure 4. Effect of the addition of lime on the plasticity properties of London Clay (Sherwood 1993)

When lime is added into the soil, the improvement mechanism can be separated into two phases. With the present of clay minerals, the clay anion is immediately isolated by the calcium cation Ca^{2+} in the lime from other weaker cations existing in the soil, hence the soil texture is changed. This ion exchange leads to flocculation in the first phase and it dramatically reduces the plasticity of the soil as seen in Figure 4 (Sherwood 1993 [11]). For the clay whose water content is 35% and plastic limit is 25%, it is plasticity and not preferred for construction. But by adding 2% of lime, the plastic limit is upgraded to be 40%, consequently makes the soil be dry and possibly ready for construction purposes.

The appearance of hydroxyl anion from lime increases the pH to about 12.4 and helps to dissolve the silica existing in soil; hence the pozzolanic reaction happens. Depends on the mineral components of the soil that this stabilized matrix is strong or weak and shows a clear improvement or not. In general in the case of lime this process is relatively slow.

For Portland cement, the hydration of the clinkers happens as soon as the reagent is added into the soil and contacts with water, creating the hydrated calcium silicates and also the calcium hydroxide. Consequently, the immediate effect of drying the soil is also seen due to the water consumption and the flocculation because of the appeared calcium hydroxide.

2.1.2. Siliceous materials to be the secondary reagent

A pozzolan, according to V. M. Malhotra and Mehta [23], "*is a siliceous or siliceous aluminous material, which in itself possesses little or no cementious property but which will, in finely divided form and in the presence of moisture, chemically react with calcium hydroxide at ordinary temperature to form compounds possessing cementing properties*". This definition is the one used in the ASTM C618, and the compound is calcium silicate hydrate. The cementing property is shown in process of expansion and hardening through the time within the mixture, hence joins all the particles into a consistent mass. Fly ash is the most popular source of pozzolan for construction, but recently rice husk ash has become more attractive due to much promising result in research of different researchers.

The pozzolanic reaction between the silica and calcium hydroxide with the appearance of water is the expected reaction, so the solubility characteristic of the silica is main factor to govern the reaction. Soluble silica at low concentration is a weak acid and it is often called monosilicic acid. At higher concentration, the polymerization starts rapidly so that the polysilicic acid is formed, and the enlarged form from this one is called colloidal silica.

The solubility of silica can be modified largely by adjusting the pH value as observed in the work of G.B. Alexander et.al. The solubility increases from 120 mg/kg at the pH of 6-8 to 879 mg/kg at the pH of 10.6 [24]. This helps to explain the mechanism of the pozzolanic reaction within the soil with the mixture of the lime and the siliceous material. As the hydroxide ion added into the wet soil increased the pH value of the soil environment, it accelerates the dissolution of the silica, hence support the reaction between the (SiO_4) groups with the Calcium ion on the soil surface to create the calcium hydrate silicate.

Particle size of the silicious material is an important parameter governing the solubility of the material. As seen in the Figure 5 [25], the smaller the positive radius the larger the solubility. When the particles are smaller than 5nm, the effect of this parameter surpasses the effect of the pH value, so the silica is able to be highly soluble even at low pH. The negative curvature can appear if there are holes on the silica surface or at the contact point between the particles, and due to the low solubility at these areas that the soluble silica can deposit here, forming colloidal silica.

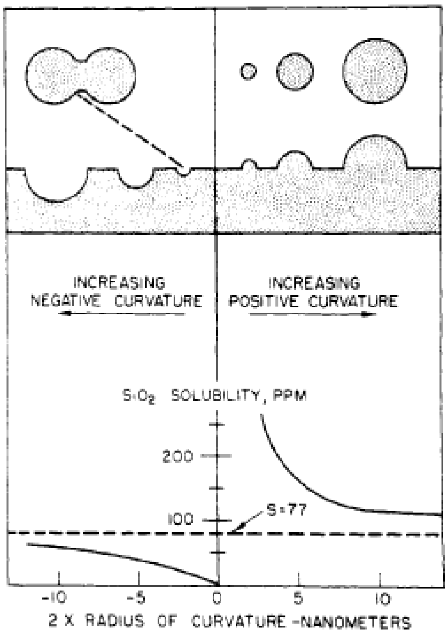

Figure 5. Variation in solubility of silica with radius of curvature of surface (Iler 1979)

2.2. Rice husk ash to be a siliceous

Silica in the rice husk ash as well as other plants comes from the dissolution of earth minerals during its life time. Silica is the major component of the earth's crust, and by dissolution and deposition it is transported into organism, so it is one of the fundamental element of the life [26]. Research by Whittenberger showed that the plant roots has their own substance to bring silica into solution in the form of soluble silicic acid for absorption, and this is the mechanism that weathers the rock to become the soil [27].

Within the plant, the silica is still in the form of the soluble acid for transportation and then is deposited due to evaporation. The concentration rate and location of silica within the plants then depends on the evaporation. In the case of wheat and corn, the most highly silicified place was found at the edges of the leaves where the water is lost the most rapidly [28]. In rice plants, the silica concentrates the most at the rice husk and can hold about 20% by mass of the rice husk.

The soluble silica comes out of the acid solution as amorphous form and this is confirmed by the research of Krishnarao and Godkhindi [29]. Silica in amorphous form is much more soluble than other crystallized form as at 25 °C, amorphous silica has a solubility range from 70 to more than 150 mg/kg while this value of crystallized silica is less than 10 [25]. Hence, the burning process producing the rice husk ash is expected to eliminate only the organic contents and remain the silica to be amorphous.

2.2.1. Burning condition dependence of the rice husk ash activity

Rice husk ash is the rich silica source collected from pyroprocessing of the rice husk, but because silica structure which influences the activity of the material is sensitive to temperature and burning duration, and the organic components need sufficient time to be burnt appropriately, so the rice husk ash properties strongly depend on the burning condition.

Along with the increase of the temperature during the pyroprocessing, at about 100 ^{o}C water evaporates and about 300 ^{o}C organic components start to burn. Up to 500 ^{o}C it was observed in the work of different researchers that almost all the these components have been transferred to gas phase, causing a sharp decrease in the weight of the material before it reaches to a stable mass as seen in Figure 6 [22]. The residue at this state is the rich silica ash. However the organic materials need time to be removed completely and it was seen in the work of Deepa G. Nair et.al [30] that burning at 500 ^{o}C in 3 hours is still not enough for this purpose. There is a large reduction in the percentage of ignition loss between the duration of 3 hours and 12 hours and only after 12 hours the mass of the material is stable, i.e. the organic components are removed completely.

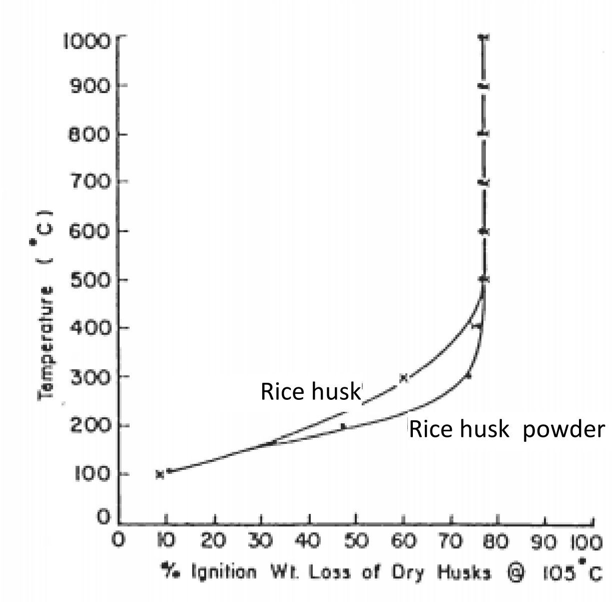

Source: Cook *et al* (23).

Figure 6. Characteristic of rice husk on ignition (UNIDO, 1984)

However the long burning duration cause a growth of the silica crystals as stated in the work of Chopra et.al [31]. The researchers used the X-ray diffraction techniques to capture the silica structure, and they observed that up to 700 ^{o}C silica was in amorphous form, but burning in long duration at this temperature caused the silica to crystallize. In one of the earliest research about rice husk ash by Mehta [32], prolonged period at 500 ^{o}C can keep the silica to be amorphous, but it can just be kept in this form in the first minute when the temperature goes above 680 ^{o}C. Another crystallization point was recorded in the work of Yeoh et.al. and it is at 900 ^{o}C within 1 hour or 1000 ^{o}C within 5 minutes [33]. So it can be concluded that the crystallization of silica can start at different temperature which is above 500 °C with differently sufficient burning duration.

The condition which can produce the active rice husk ash was optimized in the recent work of A. Muthadhi and S. Kothandaraman [34]. Taking into account the balance between the energy consumption and extraction of burning rice husk, the optimum condition which can produce an active ash with maximum amorphous silica content and other parameters at good rate but consume the least energy is a burning duration of 2 hours at 500 °C.

2.2.2. Pozzolanic activity evaluation

The activity of the rice husk ash is evaluated through its ability in reacting with the calcium hydroxide and it is governed by the solubility as well as the amount of the silica. As mentioned in the section 2.1.2, the particle size and the crystal form are the main factors that control the silica solubility. Accordingly, the reactivity of the rice husk ash is normally evaluated by the parameters of the particle size, which are the grain size distribution and the specific surface area, the amount of the amorphous silica and the reaction rate with the calcium hydroxide.

- *Particle size by specific surface area determination*

The most common method to determine the specific surface area of a material is the BET method using the adsorption of nitrogen gas. The principle of the method is that using the adsorption of nitrogen gas whose atoms are independent with each other and only one atom can occupy one site on a surface to cover the sample surface by a molecular layer to derive the specific surface area of the sample by the BET calculation [35].

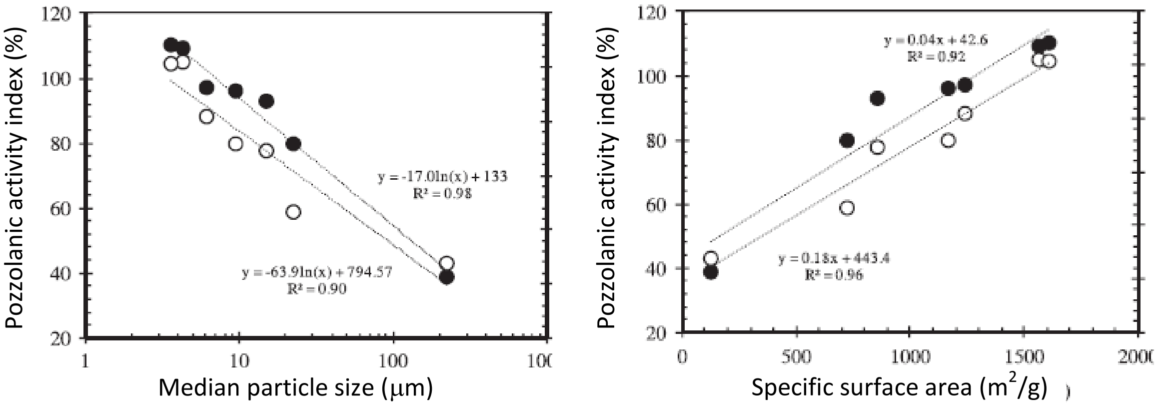

Figure 7. Relation between pozzolanic activity index and particle size and specific surface area (Cordeiro et al., 2011)

The correlation between the parameters is that a larger specific surface area normally comes along with a smaller diameter and brings a higher reactivity. The influence of particle size and specific surface area to the activity of rice husk ash was studied in the research of Cordeiro, G.C., et al., and it also show a positive effect of a small size grain with large specific surface area as seen in Figure 7 [36]. Rice husk ash in this research was collected from boilers at temperature between 600 ^{o}C and 850 ^{o}C which can easily lead to the crystallization of silica, and it also had high carbon content, so this ash was not expected to be highly active. But result of this research shows that energy for grinding can help to increase considerably the activity of the ash.

- *Amount and structure form of the silica*

Amount of the silica in the rice husk ash can be determined by an X-ray fluorescence (XRF) spectrometer. The principle of the method is that atoms of particular elements would release a characteristic energy when one of its inner electron is replaced by an outer electron. A short wave length which has high energy such as X-ray is used to impact the atoms and the released energy is fluorescent radiation. The results might be effected in the case the powdered sample has a wide range of grain size or different elements[37], and the tolerance might be considerable.

The crystal phase of the silica can be determined by X-ray powder diffraction (XRD). This technique takes the advantage of the characteristic diffraction of an X-ray radiation on a crystal lattice to identify the phase of a crystalline material. The diffracted X-ray is collected and diffraction peak is conversed to the distance of the crystal lattice d-spacing. Because d-spacing is a unique parameter of a mineral, it is used to identify for the phase identification of the crystal [38] and the density of the diffraction peak can give a rough estimation about the quantity of the crystal.

- *Reaction rate with calcium hydroxide*

Activity of the pozzolanic materials can be evaluated basing on either monitoring the reaction directly or determining the effect of reaction to the test sample. In direct methods, the varying amount of calcium hydrate showing the process of the reaction can be detected by different techniques such as X-ray diffraction or chemical titration. In indirect methods, the reaction is evaluated by monitoring the parameters which can give information about the reaction effect such as compressive strength or electrical conductivity of the sample. The correlation between typical tests was studied in the work of S. Donatello et.al and it was seen to be close correlated [39]. There is another important conclusion from this work is that the mass ratio between calcium hydrate and the pozolanas is an important parameter and it can cause interference in understanding the effect of the pozzolanic reaction.

Electrical conductivity measurement of saturated lime solution added by the siliceous is a simple indirect method and gives a reliable result so that it appears in almost all the research about pozzolanic activity. A complete process was firstly proposed by Luxán et.al in 1989, in which he figured out the optimized ratio to give an accurate result and good pozzolanic materials is supposed to have a conductivity reduction which is equal or larger than 1.2 mS/cm [40]. According to this criteria, rice husk ash is considered to be highly active as observed in the work of Deepa G. Nair et al. [30]. Result in Table 2 is taken from this research and is the conductivity of rice husk ash burnt at 500 °C and 700 °C in 12 or 24 hours with Slowly or Quickly cooling. Microscopic analysis of this researched showed that there is a large different in particle size of the rice husk ash burnt at 500 °C in different processes, but as seen in Table 2, the conductivity variations are only slight different. In other words, base on the electrical conductivity experiment, burning temperature has larger influence to the rice husk ash activity than the burning duration.

Table 2. Electrical conductivity reduction of saturated solution of calcium hydroxide added by RHA (Nair et al., 2008)

Sample	Conductivity change (ΔmS/cm)
RHA 700-12S	3.2
RHA 700-12Q	3.6
RHA 700-24S	3.0
RHA 700-24Q	3.5
RHA 500-12S	5.3
RHA 500-12Q	5.4
RHA 500-24S	5.2
RHA 500-24Q	5.2

Among the group of pozzolanic materials, rice husk ash has been recorded to be highly active. Reactions of calcium hydrate with different siliceous were tested in the work of R. Walker and S. Pavia and it was seen that the most amorphous group which includes rice husk ash is the most active [41]. Beside the statement about the amorphousness as an activity controller, this research also found the dominated governing role of the specific surface area to be in water demand. In the role of cement replacement materials, different pozolanas were tested in the work of S.K. Agarwal [42] and rice husk ash with particle size smaller than 45μm gave the highest pozzolanic index improvement.

2.2.3. Effect of rice husk ash in soil stabilization

As mentioned above, appropriate pyroprocessing can change the rice husk to be a rich silica material. So this ash can be used as a cement replacement in the cement stabilization methods, or cooperate with lime to enhance the lime stabilization methods. Being a cement replacement materials, rice husk ash can help to reduce considerably the required amount of ordinary Portland cement to archive the same strength in the case of cement only. With a fixed amount of cement, added rice husk ash can improve largely the strength as observed in the work of Basha et.al. [43].

In cooperation with lime, among different siliceous, rice husk ash gives the most significant result as seen in the work of A. Seco et.al (Figure 8) [44]. In this research, 5% of rice husk ash helped to decrease the swelling of an expansive soil sample from almost 5% to 0.5%, and this is the largest reduction among different tested additives. However

5% is not the optimized proportion found in other research working with expansive clay. In deed the optimized proportion was seen to be 12% in the research of R. M. Brook [45] and R. S. Sharma et.al. [46]. The optimized ratio between lime and RHA was figured out to be 1:3 by R.S. Sharma, which means 4% of lime is required for a well-burnt rice husk ash. But in a research about utilization of uncontrolled burnt rice husk ash with expansive clay in Indonesia by A. S. Muntohar [47], the ratio is 1:2 and the required amount of lime is 6%. This author also did the experiment with laboratory expansive clay which is the kaoline and bentonite mixture [48], and 6% is still the required amount of lime, but the amount of rice husk ash also reduced to this proportion. So the first conclusion from this disagreement is that the optimized ratio and proportion of lime and rice husk ash is a parameter depending on local conditions, and the result can be significantly affected by the burning condition of rice husk ash.

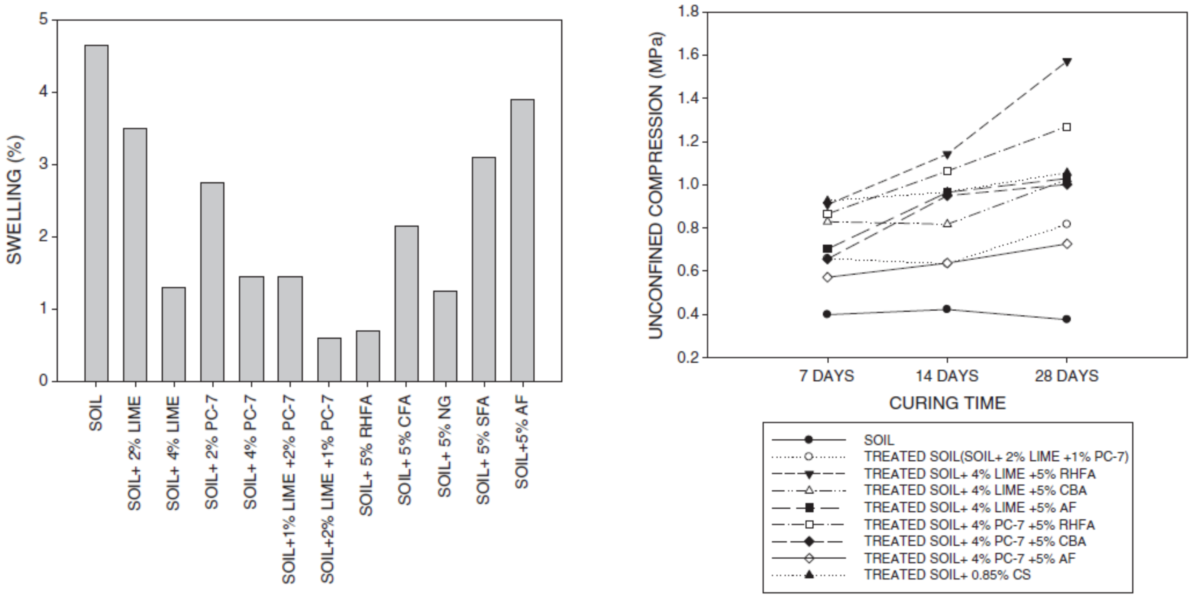

(a) (b)

Figure 8. Expansive soil with differen additives* (a) influence to swelling; (b) influence to the unconfined compression strength (A. Seco et al., 2011)

* PC-7: magnesium oxides; RHFA: Rice husk fly ash; CFA: Cereal fly ash; NG: Natural gypsum; SFA: Steel fly ash; AF: Aluminate filler

While proportion of 5% is not the optimized for expansive clay, this is the proportion found in the research with other soil types by different researchers, although the ratio with lime varies largely. For the fine grained soil classified to be ML, 5% of RHA showed the most improvement in all the cases of lime [49], while for lateritic soil classified to be CH, 6% of lime was the suggested amount of lime to combine with about 4% to 6% of rice husk ash [50]. The ratio was reduced for the organic soil classified to be OL as 2% of lime with 5% of rice husk ash was the outcome [51].

In the work of these types of soil, the rice husk ash was controlled burnt at appropriate condition because high expectation for this well burnt ash is the common sense. But there was research about open-air burnt ash and it showed that 6% of this ash can also help to improve a residual soil [52]. So in general, the promising effect of rice husk ash is not only governed by the activity of the ash and it is the synthesis of the ash quality with also the soil properties, the mixing amount and the ratio with lime.

While the optimized ratios and amount should be figured out for every individual case of soil types in different locations, the correlation between rice husk ash activity and the soil improvement effect should be generalized. This can help to reduce the input effort of obtaining an active ash from a strictly controlled burning condition by a less strictly one, hence increase the utilization opportunity of rice husk ash.

2.3. Literature summary

In the group of pozzolanic materials, the rice husk ash appeared to be one of the most reactive, and the optimum burning conditions between the energy consumption and the quality of the rice husk ash were suggested to be 500^oC in 2 hours. To be a secondary reagent for soil stabilization, its results was seen also very promising.

Among results of the different researchers about the ability of the rice husk ash in soil improvement, there were some researcher paying attention in the reactivity of the material and intended to produce a high quality ash for the experiments, while there were also some researchers intended to use uncontrolled burnt ash in order to utilize the local agricultural waste. In some other papers the researchers did not mention about the reactivity of the materials and how it had been produced. Interestingly in all the cases, the rice husk ash still showed a positive result. Because these researchers worked independently of each other and with different soil types in different regions, it is difficult to compare the effect of the controlled and uncontrolled burnt rice husk ash. Nevertheless, the positive results of the uncontrolled burnt ash expresses a possibility that might the investment of energy into rice husk ash production can be reduced at a certain level, then the investigation of the burning conditions to the applicability of the rice husk ash in soil improvement is useful.

3. Rice husk ash production and characterization

Because of the dependence of the rice husk ash characteristics on the burning conditions, the ash burnt in different durations and temperatures were classified and evaluated in order to understand their role and influence to the soil afterward. Their reactivity would be concluded based on the investigation of particle size, reaction rate with calcium hydroxide, and the crystal form.

3.1. Production and classification of rice husk ash from burning conditions

Rice husk ash is a silica-rich material and it requires a strict burning process to maintain the silica in the amorphous form while eliminating almost all the organic components. As mentioned in the section 2.4, based on literature values, pyroprocessing of 2 hours at 500°C was concluded to be sufficient to produce an ash with the desired high amount of amorphous silica combined with a low amount of carbon. However, due to the exothermic nature of the rice husk conversion, the temperature of the rice husk bulk is probably not well controlled even though a controlled system is used. It is possible that within a sample, the inner part of the husks experience a higher temperature so that the silica starts to crystallize, while at other points the temperature is lower, and thus the organic component is still not burnt completely and remains present.

Accordingly, rice husk ash burnt at the ideal temperature and duration can still be less reactive due to local temperature gradients and may consist of the undesired crystallized silica and/or contain carbon. In order to clarify the influence of the silica phase and the carbon content on the efficiency of the rice husk ash, these parameters were modified to be dominant in different sample of the ash. Accordingly, the three types of rice husk ash produced were categorized as “active ash”, “carbon ash” and “crystallized ash” and labeled to be A-RHA, C-RHA and Cr-RHA respectively.

- A-RHA: the name is derived from “amorphous” or “active”. This ash was burnt in the condition suggested to be ideal, which is duration of 2 hours at 500°C. The oven was set up to about 250°C before putting the rice husk in for burning. It took about 30 minutes when the temperature reached to 500°C, the mass then was left for 2 hours, and it was quickly cooling down by immediately removing from the furnace and storing in room temperature.

- C-RHA: the name stands for carbon. This ash was open-air and uncontrolled burnt; it was taken out of the fire when all the husks were burnt to be black; the temperature of the flame is normally 300^{o}C.
- Cr-RHA: the name comes from the "crystal". The ash was collected from slow burning process, in which the rice husk was put into the furnace from the atmosphere temperature. After that the furnace was turned on and after about 7 hours the temperature was between 600^{o}C and 700 ^{o}C. Then the furnace was turned off and the rice husk ash was kept in the furnace overnight for cooling down.

The burning process of A-RHA and Cr-RHA was implemented in Deltares with the rice husk originated from Hanoi, Vietnam, while the C-RHA was burnt in Vietnam according to local practice before transportation. The appearance of the ash before grinding is shown in Figure 9. After burning, the raw rice husk ash was ground by the HERZOG HSM 100 vibration grinding mill, capacity of 10ml, in 30 seconds to obtain a fine ash.

Table 3. Rice husk ash classification

Ash	Burning condition	Color	Expectation
A-RHA	500^{o}C in 2 hours, quick cooling	Grey	Highly active
C-RHA	Open-air and quick burning	Black	Averagely active due to high amount of carbon
Cr-RHA	Slowly burning and cooling in range of 600 ^{o}C and 700 ^{o}C	Pink	Averagely active due to crystallized silica

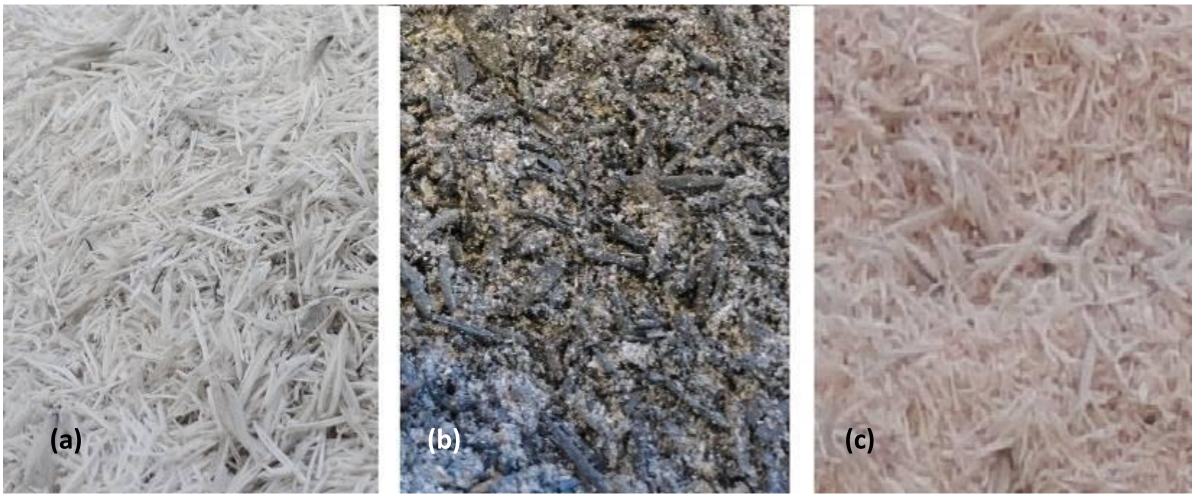

Figure 9. Rice husk ash classification. (a) A-RHA; (b) C-RHA; (c) Cr-RHA

Characteristics and expected properties for these three types of ash is generalized in Table 3. By burning under the appropriate condition, the A-RHA is expected to be highly active because of the low amount of carbon content and the silica remained at amorphous phase. As seen in Figure 9a, the A-RHA is lightly grey which interprets a low carbon content, while the black color of the C-RHA in Figure 9b is a clear evidence for the existence of much unburnt carbon. The Cr-RHA has several grey points as seen in Figure 9c, but the main color is lightly pink.

3.2. Rice husk ash characterization

The main factors governing the activity of the material were determined by the techniques introduced in the section 2.2.2. Besides, they were also observed by the Environmental Scanning Electron Microscope and their particle density was also determined.

- *Specific surface area*

Specific surface areas of the three types of rice husk ash were determined by BET method with the Gemini VII 2390, Micromeritics^R in the Microlab of the Faculty of Civil Engineering and Geosciences. The samples were put in the oven at 105 ^{0}C in 2 hours before doing the experiment. The C-RHA has a specific surface area of 68 m^2/g, which is the largest. The Cr-RHA which has large particles together with the agglomerations has the smallest value which is 27 m^2/g, and for the A-RHA it is 47 m^2/g.

- *Environmental Scanning Electron Microscope images*

The rice husk ash and also the rice husk were observed by the XL30 ESEM, Philips in the Microlab of the Faculty of Civil Engineering and Geosciences. The image of the rice husk Figure 10 shows a clearly separated white layer which probably is the silica precipitated from the solution within the rice husk.

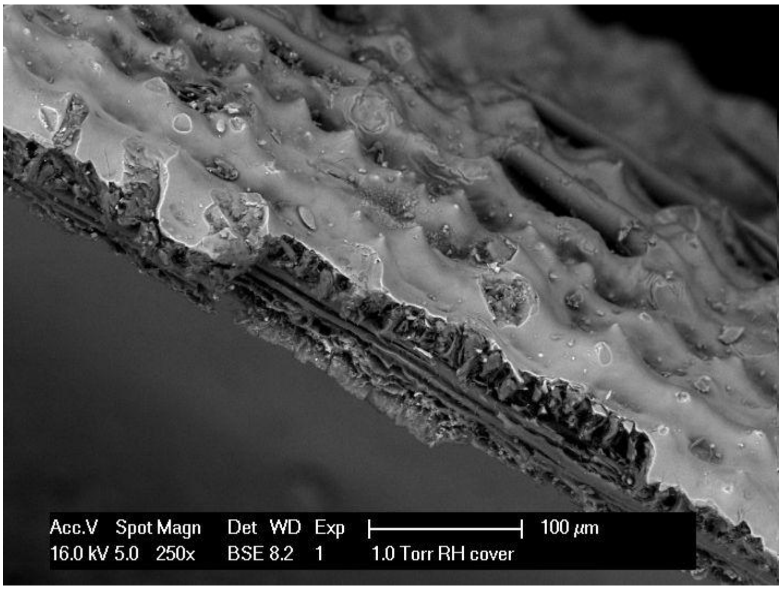

Figure 10. Rice husk image

The images of the rice husk ash show that the particles of all the three types of ash are angular although their size is different. The C-RHA appears to be the finest and also uniform as seen in Figure 12, while the image of A-RHA suggests a well graded size distribution as seen in Figure 11. From the scale of the images, the average size of the particles in C-RHA or A-RHA is estimated to be between 10 μm and 20 μm. The Figure 13 is the image of Cr-RHA and there are a number of larger particles seen together with some agglomerations. The diameter of the agglomerations is larger than 100 μm, and there are particles whose equivalent diameter is larger than 50 μm. The same grinding energy breaking the ash to different levels of dimension can be a suggestion of the firmness of the different types of rice husk ash.

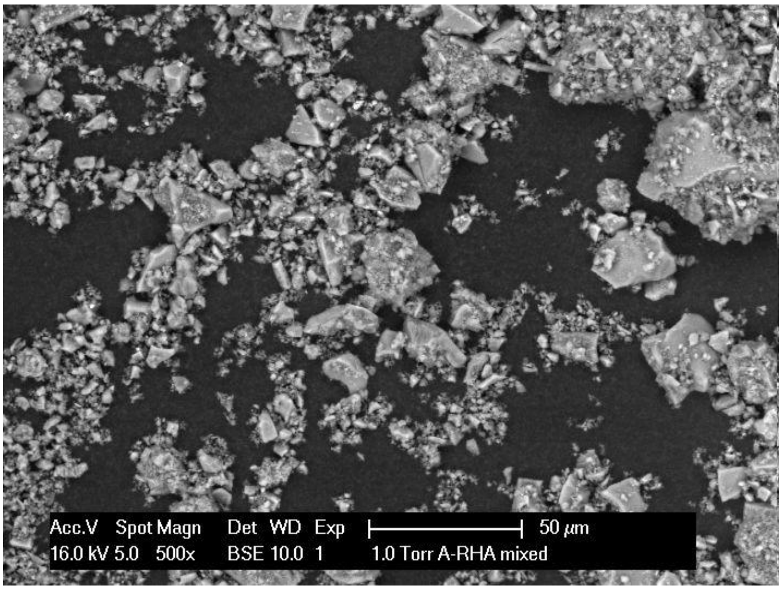

Figure 11. A-RHA particle image

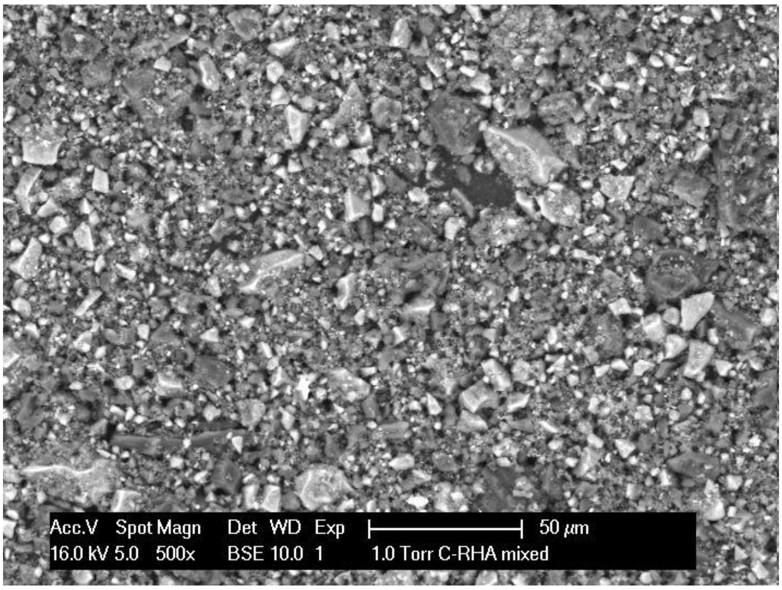

Figure 12. C-RHA particle image

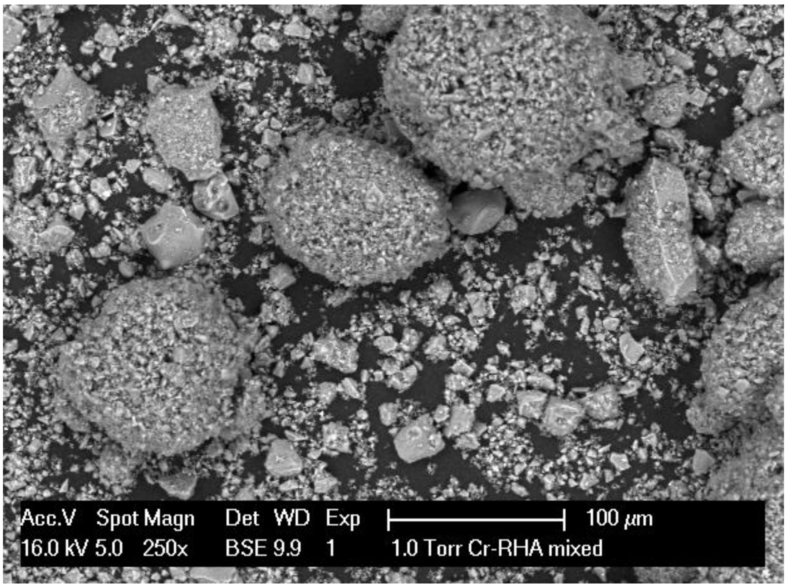

Figure 13. Cr-RHA particle image

- *Particle density*

Particle density of the ash was also determined by the pycnometer and the used liquid was ethanol. For each type of ash, the parameter was identified several times and the average value was used, data is shown in the appendix 2. The values of A-RHA and Cr-RHA are similarly, as they are 2.08±0.09 and 2.05±0.11 g/cm^3, while the C-RHA is considerably lighter as its particle density is 1.71±0.05 g/cm^3.

- *Elemental analysis*

Components of the ash were analysis by an XRF Spectrometer which is the Epsilon 3XL Panalytical in the Recycle laboratory of the faculty of Civil Engineering and Geoscience. For the A-RHA and Cr-RHA, the amount silica was captured to be 94%. For the C-RHA, the amount of silica was 55% but the total mass recorded after the test was only 60% while this situation did not happen with the other two types (Figure 14). Because the machine cannot capture the carbon, this loss was assumed to be the amount of the carbon. Specified proportions of the elements which is larger than 0.1% can be seen in the Table 4a, while Table 4b shows the components in mol. Detail results of the XRF analysis is presented in the appendix 2.

Table 4a. Mass percentage

	Total mass %	**SiO_2** %	**K_2O** %	**CaO** %	**MgO** %	**Fe_2O_3** %	**Al_2O_3** %	**P_2O_5** %	**SO_3** %	**Others*** %
C-RHA	61.6	54.9	1.17	0.86	0.31	0.42	0.88	0.56	0.47	0.41
A-RHA	100.0	94.5	2.18	0.88	0.45	0.16	0.61	0.55	0.34	0.27
Cr-RHA	100.0	94.2	2.10	0.93	0.44	0.21	0.62	0.60	0.63	0.26

* Others: MnO, NiO, ZnO, CuO, SnO_2, Cl, TiO_2, Cr_2O_3, PbO, As_2O_3

Table 4b. Mol in 1kg ash

	C**	SiO_2	K_2O	CaO	MgO	Fe_2O_3	Al_2O_3	P_2O_5	SO_3
C-RHA	33.3	9.1	0.12	0.15	0.08	0.03	0.09	0.02	0.06
A-RHA	-	15.7	0.23	0.16	1.11	0.01	0.06	0.02	0.04
Cr-RHA	-	15.7	0.22	0.17	0.11	0.01	0.06	0.02	0.08

** This amount of carbon was derived by the absence mass after the experiment

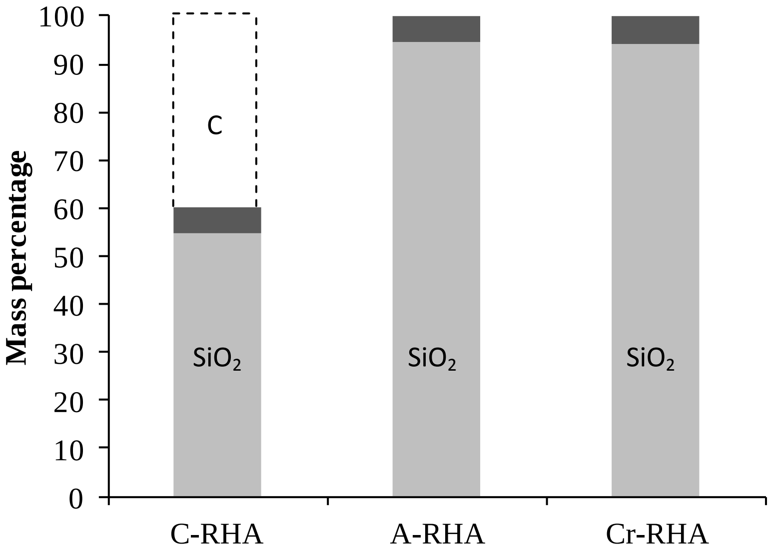

Figure 14. Elements of the rice husk ash

A remark from these results is that there are variable elements in the samples with a very small proportion; hence the accuracy might be affected by the tolerance of the machine, according to the technician this value can be 2% point. But the more important point is the dominant of silica in A-RHA and Cr-RHA, and the large amount of the carbon in the C-RHA.

- *Crystal structure*

The structure of the particle was analyzed by X-ray diffraction on a Bruker-AXS D5005 diffractometer of the X-ray diffraction facilities in the faculty of 3mE. The large and smooth raise of the diffraction density in the 2θ range of 15° and 30° appearing in all the samples shows that they are mainly amorphous together with the detection of the quartz. The red sticks is the scale of the quartz, and the C-RHA is seen to be closest to this scale as there appeared a peak at the position of 21° in this sample while there did not for the other two cases; besides the peaks at other position such as 37° or 50° were also clearer; accordingly it is supposed to contain the highest quartz content. Graphite was also detected in the C-RHA and the extremely high peak of the diffraction at the angle of 27° is highly caused by both the graphite and the quartz.

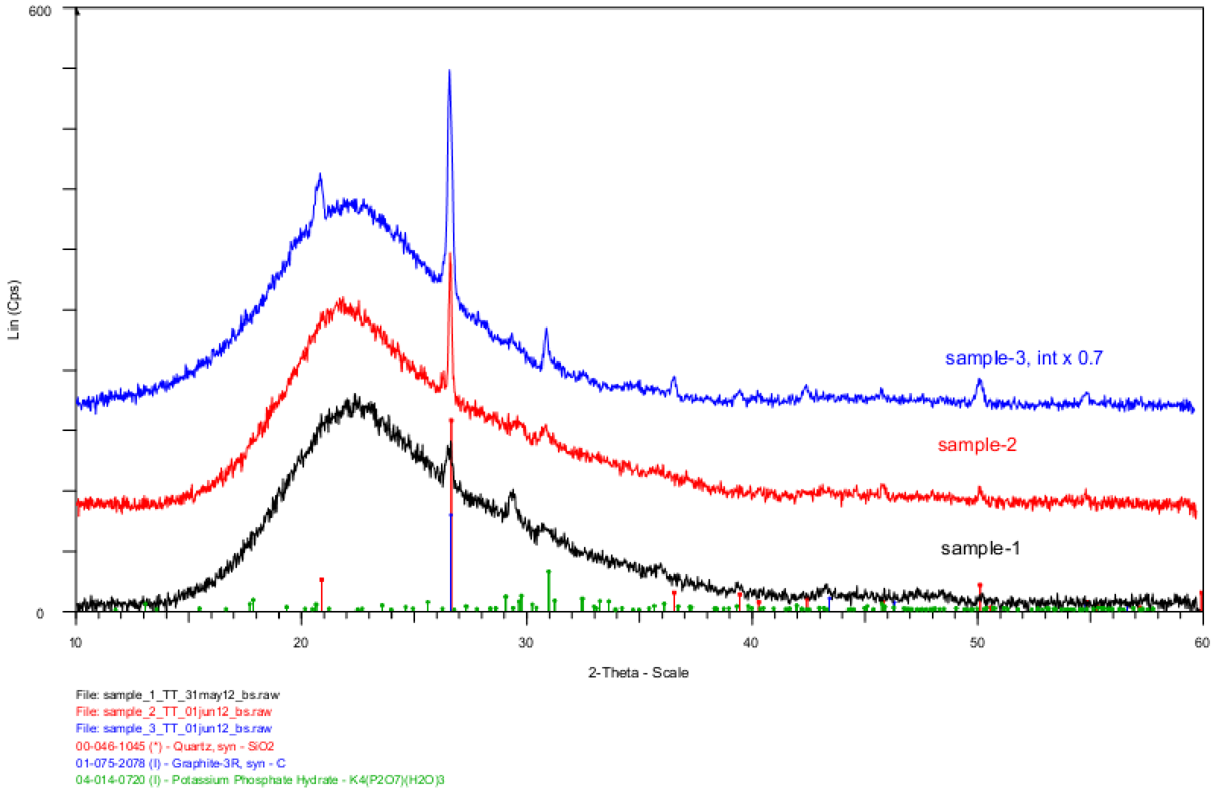

Figure 15. XRD results of the three types of ash. Sample-1: A-RHA; sample-2: Cr-RHA; sample 3: C-RHA

3.3. *Evaluation of pozzolanic activity of RHA by the conductivity measurement*

3.3.1. Principle:

Based on the solubility of amorphous silica at high pH, the pozzolanic activity of rice husk ash can be evaluated by its reaction in the saturated solution of calcium hydroxide. The chemical process within the solution is the dissolution of the amorphous silica from the rice husk ash in the high pH solution followed by the pozzolanic reaction. The chemical reactions can be written as:

$$SiO_2 + 2H_2O \xrightarrow{OH^-} 4H^+ + SiO_4^{4-}$$

$$bSiO_4^{4-} + aCa^{2+} + 2xOH^- \rightarrow Ca_aSiO_b.xH_2O$$

As the ion concentration changes due to these reactions, measurement of electrical conductivity in the solution is a reliable method to evaluate the activity of the material. As the conductivity and the concentration of the ions is correlated, conductivity reduction reflects the rate of consuming reagents for the reaction; hence, the reactivity of the material is revealed.

3.3.2. Materials and process

The Electrical conductivity method of Luxán et al. [40], which was discussed in section 2.2.2, was used to evaluate the pozzolanic activity of the rice husk ash. 200 ml of saturated calcium hydroxide solution was put into glass beaker and together with the magnetic stirrer they were kept in a stove which was set at 40°C preliminarily. Then, EC and pH electrodes were installed and the stirrer was turned on; data was collected at a time interval of 10 seconds. When temperature was recorded to be stabilized at 40±1°, 5 g of the sample was added into the solution. The solution was kept to be stirred all the time.

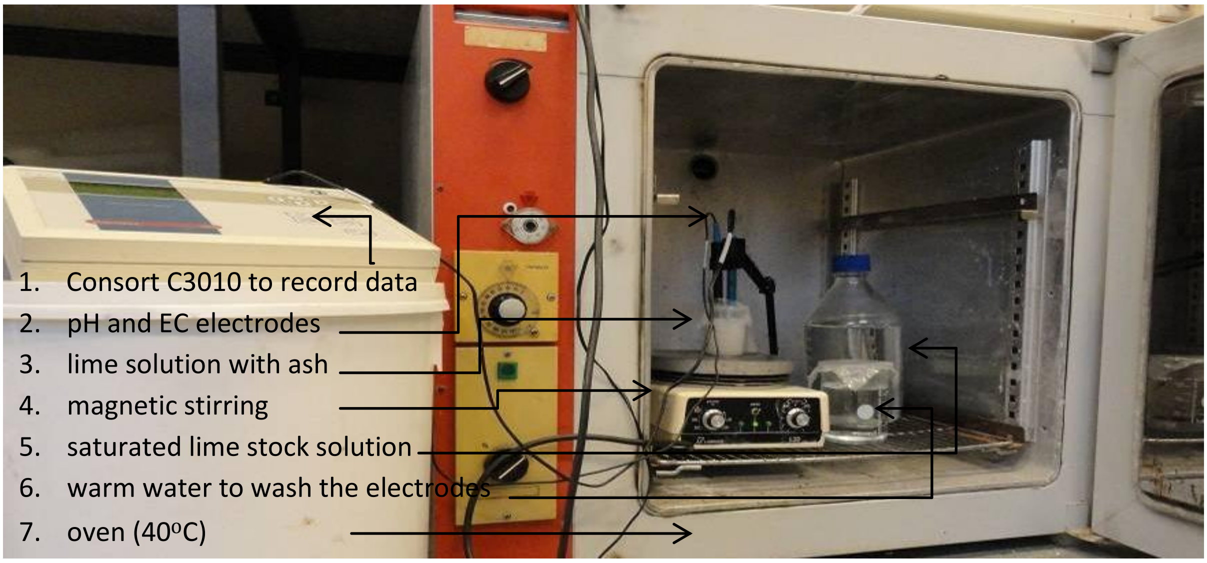

Figure 16. Setting up for electrical conductivity measurement

The three ash types, C-RHA, A-RHA and Cr-RHA, were tested; reagent used in this experiment was calcium hydroxide solution which was saturated at 40°C. The solution was made by dissolving an excess amount of calcium hydroxide powder in deionized water at 40°C, then storing at the same temperature for stabilization and finally filtering two times with filter paper. In order to maintain the temperature of the solution, all the tools were put in the oven previously and the filtering was implemented also in the oven.

3.3.3. Results

The following graphs show the result of conductivity and pH variation of the three types of ash in the saturated solution of calcium hydroxide. A similar trend of reduction in EC was recorded for all the cases, and the largest reduction happened in the first minute after the rice husk ash was added. However, there is a considerable difference in the reduction rates between the ash types. Figure 17 shows that the C-RHA has the largest reduction in EC value, which dropped by 2.34 mS/cm in the first minute, while the reduction of Cr-RHA was only 1.19 mS/cm. The EC reduction of A-RHA was close to the value of the C-RHA, but along with time the difference was enlarged.

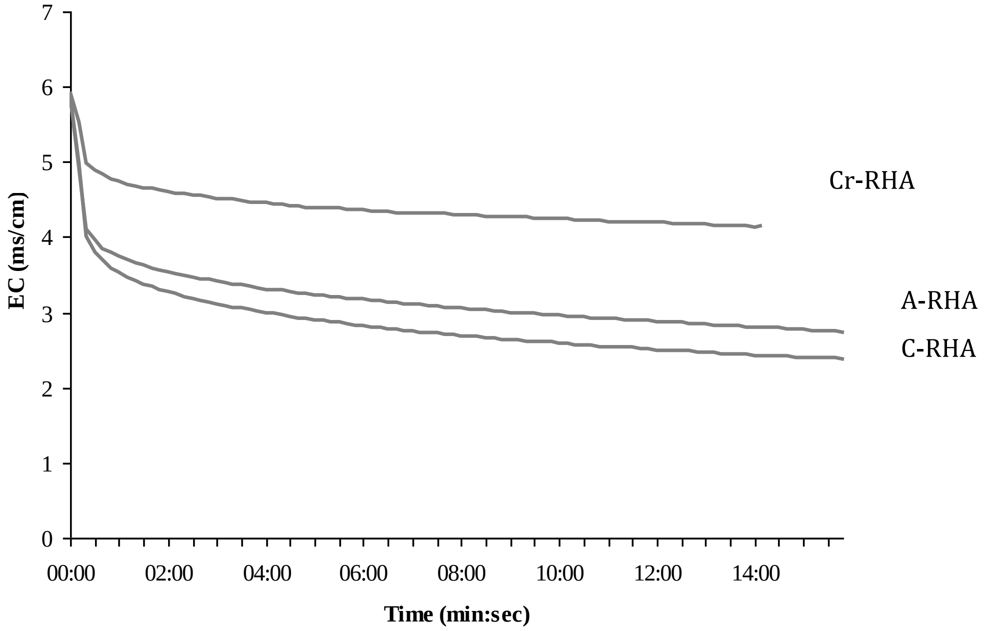

Figure 17. Electrical conductivity variations

The gradual reduction of the pH value in all the cases indicates that there was a reaction between the base solution and the silicic acid. Similarly to the EC variation, C-RHA had the largest reduction in pH, which dropped by 0.36 units to 11.08 after 15 minutes. The pH value of the solution with A-RHA was slightly above 11.1 after 15 minutes as seen in Figure 18, while the value of the solution with Cr-RHA stayed at a higher level, which was above 11.3. Data of the experiment was presented in the appendix 3.

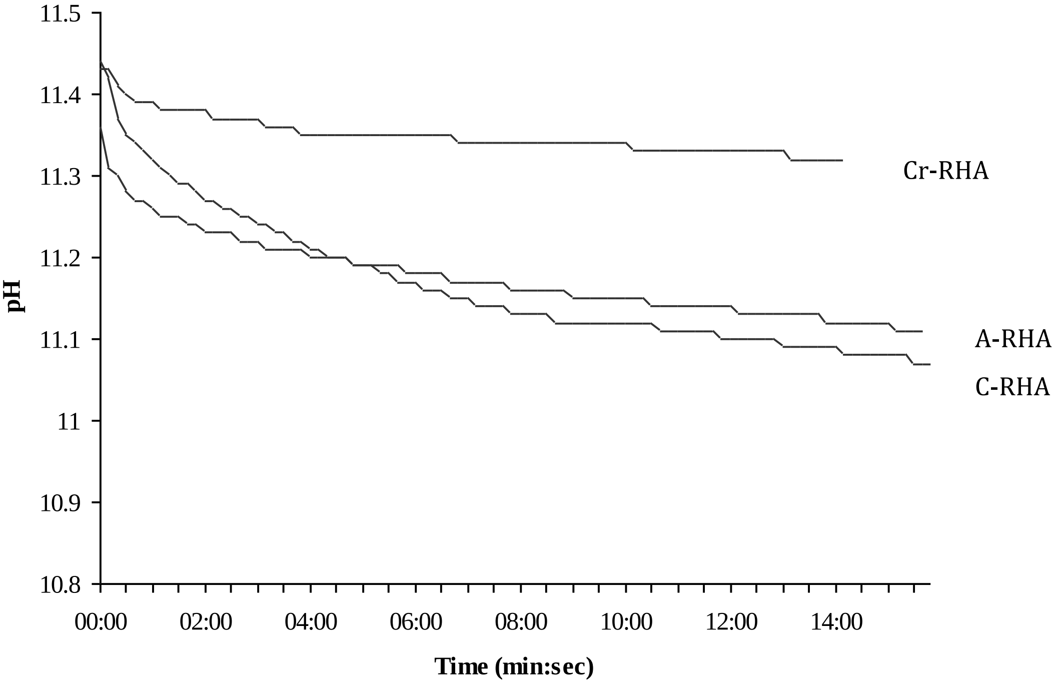

Figure 18. pH variations

3.4. *Identification of the reactive silica content by chemical treatment*

3.4.1. Purpose and principle

The reactive silica is defined in the standard of NEN-EN 197-1 to be "*the fraction of the silicon dioxide which is soluble after treatment with hydrochloric acid (HCl) and with boiling potassium hydroxide (KOH) solution*". This is the part which is able to take part in the pozzolanic reaction to create the calcium silicate hydrate and this ability is controlled by the solubility of the material. In other words, the amount of silica in the amorphous form and imperfect crystal form holds the role of governing the reactivity of the material due to its strongly soluble characteristic compared with the crystal forms.

The first step of the treatment is with hydrochloric acid to minimize the precipitation of the soluble silica and also dissolves the metal oxides in the rice husk ash, while the subsequent treatment with the boiling potassium hydroxide solution dissolves the reactive silica and the nonmetal oxides. Consequently, the insoluble residue after the treatment is dominated by the non-reactive silica. The un-burnt carbon (if present) will be converted to CO_2 in a burning step at 1000^oC.

3.4.2. Material and process

The experiments were implemented with the three types of rice husk ash, the rice husk and a reference which is quartz flour. The flour is the silverbond M6 supplied by the Sibelco Company and was used in the project number 1206571 of Deltares. It is mainly quartz whose proportion is larger than 98%, and average diameter d_{50} was identified to be 51 μm. For the rice husk, from the burning process producing A-RHA and Cr-RHA, it showed that the ash is only 12% by mass of the rice husk, so in its experiment all the mass was double so that the collected residue would be visible.

The procedure of the experiments follows the instruction in NEN-EN 196-2, section 10.2. The reagents used in these experiments were the hydrochloride acid at the concentration of 9.44 mol/L, 2.60 mol/L, and 1.15 mol/L, and the potassium hydroxide solution at the concentration of 2.80 mol/L. The filter papers were needed and the used ones were Whatman cellulose filter paper with the minimum particle level of 2.5 μm.

A mass of 1g of the solid was dispersed firstly in 25ml water, then 40ml of the HCl 9.44M solution. The solution was gently heated and evaporates to dryness in a water bath at 100^oC. The acid treatment was continued by heating and evaporating two more times with 20 ml solution of HCl 9.44M before heating in 100ml of the HCl 2.6M solution and being filtered. The filter paper and its content was transferred to a 250 ml conical flask and was added with 100 ml of the KOH 2.8M solution, then was left overnight. The base treatment was continued by heating this flask in boiling water for 3 hours under reflux. After that it was filtered and washed by 100ml of HCl 1.15 M solutions, then by nearly-boiling water. At the end, the filter paper and its content was ignited at 950^oC, the residues are considered to be the unreactive component and were weighed.

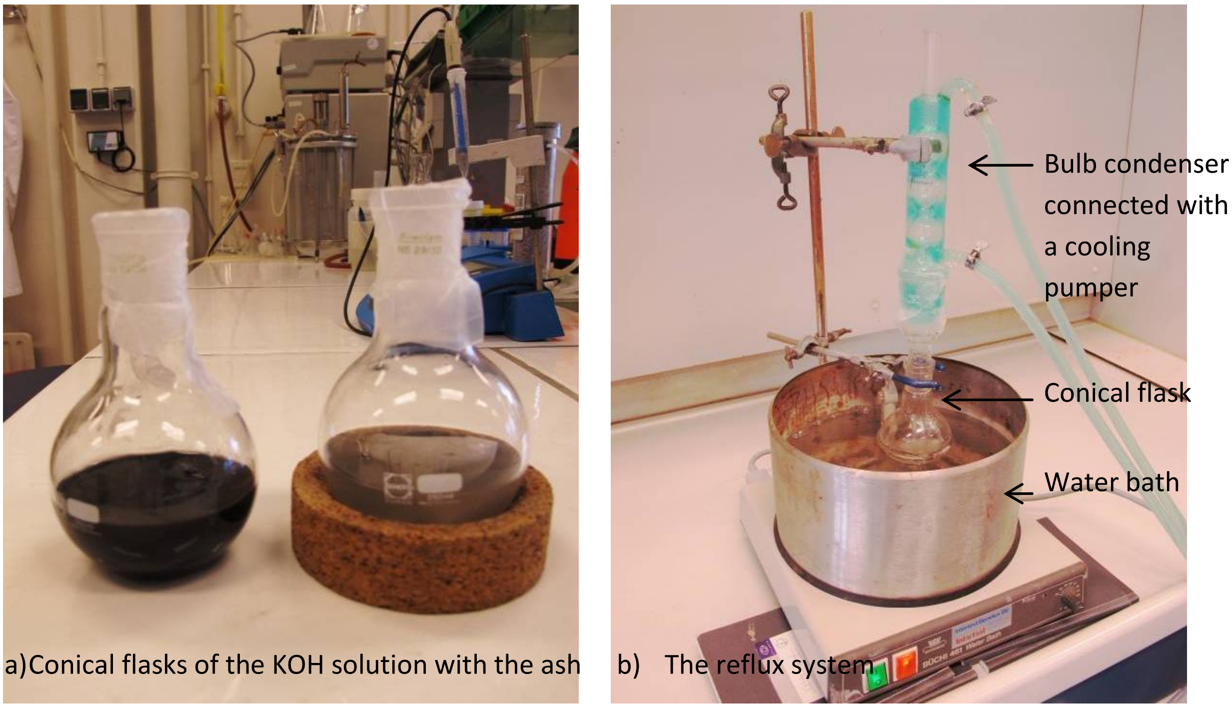

a)Conical flasks of the KOH solution with the ash b) The reflux system

Figure 19. Set up for experiment of non reactive silica content

3.4.3. Results

Table 5. Reactive silica amount identification

	Rice husk	Quartz flour	A-RHA	C-RHA	Cr-RHA
Total mass (g)	1.9915	1.0321	1.03	1.00	1.05
Total silica (g)	0.23898	1.01146	0.97335	0.549	0.9891
Plate (g)	50.1694	50.3355	51.3029	50.1669	53.9139
Plate + ash after ignition (g)	50.1758	51.3366	51.3125	50.1954	53.9283
Residues (g)	0.0064	1.0011	0.0096	0.0285	0.0144
Total silica/total mass	12%±2%	98%±2%	94.5%±2%	54.9%±2%	94.2%±2%
Reactive silica/total mass	11.7% ±2.0%	1.0% ±2.0%	93.6% ±2.0%	52.1% ±2.6%	92.8% ±2.9%
Residue/total mass	0.3% ±0.01%	97.0% ±0.03%	0.9% ±0.02%	2.9% ±0.08%	1.4% ±0.05%
Residues/total silica	2.7% ±0.6%	99.0% ±2.1 %	1.0% ±0.1%	5.2% ±0.4%	1.5% ±0.1%

After ignition there were residues in all the cases but with a very small amount except the case of the quartz flour as seen in Figure 20 and Table 5. The quartz flour mass was almost equal to its original used mass, while for all the other cases the residues was very small. Total silica in the material was chosen to be the scale then it is seen that the quartz remained after the treatment. For the rest of the cases, the C-RHA has the largest ratio which was 5.2% (±0.4 percentage point) of the total silica and this is considerable, while for the others the amounts were smaller than a half of this proportion. The tolerances of the results were derived from the errors of the balances which were set to be ±0.0001 and ±0.02, together with the tolerance of the XRF results.

The effect of these treatments on the rice husk was seen very clearly in the Figure 22. After the acid treatment the color of husk changed from yellow to black, and they became thinner and partly transparent after the base treatment. After ignition, it is hardly to observe the residues of rice husk or the rice husk ash, but for the quartz flour it can be easily seen to stay almost the same with its original state as shown in the Figure 20. However there has also some transformation within the quartz mass as there were large crystals as seen in the Figure 23.

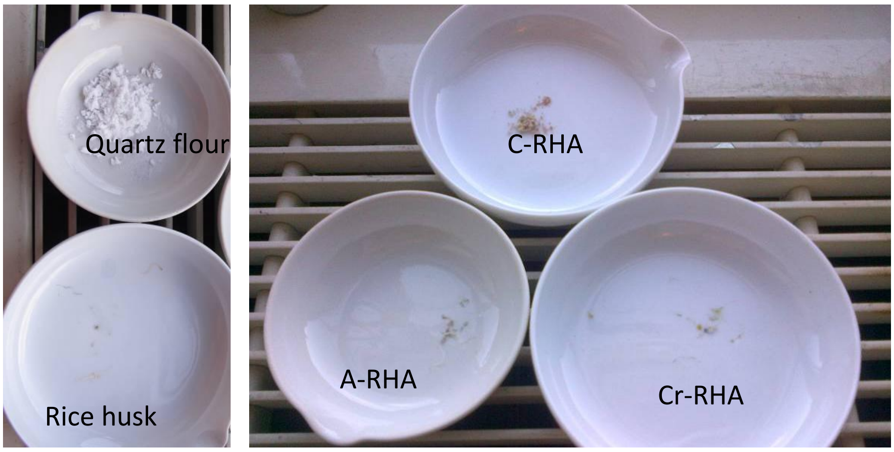

Figure 20. Residues after ignition in the experiment of non reactive silica content

Figure 21. Rice husk

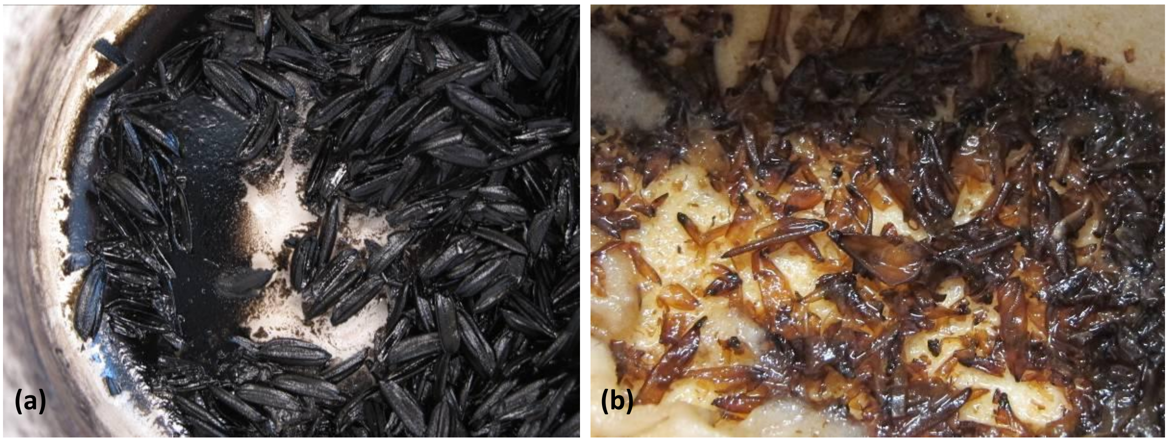

Figure 22. Rice husk after treatment. (a) the first treatment with acid; (b) the second treatment with base

Figure 23. Partly quartz transferred to another form of crystall after ignition at 950°C

3.5. Rice husk ash activity evaluation

From the classification in section 3.1, the rice husk ash is classified into three: A-RHA, C-RHA and Cr-RHA. The A-RHA which was burnt under the theoretically appropriate burning conditions is expected to be the most active while the carbon content of C-RHA is expected to be high due to quick burning and is predicted to hinder the silica activity; for the Cr-RHA its silica is supposed to partly converted into crystal form because of a slow burning at high temperature so the activity is also decreased.

The results of the rice husk ash identification were generalized in the Table 6.

3.5.1. Physical properties and main components of the rice husk ash

The ESEM images in section 3.2 show that Cr-RHA has the largest particle size. This is consistent with its lowest specific surface area determined by the nitrogen gas adsorption. The same energy was used to grind all the ash, so these big pieces of Cr-RHA indicate the solid is harder than the other ashes, which is an indication of the presence of crystallized silica.

In contrast, the XRD results indicate that the amount of quartz is the highest in the C-RHA, not the Cr-RHA, while the A-RHA has a moderate amount. This observation is consistent with the results of the non-reacted silica concentration (determined as the non-soluble fraction while boiling in KOH) as described in the section 3.4. This amount of the C-RHA was about 3% of the total mass, while for the other two types it was about 1%. These are probably the total quartz presenting in the ash because the result with the quartz flour showed that it was not dissolved by the boiling KOH solution. So in term of the crystal content the results were not as expected, but indeed the large amount of quartz in the C-RHA is reasonable. This is because although the temperature of the flame tip is about 300°C, the peak value can be about 900°C [53], so this might be the reason that made the silica in the rice husk crystallize locally and the quartz appeared more clearly in these experiments.

The black color of the C-RHA is a clear indication of the presence of the carbon in this ash. The XRF results confirmed this and showed that the carbon content is relatively high at about 40%. This carbon is the main reason that this ash type has the smallest particle density. The A-RHA and Cr-RHA contain mainly the silica so a relatively equal particle density of these two types is reasonable.

Table 6. Rice husk ash identification

Type of rice husk ash				**A-RHA**	**C-RHA**	**Cr-RHA**
Prediction from literature				The most reactive	Moderately reactive	Moderately reactive
Identified parameters	**Particle size** estimation (ESEM)		(μm)	20	10	50
	Specific surface area (Nitrogen Gas Adsorption)		(m^2/g)	47	68	27
	Particle density (pycnometer with ethanol)		(g/cm^3)	2.08 (±0.09)	1.71 (±0.05)	2.05 (±0.11)
	Silica and carbon component (XRF)	SiO_2	%	94.5(±2)	54.9(±2)	94.2(±2)
		C	%	-	40.0(±2)	-
	Crystal structure (XRD)			All the three types are mainly amorphous but quartz is identified		
	Activity (Electrical conductivity reduction in the first 2 minutes)		(mS/cm)	2.36	2.61	1.33
	Silica component (solubility in boiling KOH treatment)	Reactive	%	93.6 (±2.0)	52.1 (±2.6)	92.8 (±2.9)
		Nonreactive	%	0.9 (±0.02)	2.9 (±0.08)	1.4 (±0.05)

3.5.2. Chemical properties in term of the reactivity

Using the specific surface area to predict the activity, the Cr-RHA has the lowest value, which indicates a low activity. This is confirmed by the conversion rate in saturated calcium hydroxide, as the Cr-RHA presented the smallest reduction in both the electrical conductivity and pH of the solution.

Interestingly, the specific surface area and the EC reduction are also consistent with each other in the case of A-RHA and C-RHA, but not to state that the A-RHA is the most active as expected. In the experiment with the saturated calcium hydroxide solution, the A-RHA with the expectation of being the most active was expected to have the largest electrical conductivity reduction rate, but it turned out that the C-RHA had the largest EC reduction despite the large amount of carbon content and the quartz, and also the smallest amount of silica compared with the A-RHA and Cr-RHA. Similarly, the specific surface area of the A-RHA is not the largest as expected but the C-RHA is. In other words, the C-RHA is the most active in these experiments. So in case the carbon content really hinders the activity of the ash, then the C-RHA without the carbon can even be more reactive.

3.5.3. Clarifying the factors governing the reactivity of the rice husk ash

The most reactive characteristic of the C-RHA is resulted simultaneously by the large specific surface area and the nature of the silica. So in order to evaluate the silica itself, the effect of the specific surface area was eliminated by the divide of EC reduction by the surface area. This surface area is the total surface area of the ash used in the conductivity experiment at the concentration of 5g of the ash over 200ml. As the purpose is to compare the reactivity of the ash, the Cr-RHA was chosen to be the reference and the derived results would be compared in terms of ratio.

Table 7. Separating the effect of the surface area from RHA activity

		C-RHA	A-RHA	Cr-RHA
EC reduction after 2 minutes	(mS/cm)	2.61	2.36	1.33
Specific surface area	(m^2/g)	68	47	27
Proportion of reactive silica	-	52.1%	93.6%	92.8%
Surface area at the concentration of 5g/200ml	(m^2/m^3)	17×10^5	11.75×10^5	6.75×10^5
EC per area	$\left(\frac{S/m}{m^2/m^3}\right)$	1.53×10^{-7}	2.01×10^{-7}	1.97×10^{-7}
EC per area Proportion (for rice husk ash)	-	0.78	1.02	1
Unit EC proportion (for reactive silica)	-	1.33	1.02	1

After eliminating the influence of specific surface area, the C-RHA has the smallest conductivity per area as seen in the Table 7. In other words, if the three types of ash have the same specific surface area then the C-RHA is the least reactive while the A-RHA and Cr-RHA reactivity are equal. However, because the amount of reactive silica in the C-RHA is just a half of the other two cases, so an extra calculation was made by dividing the EC per area proportions by the percentage of the reactive silica while still taking the value of Cr-RHA to be the reference. The quantity of the EC after this divide is supposed to be the unit EC which expresses the reaction rate of one mass unit of reactive silica presenting in the rice husk ash. In other words, this so-called unit EC expresses the solubility of the rice husk ash in the saturated lime solution, and it shows that the C-RHA is the most soluble.

Nevertheless, the C-RHA also has the largest amount of quartz. A possible explanation for this difference is that for the C-RHA, although the crystallization occurred locally due to the high temperature, the burning duration was short so that the rest of the silica still remained at its initial state (which is amorphous silica precipitated from solution [25], hence the most soluble and consequently the most reactive); while the A-RHA and the Cr-RHA were burnt in a controlled environment and the temperature gradients were limited but affected to the whole mass of the materials. As the temperature increased the crystallization occurred gradually, in this way the silica in A-RHA or Cr-RHA was not strongly crystallized to quartz but still had a reduction in its solubility. This statement leads to a conclusion about the effect of the burning process that it is only needed to remove the organic components and its impact to the amorphous silica should be minimized as much as possible.

In this interpretation, the influence of the carbon was seen in only the term of quantity as it reduces the proportion of the silica. Besides, the specific surface area of the C-RHA is the total value of both the carbon and the silica, so the real area of the silica might be considerably smaller, then the calculation in Table 7 can bring out a much higher value of unit EC for the C-RHA. In the other hand, there might be a situation that the carbon (the unburnt completely organic components) can attract the ion within the solution and cause the reduction of the electrical conductivity of the solution. So these matters need to be clarified by investigation of the original rice husk in details.

In overall, the three types of ash are confirmed to be fitted into the classification, as the C-RHA has the large amount of the carbon content and the Cr-RHA has a clear indication of the crystal. But their activity has been determined not to be as expected. Between the two cases of controlled burning which are A-RHA and Cr-RHA, the results are consistent with the statement of A. Muthadhi and S. Kothandaraman [34] as the A-RHA is seen to be more reactive thanks to the results of a larger specific surface area and also larger drop of the electrical conductivity. But because in the literature the uncontrolled burnt rice husk ash was not dealt with so the result of the C-RHA in this research is a step further from the literature.

The C-RHA has the smallest amount of silica because of not being burnt completely, also contains the largest amount of the quartz, but it has the highest activity expressed by the EC variation and the largest specific surface area. These results reflect the correlation between the particle size and the crystal form of the silica, and they surpass the quantity factor to govern the reactivity of the rice husk ash. They also confirm the expected effect of the burning process which is only eliminating the organic components while remaining the silica in the amorphous form, but suggest that there is a hierarchy of solubility rate and the burning duration should be short so that the silica can stay at the highest amorphous state which corresponds to the highest activity.

4. Effect of rice husk ash on the engineering properties of clay

In this part the soil improvement ability of the rice husk ash collected from different burning conditions was examined. Being a secondary reagent, the rice husk ash needs calcium hydroxide to be activated so it will be combined with this reagent by the mixing ratio of 1:1. Effect of the additives is evaluated through the variations of the main engineering properties of the mixed soil.

4.1. Soil properties

The soil type chosen in this work was the Dutch river clay. The initial water content of the clay, unit weight together with plastic and liquid limit were determined in the laboratory according to the British Standard BS1377-2:1990 [54]. The results are shown in Table 8. According to the unified soil classification system used in the standard BS 5930:1999 section 6 [55] this soil is classified as a clay with high plasticity (CH).

The liquid limit was indirectly identified from the correlation between the cone penetration depth and the water content as described in the ISO/TS 17892-6:2004 [56]. According to this document, the undrained shear strength can also be derived from the cone penetration depth, so the variation of this parameter along with the water content was also interpreted and the result was plotted together with the cone penetration depth as shown in Figure 24. The undrained shear strength of the clay at the plastic limit and liquid limit state were derived to be 140 kPa and 1.57 kPa respectively.

Due to the large occurence of soft clay with high water content in practice, the clay was soaked to obtain a higher water content which was 48%, and corresponding unit weight was 1.78 g/cm^3; the Liquidity Index then changed from 0.39 to 0.76. This soaked clay will be the objective of this research.

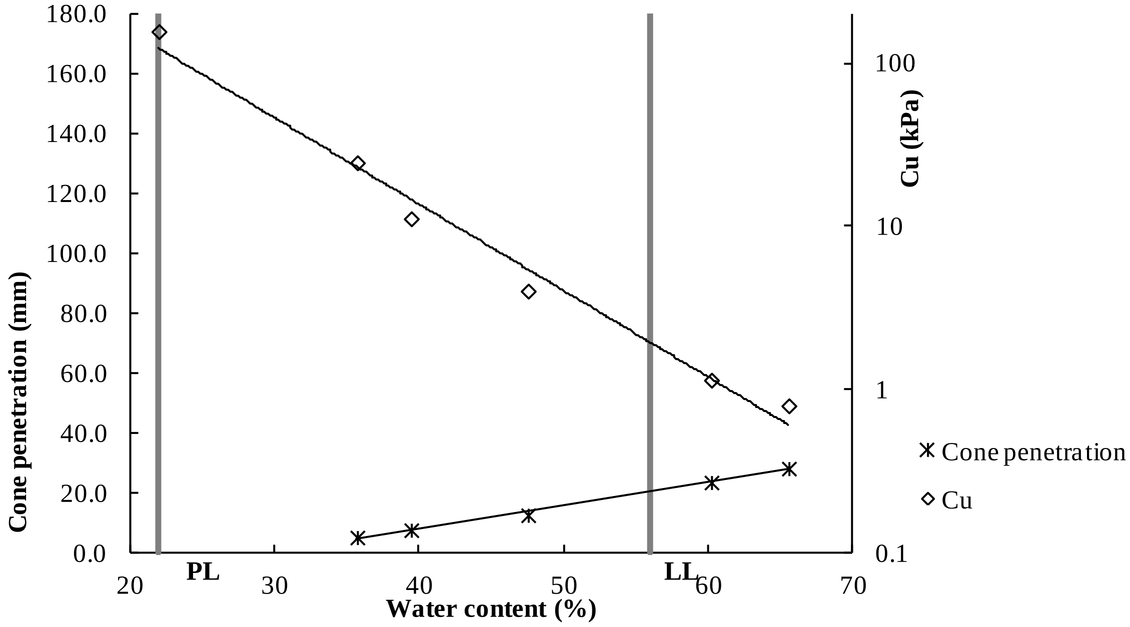

Figure 24. Undrained shear strength along with the water content

Table 8. Properties of the clay

Parameter		Value	Number of test
Plastic Limit	%	21.96	2
Initial water content	%	35.14	2
Liquid Limit	%	56 %	
Plastic Index	%	34.04	
Liquidity Index	-	0.39	
Increased water content	%	47.94	10 (Deviation is 0.5 %)
Decreased unit weight	(g/cm^3)	1.76	2
Liquidity Index	-	0.76	

4.2. Plasticity modification

4.2.1. Method and process

When clay is mixed with lime and rice husk ash, there is an instant change to the soil plasticity which isdesribed in this part. The soil was mixed with different amounts of lime only and with mixtures of lime and different types of rice husk ash. Then its water content and the Atterberg's limits after mixing were determined. The mixing ratio of the ash and the lime was kept to be one in all experiments.

To evaluate whether a change in water content was due to the pozzolanic reaction in which water is consumed or due to evaporation, a sub-experiment was performed with the C-RHA. After the mixing process was completed in the first ten minutes, the water content of the mixed soil was determined several times during the first hour. The test was also done with a sample of soil without addition of RHA, but with continuously mixing so that the evaporation rate due to the mixing could be identified.

4.2.2. Results

By mixing the clay with the additives, the water content of the soil was considerably reduced as seen in Table 9. Nevertheless the reduction difference between the different additives was not large. The influence of the additives was expressed clearer in the change of the plastic and liquid limits. Figure 26 shows that the additives help to increase both limits, but they were only proportional with the amount of lime when the added amount was less than 3%. Above 3% no increase in both consistency limits was observed. Because the two limits had a similar rate of increasing, the Plasticity Index stayed quite constant independent of the type of additives. Figure 26 also shows that the effect on the Atterberg limits of adding different types of ash with the lime was not different from the results of adding lime only.

Figure 25. Clay after mixing with lime and RHA (lime : A-RHA =1).
(a) 1% lime; (b) 2% lime; (c) 3% lime

To evaluate whether the instant reduction in water content, which was observed when clay was mixed with additives was caused by an increase in solid mass only or by a rapid chemical reaction or evaporation during mixing, the water content of the soil before and after mixing were determined in an experiment with C-RHA, which is the most sensitive with calcium hydroxide as observed in the electrical conductivity measurement (section 3.3). As seen in Figure 27, after ten minutes of mixing the water content reduced approximately 2% from its calculated value based on the initial water content and amount of added solid mass. After the mixing was stopped the water content for the soil with the additives stayed constant. For the clay without the additives, the mixing was still continued and the water content kept decreasing with the same rate, which proved that the evaporation during mixing was the main factor causing the change in water amount of the soil. Data of the experiments in this section is presented in appendix 4.

Table 9. Plasticity modification by the additivies

Soil	**W** (%)	**LL** (%)	**PL** (%)	**PI** (%)	**LI**
Clay	48	56	22	34	0.76
Clay + 1% lime	45	75	37	38	0.22
Clay + 2% lime	45	76	44	32	0.04
Clay + 3% lime	46	79	44	36	0.07
Clay + 6% lime	43	80	43	37	-0.01
Clay + 2% lime + 2% C-RHA	43	77	42	35	0.03
Clay + 3% lime + 3% C-RHA	43	77	45	32	-0.06
Clay + 4% lime + 4% C-RHA	43	75	41	34	0.05
Clay + 3% lime + 3% A-RHA	43	78	43	35	0.01
Clay + 1% lime + 1% Cr-RHA	44	-	37	-	-
Clay + 2% lime + 2% Cr-RHA	45	79	43	36	0.05

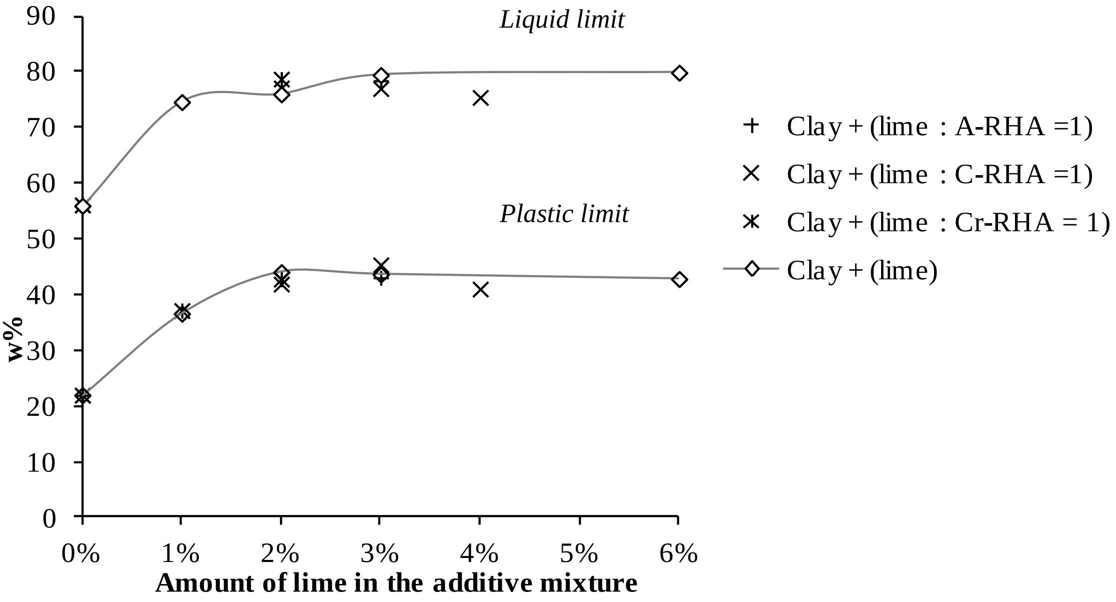

Figure 26. Plasticity modification by the additives

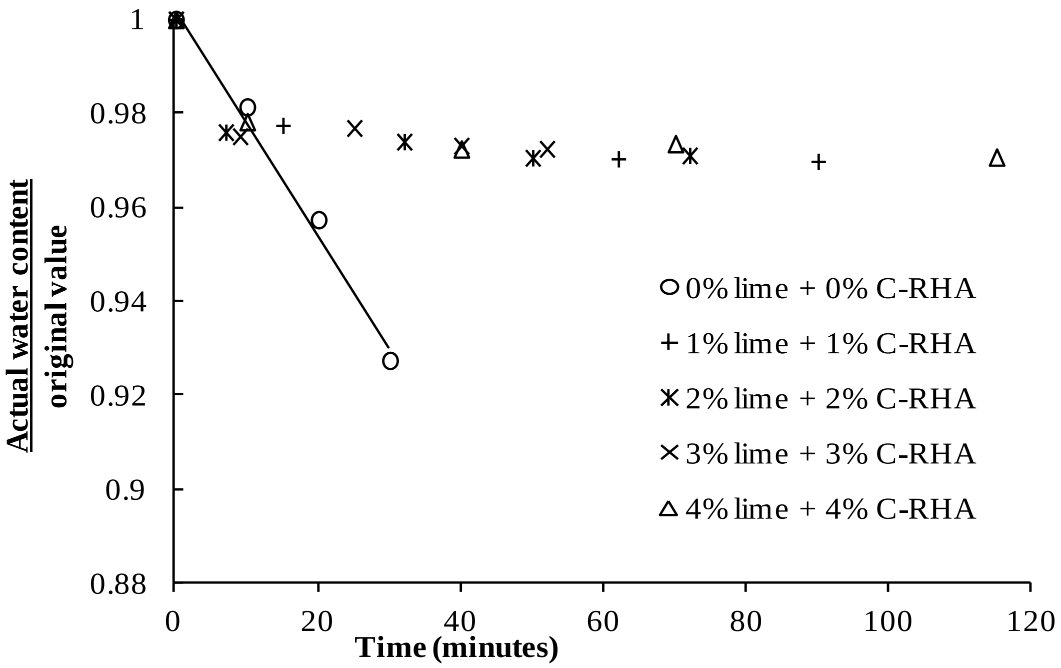

Figure 27. Water content change within the clay mixed with lime and C-RHA

4.3. Undrained shear strength improvement

4.3.1. Method

To evaluate the strength improvement of the clay mixed with the additives the undrained shear strength was measured using the fall cone test according to ISO/TS 17892-6:2004 [56]. In this test the penetration depth of the fall come is measured, which is correlated to the undrained shear strength according to:

$$c_u = cg\frac{m}{i^2}$$

where

c_u	is the undrained shear strength, in kPa;
c	is a constant depending on the state of the soil and the tup angle of the cone. For cone with 30° tip c = 0.8;
g	is the acceleration at free fall. It is 9.81 m/s^2;
m	is the mass of the cone, in g;
i	is the cone penetration, in mm.

The additives were the three types of ash, which are C-RHA, A-RHA, Cr-RHA, in combination with lime in the ratio of one. The amount of the of additives was varied from 1% to 3%. In other words, the amount of (RHA : lime) was 1%:1%, 2%:2%, and 3%:3%. The effectiveness of only lime was also investigated by adding 1%, 2%, 3% and 6% of lime into the clay. This proportion is the mass ratio between the dry additive and the wet clay which had been soaked to the set-up water content. The strength development was observed in one month.

4.3.2. Procedure

The development of the strength was observed in 1 month. The clay mixed with the additives was put in plastic cups and covered by plastic foil wrap. Tight caps were put on top so that evaporation during the time was prevented. For each time of data collecting, at least three measurements were done at different cups and there would be unused cups at the end of the process for the measurements of the later strength. If the difference between the measurements was larger than 1 mm (reading was larger than 10), more measurements were done.

Figure 28. Fall cone test for undrained shear strength identification

4.3.3. Results

Over one month, the undrained shear strength of the mixed clay showed a considerable development. Figure 29 shows the development of the c_u for different amount and types of the additives at the first day, 7th day and 28th day. It is seen from the figure that the strength and the amount of the additives are proportional within the range of the experimented amount of the additives, but the increase rates over time are largely different. As seen in Figure 29a, the strength of the clay mixed with only lime is approximately equal to the strength of the clay mixed with the mixture of lime and rice husk ash in the first day after mixing. After one week, the soil with lime and rice husk ash shows a higher strength than the soil with only lime, and this difference was enlarged over 28 days. The C-RHA expressed the largest improvement. In the Figure 29c the undrained shear strength of the clay mixed with 3% C-RHA and 3% lime after 28 days is about double the strength of the clay mixed with only 3% lime, and is approximately equal to the strength of the clay mixed with 6% lime.

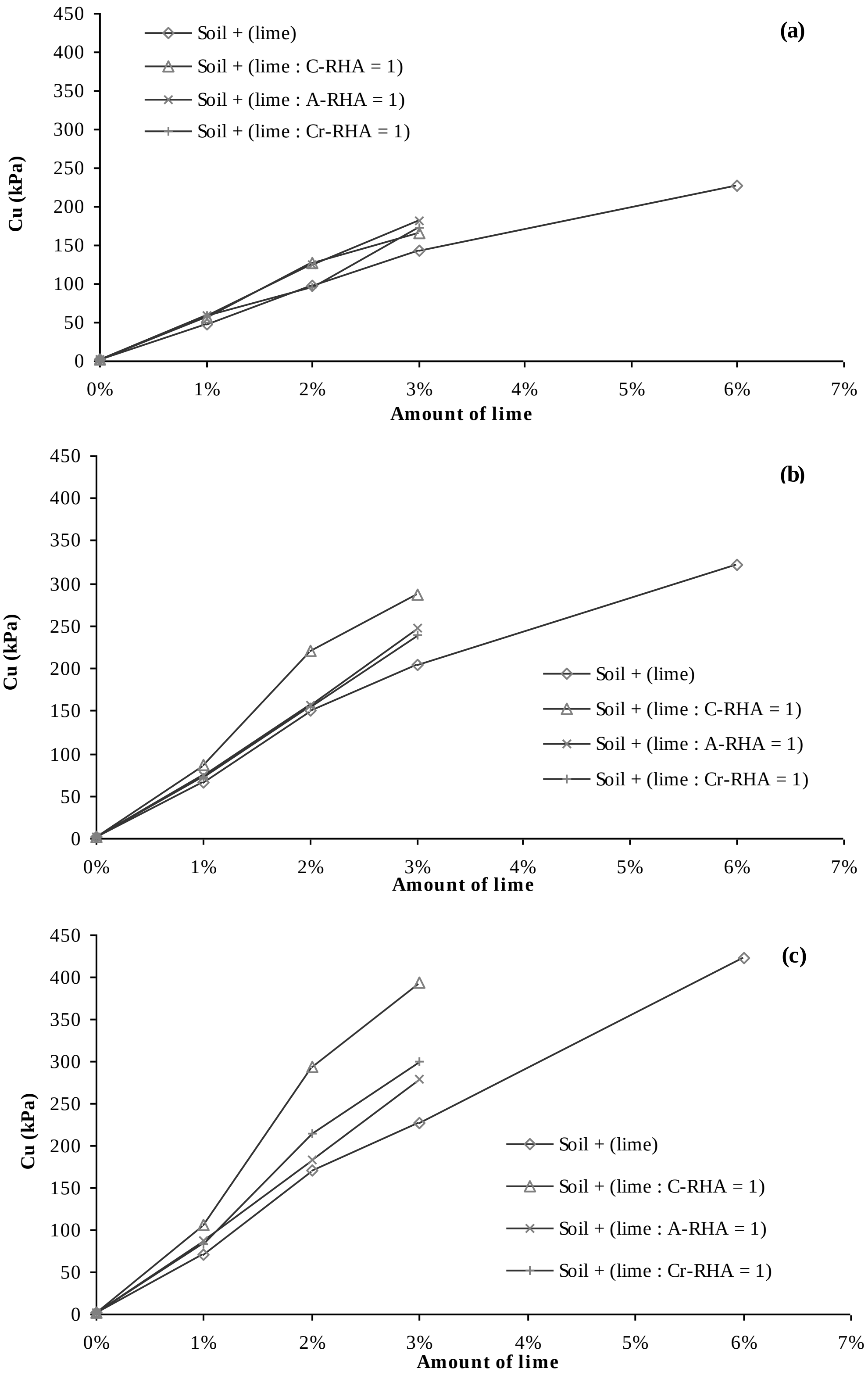

Figure 29. Undrained shear strength at the (a)-1st day, (b)-7th day, (c)-28 day

Strength development over time of the clay mixed with 3% only lime and the mixture of 3% lime with 3% rice husk ash were plotted in Figure 30 for comparison. Result of the case of only 6% lime and only 6% of C-RHA was also plotted in the figure. The clay mixed with only the rice husk ash did not show considerably improvement compared with all the other cases with lime. The largest development of the strength appeared in the first 3 days for almost all the cases except the for the C-RHA case. Comparing the 6% lime with the 3% C-RHA/3% lime mixture, for the clay with lime only about 75% of the strength had already developed within the first week, while for the case of C-RHA the strength developed at a slower pace but continued to develop considerably and approached the strength of the clay mixed with 6% lime after two weeks.

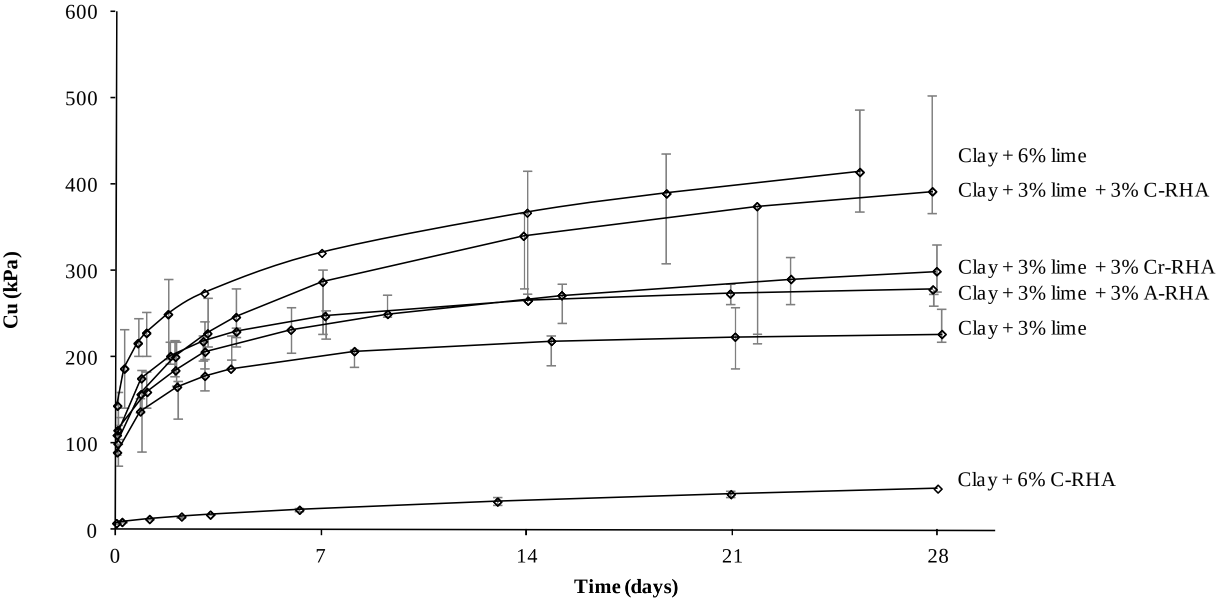

Figure 30. Strength development over time

4.4. *Compressibility and consolidation*

4.4.1. Materials and methods

The effect of mixing additives (lime and rice husk ash) with clay on the compressibility and consolidation behavior was investigated by oedometer tests, which were performed according to the standard ISO/TS 17892-5 [57]. The mass ratio between rice husk ash and lime was kept at 1, and the amount of single additives was 3%. In other words, the considered cases were 3% RHA mixed with 3% lime, then added into the soil. The proportion was the ratio of the additive over the wet soil mass. The case of only lime was implemented with the proportions of 3% and 6% in order to have a reference.

Result from the undrained shear strength development showed that the strength increased largely in the first several days, and the plasticity of the soil was also improved considerably right after mixing, so in the field the clay can be ready for construction immediately after treatment. Accordingly, specimens for the consolidation tests were undertaken with the first load of approximately 35 kPa in 7 days. After that, additional load steps were applied to be approximately double the previous load, which were 70 kPa, 139 kPa, 278 kPa, 557 kPa and 1.1 MPa. Each load step was ended when the end of the primary consolidation period could be observed on the logarithmic time scale by the start of the secondary compression.

4.4.2. Results

By adding the additives, the compressibility of clay was improved considerably as seen in Figure 31. Although the compression index C_c of the soil after treatment was increased in comparison with the value of the original soil as shown in Table 10, the additives created a large apparent pre-consolidation pressure which is about 200 kPa. The additives also helped to decrease the reloading compression index Cr by a half as seen in Table 10.

In the second loading, a very small settlement was recorded in all the cases of treated soil as shown in the Figure 32. Detail data is shown in appendix 6.

Table 10. Effect of the different additives to the compressibility parameters

Soil	**σ'_p** (kPa)	**C_c** -	**C_r** -	**σ'** (kPa)	**t_{50}** (s)	**C_v** (m2/year)	**C_α** $\times 10^{-3}$
Clay	17.1	0.373	0.036	34.91	2225	0.225	5.83
				64.48	1711	0.270	-
				123.69	1472	0.282	4.25
Clay + 3% lime	200.0	0.412	0.019	278.40	77	6.527	1.616
				557.29	68	6.634	2.102
				1104.45	67	5.861	2.164
Clay + 3% lime + 3% A-RHA	172.2	0.419	0.020	277.08	98	5.084	1.487
				555.96	79	5.676	1.949
				1103.13	78	5.026	1.680
Clay + 3% lime + 3% C-RHA	215.8	0.441	0.018	275.75	73	7.031	1.985
				554.64	75	6.186	1.893
				1101.80	67	6.034	2.153
Clay + 3% lime + 3% Cr-RHA	216.3	0.422	0.019	276.42	86	5.907	1.413
				550.00	68	6.775	1.952
				1097.17	61	6.615	2.164
Clay + 6% lime	232.5	0.407	0.014	278.59	77	6.727	1.256
				554.38	66	7.156	1.782
				1105.96	62	6.728	2.125

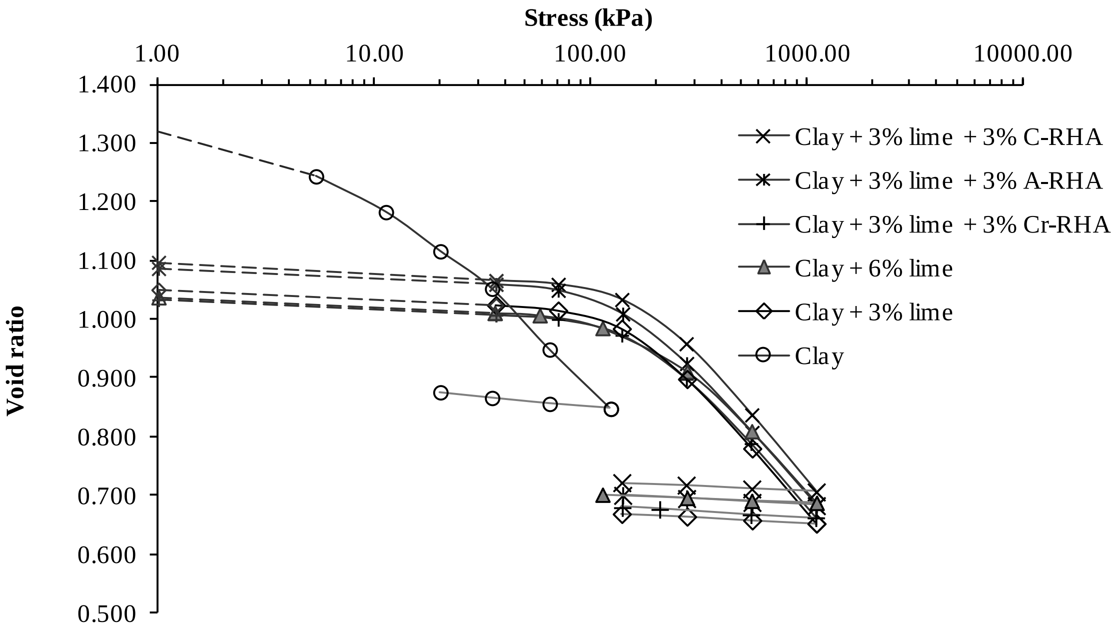

Figure 31. Effect of the different additives to the deformation behavior of the soil

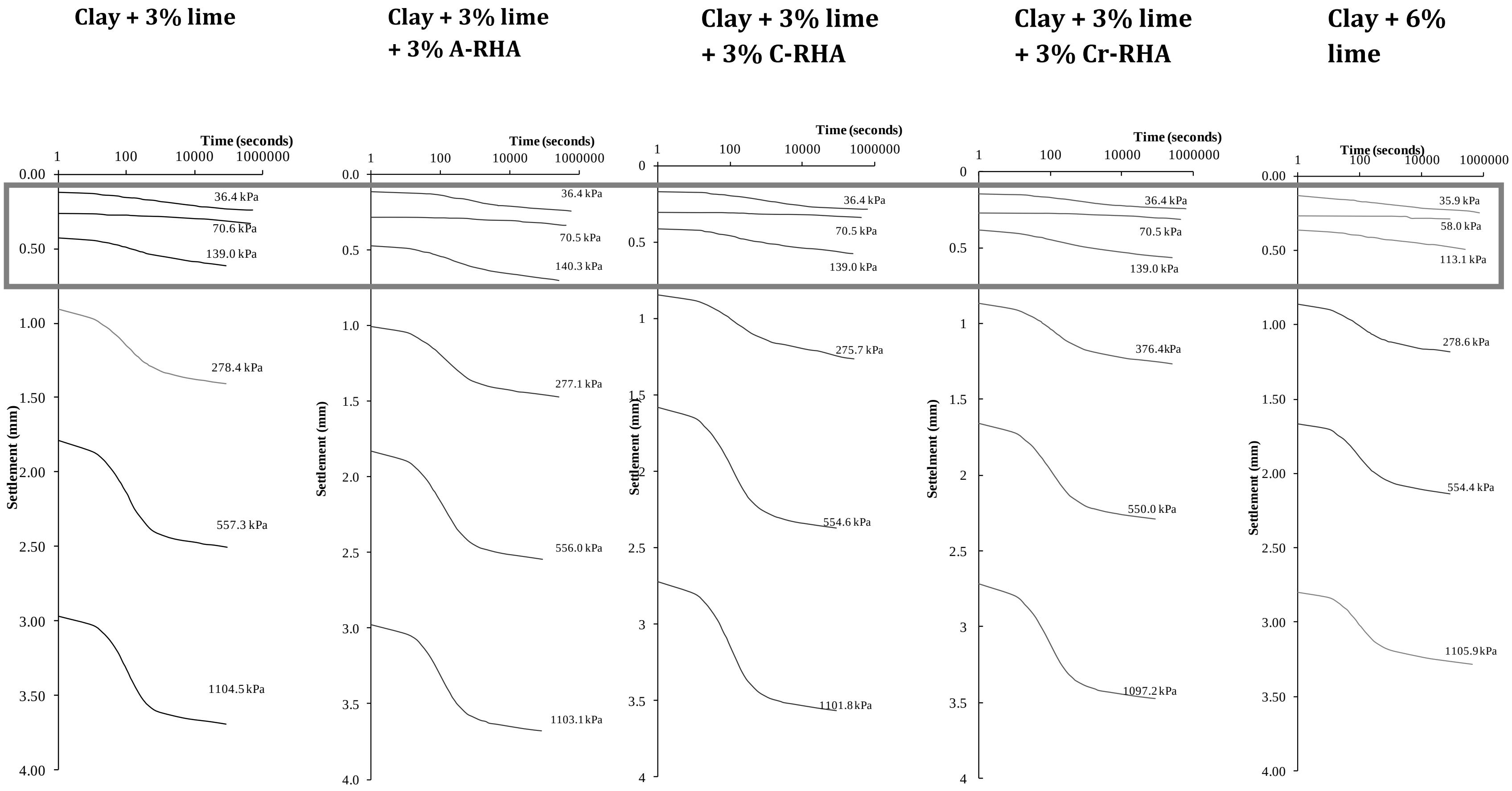

Figure 32. Time-settlement curves for the consolidation experiment

Table 11. Soil improvement

Parameters			Clay	Clay + 3% lime	Clay + 3% lime + 3% A-RHA	Clay + 3% lime + 3% C-RHA	Clay + 3% lime + 3% Cr-RHA	Clay + 6% lime
Atterberg limits	**Water content**	%	48	46	43	43	-	43
	Plastic limit	%	22	44	43	45	-	43
	Liquid limit	%	56	79	78	77	-	80
	Plastic index	%	34	35	35	32	-	37
	Liquidity index	-	0.76	0.06	0.00	-0.06	-	0.00
Undrained shear strength at 28th date		(kPa)	3.0	227.1	278.9	393.0	300.0	423.5
Consolidation	**Pre-consolidation stress**	(kPa)	17.1	200.0	172.2	215.8	216.3	232.5
	Compression Index	-	0.373	0.412	0.419	0.441	0.422	0.407
	Reloading compression index	-	0.036	0.019	0.020	0.018	0.019	0.014
	Consolidation coefficient	(m^2/yr)	0.282	5.861	5.026	6.034	6.615	6.728
	Secondary consolidation coefficient	($\times 10^{-3}$)	4.25	2.164	1.680	2.153	2.164	2.125

4.5. Effect of the rice husk ash in clay improvement evaluation

The clay treated with lime and the mixture of lime and rice husk ash was investigated in terms of the plasticity, strength and consolidation. It was seen that all the additives helped to improve the soil considerably, and there is difference in the effect of the different additives. Table 11 is the generalization of the results.

4.5.1. Immediate effects

The additives helped to improved considerably and almost immediately the plasticity of the soil as described in the section 4.2. After mixing, the soil from almost being liquid changed to be dry and formed agglomeration as seen in the Figure 25, and this is the result of the sharp reduction of the Liquid index as shown in Table 9. The effect of lime to the river clay used in these experiments seen in the Figure 26 is different with its effect to the London clay seen in the Figure 4 (Sherwood 1993) in term of Liquid limit, and this is highly because of the variation the soil properties due to the different regions; but they both show a large and smooth increase of the Plastic limit. In these experiments, this Attenberg limits were brought close to the water content of the treated soil. If evaluating the engineering properties of the treated clay by the Liquidity Index, the soil can be considered to be good as this parameter is close to zero, corresponding to a state of semi-plastic solid.

Nevertheless, this immediate effect is confirmed to be the result of lime only, and the rice husk ash did not show any influence as seen in Figure 26. Even though with C-RHA, the ash type appeared to be the most active in the experiment with calcium hydroxide solution as described in section 3.3, its results in this experiment is also not visible. This derives that the pozzolanic reaction if occurring in the soil would be a gradual process and need a certain time to strengthen the soil to the ultimate strength.

4.5.2. Long-term effects

The development of the undrained shear strength of the treated clay described in the section 4.3 has confirmed the occurrence of some reactions. In this case it is supposed to be the pozzolanic reaction and the hardening process of the calcium silica hydrate in the treated clay. In Figure 29a, the strength of the all the cases did not show a considerable difference in the first day; in other words this is the confirmation of the immediate effect of the lime. Along with time, the gap between the cases was enlarged, and the remark was seen with the C-RHA as it showed the largest improvement. This is consistent with the result of the electrical conductivity variation in section 3.3, as the C-RHA showed the highest activity with calcium hydroxide. In the other hand, using only C-RHA did not show a considerable effect compared with the other cases with lime, and it confirms that the rice husk ash needs a primary reagent such as lime to be activated.

The carbon content might have a considerably hindrance to the formation of the cementious matrix in a concrete mass, because it can easily absorb on the surface of the aggregates whose size is much larger than the ash particle. But in the clay where the particle is in an approximately equal size, then might the negative effect of the carbon content was much less considerable as the rice husk ash particle can be not only the cementation reagent but also the aggregates. In this way a large amount of the carbon might not a serious problem. Besides, for soil treatment the required strength is much less than that of the cement or concrete mass, hence, effort of eliminating completely the carbon in the rice husk ash is not necessary. In the other hand, considerable amount of quartz can even bring the benefit to the soil thanks to its firmness.

In overall, using the rice husk ash in lime treatment helps to increase the strength of the soil considerably, especially with the type of C-RHA. Replacing half the amount of lime by this ash type still can improve the soil to an approximately equal strength, although it takes a longer time which is about 2 weeks. Because the C-RHA is the most active with the lime, its most positive effect is consistent with the explanation of the calcium silica hydrate hardening from the pozzolanic reaction.

There might be a question that if just a small amount of the naturally amorphous silica can be very active then is it necessary to burn the rice husk. Indeed the burning is still required to transfer the rice husk to ash so that the reaction with the lime would be the most effective. Another disadvantage if using only the rice husk is that this is a very bulk material, and the decay of the organic component in the rice husk after construction might cause large deformation.

4.5.3. Compressibility and consolidation behaviour

Similarly to the undrained shear strength, deformation of the treated clay was improved considerably although the differences between the cases are not large. If the additives are the results of this difference, not the certain factors of experiment work, then the C-RHA is still the type which gave the most positive result, as seen in Figure 31.

The small settlement in the second load step is the confirmation of the hardening process happening in the soil due to the additives. The specimens were left under the first load in about one week, which is approximate with the time that the strength developed to about 75% of its final value as seen in Figure 30, and in the second load step, all the treated clay appeared to be much stiffer than its initial state, shown by a small coefficient of volume compressibility. Figure 32 shows a neglected settlement in this load step for all the cases, and it derives a developed cementious matrix within the soil mass. This firmness was not remained during the following load steps, and this expresses that the third load step has exceeded the capacity of the newly formed matrix.

In the experiment, the waiting time for the first load step was chosen to be one week, and the result show that the strength of the cementious matrix appeared not to fully developed, as the capacity was exceeded at the third load step. This leads to a curiosity about the optimized waiting time, as it is not worthy to wait for the completed development of strength because the calcium silicate hydrate still keeps hardening during the loading process, but it also needs a sufficient time for the newly cementious matrix to obtain a certain strength and stiffness so that the hardening process would not deteriorate due to the process of loading.

5. Conclusion

The most positive results in soil improvement of the C-RHA is consistent with its highest reactivity, and it confirms that a small amount of “highly” amorphous silica can be very valuable, and the burning process should be only useful in eliminating the organic content of the rice husk. The burning condition which was suggested to be successful in completely consuming the organic content while remaining the silica in the amorphous state, which was used to produce the A-RHA, unfortunately has still affected the activity of the silica although this silica was seen to be still amorphous. Between the two cases, the quick burning process which does not effectively eliminate the carbon content and even causes the crystallization locally but considerably less effect the rest of the amorphous silica, and the controlled burning process which completely eliminates the carbon but also negatively affect the activity, the product of the former condition is still highly more reactive. Accordingly this is the preferred condition to obtain a highly reactive rice husk ash.

In the clay, rice husk ash even at low reactive level still has a considerably positive effect to the soil, so it confirms the promising utilization in soil treatment which has been raised by different authors previously. The C-RHA which was identified to be the most reactive gave the most positive improvement, while the large carbon content is supposed not to be a serious problem, so the quick and open-air burning to produce this ash type is the preferred alternative for soil improvement purposes. This burning process also has the advantage of less consumed energy, and it can enlarge the opportunities of rice husk ash utilization in geo technology.

The range of the strength and the deformity improvement of the clay were seen not to be extremely high if it is compared with the expectation of a strong foundation for large loads, but together with the immediate effect of improving the plasticity of the soil, this is sufficient with the infrastructure construction such as road or dykes and levees constructions. This soil improvement method can promote all its advantage in the area where the soil lacks of the active silica in its component and only lime treatment is not sufficient.

From this research, the rice husk ash production for soil improvement was found out not to be necessarily strict. This is the start point for the application of the rice husk ash with other soil types than clay and peat is a challenge. A completed investigation about the effect of rice husk ash to different soil types, the range of improvement and the optimum mixing ratios for each soil types are interesting topics and can be useful in practical. Investigation of rice husk and the role of the carbon to the reactivity are also recommended in order to completely understand the material.

REFERENCE

1. NEN, *Identification and classification of soil - Part 2: Principle for a classification (ISO 14688-2:2004)*, in *Geotechnical investigation and testing*2004, European Committee for Standardization.
2. NEN, *NEN 6740 - Basic requirements and loads*, in *Geotechnics*2006, Nederlands Normalisatie-instituut.
3. Walker, J.D. and J.W. Geissman, *2009 Geologic Time Scale*, timescl, Editor 2009, The Geological Society of America.
4. *Report of population and accommodation April 1st 2009*, 2009, Central Committee of Overall Investigation of Population and Accommodation (Vietnamses).
5. *Into Dutch soils*, E.a.S. Planning, Editor April 2010, Ministerie van VROM.
6. *Mekong Delta*. June 17th 2012]; Source: Le Dien Duc and reference]. Available from: http://www.arcbc.org.ph/wetlands/vietnam/vnm_mekdel.htm.
7. Nguyễn, H.P., *Research and establish the map of soft soil regions to apply for long term development of Hanoi capital*, 2002, University of Mining and Geology: Hanoi.
8. Ohtsubo, M., T. Higashi, and M. Kanayama, *Depositional geochemistry and geotechnical properties of marine clays in the Ariake Bay area, Japan*, in *Characterization and Engineering Properties of Natural Soils*, K.K. Phoon, et al., Editors. 2006, Taylor & Francis.
9. Barends, F., *Introduction to Soft Soil Geotechnique, Content, Context and Application*2011, Amsterdam, Netherlands: IOS Press.
10. Bell, F.G., *Engineering Treatment of Soil*1993, London: E&FN SPON.
11. Sherwood, P., *Soil Stabilization with Cement and Lime*1993, London, UK: HMSO.
12. Swamy, R.N., ed. *Cement Replacement Materials*. Concrete Technology and Design, ed. R.N. Swamy. Vol. 3. 1987, Surrey University Press: London.
13. Sánches-Moral, S., et al., *Lime pozzolana mortars in Roman catacombs: composition, structure and restoration.* Cement and Concrete Research, 2005. **35**: p. 11.
14. Nguyen, V.N., *Rice production, consumption and nutrition*, in *FAO Rice Information*2002: Rome.
15. FAOSTAT. *Production / Crops*. 2010 22 Jul 2011]; Available from: http://faostat.fao.org/site/567/default.aspx#ancor.
16. Wen-Hwei Hsu and B.S. Luh, *Rice Hulls*, in *Rice: Production and Utilization*, B.S. Luh, Editor 1979, Avi Publishing Company: Connecticut. p. 736-763.
17. Catelin, M., *2010 Survey of Energy Resources - Coal*, 2010, World Energy Council.
18. REFUEL. *Intelligent Energy Europe*. 16 Feb 2012]; Available from: http://www.refuel.eu/biofuels/.
19. EU. *Renewable energy*. 16 Feb 2012]; Available from: http://ec.europa.eu/energy/renewables/targets_en.htm.
20. REFUEL, *Eyes on the track, mind on the horizon*, 2008.
21. PÖNER. *Rice husk Technology*. 22 Jul 2011]; Available from: http://www.poerner.at/fileadmin/user_upload/pdf/Brochure_Grimma_Rice_Husk_090615_web_e.pdf.
22. UNIDO, *Rice Husk Ash Cements: their development and application*1984, Vienna.
23. Malhotra, V.M. and P.K. Mehta, eds. *Pozzolanic and Cementitious Materials*. Advances in Concrete Technology, ed. V.M. Malhotra. Vol. 1. 1996, Gordon and Breach Publishers: Ontario, Canada.

24. Alexander, G.B., W.M. Heston, and R.K. Iler, *The Solubility of Amorphous Silica in Water.* Journal of Physics and Chemistry, 1954. **58**(6): p. 453-455.
25. Iler, R.K., *Chapter 1. The Occurrence, Dissolution, and Deposition of Silica*, in *The Chemistry of Silica: Solubility, Polymerization, Colloid and Surface Properties, and Biochemistry*1979, A Wiley-Interscience Publication.
26. Iler, R.K., *Chapter 7. Silica in Biology*, in *The Chemistry of Silica: Solubility, Polymerization, Colloid and Surface Properties, and Biochemistry*1979, A Wiley-Interscience Publication.
27. Whittenberger, R.T., *Silicon absorption by rye and sundflower.* American Journal of Botany, 1945. **32**(9): p. 539-549.
28. Handreckk, K.A. and H.P. Jones, *Studies of silica in the oat plant - IV. Silica content of plant parts in relation to stage of growth, supply of silica, and transpiration.* Plant and Soil, 1968. **29**(3): p. 449-459.
29. Krishnarao, R.V. and M.M. Godkhindi, *Distribution of silica in rice husk and its effects on the formation of silicon carbide.* Ceramics International, 1992. **18**(4): p. 243-249.
30. Nair, D.G., et al., *A structural investigation relating to the pozzolanic activity of rice husk ashes.* Cement and Concrete Research, 2008. **38**: p. 861-869.
31. Chopra, S.K., S.C. Ahluwalia, and S. Laxmi, *Technology and manufacture of rice husk ash masonry cement*, in *Third Workshop on Rice husk ash cement*1981, ESCAP/RCTT: New Delhi, India.
32. Mehta, P.K., *Properties of blended cements made from rice husk ash.* J. American Concrete Institute, 1977. **74**: p. 440-442.
33. Yeoh, A.K., et al., *The relationship between temperature and duration of burning of rice husk in the development of amorphous rice husk ash silica*, in *Follow-up meeting on Rice husk ash cement*1979, Proc. UNIDO/ESCAP/RCTT: Alor Setar, Malaysia.
34. Muthadhi, A. and S. Kothandaraman, *Optimum production conditions for reactive rice husk ash.* Materials and Structures, 2010(43): p. 1303-1315.
35. *Quadrasorb^{TM} SI - Surface Area and Pore Size Analyzer*, 2012, Quantachrome Instruments.
36. Cordeiro, G.C., et al., *Influence of particel size and specific surface area on the pozzolanic activity of residual rice husk ash.* Cement and Concrete Composites, 2011. **33**: p. 529-534.
37. Wirth, K., M. College, and A. Barth. *X-ray Fluorescence (XRF)*. May 29, 2012; Geochemical Instrumentation and Analysis:[Available from: http://serc.carleton.edu/research_education/geochemsheets/techniques/XRF.html.
38. Dutrow, B.L. *X-ray powder Diffraction*. June 14, 2012; Geochemical Instrumentation and Analysis:[Available from: http://serc.carleton.edu/research_education/geochemsheets/techniques/XRD.html.
39. Donatello, S., M. Tyrer, and C.R. Cheeseman, *Comparison of test methods to assess pozzolanic activity.* Cement and Concrete Composites, 2010. **32**: p. 7.
40. Luxán, M.P., F. Madruga, and J. Saavedra, *Rapid evaluation of pozzolanic activity of natural products by conductivity measurement.* Cement and Concrete Research, 1989. **19**(63-68).
41. Walker, R. and S. Pavía, *Physical properties and reactivity of pozzolans, and their influence on the properties of lime-pozzolan pastes.* Materials and Structures, 2011. **44**: p. 1139-1150.
42. Agarwal, S.K., *Pozzolanic activity of various siliceous materials.* Cement and Concrete Research, 2004. **36**: p. 5.
43. Basha, E.A., et al., *Stabilization of residual soil with rice husk ash and cement.* Construction and Building Materials, 2005. **19**: p. 448-453.
44. A. Seco, et al., *Stabilization of expansive soils for use in construction.* Applied Clay Science, 2011. **51**: p. 348-352.

45. Brooks, R.M., *Soil stabilization with fly ash and rice husk ash.* International Journal of Research and Reviews in Applied Science, 2009. **1**(3): p. 209-217.
46. Radhey S. Sharma, B.R. Phanikumar, and B.V. Rao, *Engineering behaviour of a Remolded Expansive Clay Blended with Lime, Calcium Choloride, and Rice Husk Ash.* Journal of Materials in Civil Engineering, 2008. **20**(8): p. 509.
47. Muntohar, A.S., *Utiliization of uncontrolled burnt rice husk ash in soil improvement.* Dimensi Teknik Sipil, 2002. **4**(2): p. 100-105.
48. Muntohar, A.S., *Swelling characteristics and improvment of expansive soil with rice husk ash*, in *Expansive soil: Recent advances in characterization and treatment*, Amer Ali Al-Rawas and M.F.A. Goosen, Editors. 2006, Taylor & Francis/Balkema. p. 435-452.
49. A.J. Choobbasti, et al., *Influence of using rice husk ash in soil stabilization method with lime.* Frontier of Earth Science. China, 2010. **4**(4): p. 471-480.
50. Alhassan, M., *Permeability of Lateritic Soil Treated with Lime and Rice Husk Ash.* AU Journal of Technology, 2008. **12**(2): p. 115-120.
51. Muntohar, A.S., *The influence of molding water content and lime content on the strength of stabilized soil with lime and rice husk ash.* Civil Engineering Dimension, 2005. **7**(1): p. 1-5.
52. Ali, F.H., A. Adnan, and C.K. Choy, *Geotechnical properties of chemically stabilized soil from Malaysia with rice husk ash as an additive.* Geotechnical and Geological Engineering, 1992. **10**: p. 117-137.
53. Babrauskas, V. *Temperatures in flames and fires*. 2006; Available from: http://www.doctorfire.com/flametmp.html.
54. BSI, *BS 1377-2:1990*, in *Methods of test for soils for civil engineering purposes*1990.
55. BSI, *BS 5930:1999 Code of practice for site investigation*, 1999.
56. CEN, *Geotechnical investigation and testing - Laboratory testing of soil - Part 6: Fall cone test*, 2004.
57. CEN, *ISO/TS 17892-5 Incremental loading oedermeter test*, in *Geotechnical investigation and testing - Laboratory testong of soil*2004.

APPENDIXES

APPENDIX 1 - Comparison of cement and the mixture of lime and rice husk ash by simple Life Cycle Inventory analysis

APPENDIX 2 - RHA parameters

APPENDIX 3 - Electrical conductivity and pH

APPENDIX 4 - Plasticity modification

APPENDIX 5 - cu development

APPENDIX 6 – Deformity modification

APPENDIX 1 - Comparison of cement and the mixture of lime and rice husk ash by simple Life Cycle Inventory analysis

APPENDIX 1 - Comparison of cement and the mixture of lime and rice husk ash by simple Life Cycle Inventory analysis

A1.1. Portland cement and lime-rice husk ash cement

Between lime and cement, lime-pozzolana cement is discovered to appear since the 2nd century AD in Roman catacombs [13] while ordinary Portland cement has just been used widely for the last century. It is the slow rate of hardening of the lime-pozzolana mixes that makes this system be lagged behind the Portland cement [53] . At the time the Portland cement appeared, it dominated the construction field and contributes to the global industrialization. However, the environment and energy problems coming from the cement industry requires a redirection for a sustainable development, leading to a huge investment to cement replacement materials and increasing the interest for the lime-pozzolana mixes.

Among different cement replacement materials, rice husk ash is known to be the environmental friendly option for the sustainable construction. This is because its origin is agricultural residues, so CO_2 produced by burning rice husk is equal to the consumed amount during the plant life. In other words, rice husk ash is CO_2 neutral, and its utilization can help to significantly reduce the emission and consumed energy in cement and lime production.

Lime and cement do not show a large difference in the cost aspect but they have a considerable gap in term of energy used. In the database of the Ecoinvent Centre, 1 kg of clinker consumes 3.62 MJ while the same weight of hydrated lime consumes 0.14 MJ [54]. In soil stabilization particularly, the mixture of lime and rice husk ash has seen to be able to give a similar result with cement, then choosing the mixture can give an optimistic effect to the environment and energy status. A simple Life Cycle Inventory analysis will be implemented in this section to quantitatively compare the two systems.

A1.2. Method

Life Cycle Analysis is a useful method to evaluate the interaction of a specific product with environment during its life cycle by an objective and comprehensive judgment. An appropriate functional unit is very important in this type analysis. In the field of soil stabilization, the functional unit is related to the ability of different amount of materials for strength improvement of 1 unit of soil.

Among different research done about the effect of cement and the mixture of lime and rice husk ash in soil stabilization, the work of two independent researcher with the soil having similar properties are chosen for the input of the analysis. This is the work of Sariosseiri and Muhunthan, 2009 [55] and Musa Alhassan, 2008 [33] with the additives of cement and the mixture of lime and rice husk ash, respectively. Properties of the soil are shown in Table A1. The result of the research showed that to increase the Unconfined compressive strength of the soil from 295 kPa to 1900 kPa, the required amount of cement was 4.3% as seen in the work of Sariosseiri and Muhunthan, while a mixture of 6% rice husk ash and 8% lime was needed in the work of Musa Alhassan.

Table A1.Soil used for the comparision

Parameters		**Deposit in Palous [55]**	**Laterite soil in Minna [33]**
Liquid Limit		33.1 %	45.51 %
Plastic Limit		19.6 %	25.35 %
Plasticity Index		13.6 %	20.16 %
Maximum dry density	(kN/m^3)	17.3	18.1
Optimum moisture content		17 %	15.5 %
Unconfined Compressive Strength	(KN/m^2)	294.3	295

So the Life Cycle Inventory analysis was implemented with:

- Functional unit: improving the Unconfined Compressive Strength of 1 ton of soil from 295 kPa to 1900 kPa.
- Considered systems: 43 kg of CEM I and 140 kg of the mixture in which there are 80 kg of lime and 60 kg of rice husk ash.
- Boundary of the analysis: the systems are set from secondary raw materials to the final additives.

Detail calculation for the material flow charts and the emission of the systems was based on the data of the Ecoinvent Centre [54].

A1.3. Life Cycle Inventory analysis for the two systems

a) System of CEM I 42.5

From the Ecoinvent Centre, the main components of CEM I 42.5 is 90% of clinker, 5.2% of gypsum and 4.5% of limestone. Consequently, 43 kg of the cement needs 38.83 kg of clinker, 2.24 kg of gypsum and 1.94 kg limestone.

Limestone also holds the large part in clinker production, as 100kg of clinker needs 84.1 kg of limestone. And it is the source for hydrated lime which hold 0.392% of the clinker mass, so in total the required amount of limestone for 43 kg of cement is 34.79 kg. Other materials needed for the required amount of clinker is shown in Table A2 and they are put into the material flow diagram as seen in Figure A1.

Table A2. Mass of component for clinker

	Bauxite (kg)	**Hydrated lime** (kg)	**Limestone** (kg)	**Calcarous marl** (kg)	**Sand** (kg)	**Clay** (kg)
For 100kg of clinker	0.012	0.392	84.1	46.6	0.926	33.1
For 38.83 kg of clinker	0.005	0.152	32.65	18.09	0.36	12.85

Major emissions from cement production are the particulate emission which relates to blending process of the raw materials, the CO_2 emission which relates to the incineration of the limestone in the mixture, and the consumed energy for the blending and the combustion of the mixture. So the analysis was based on these parameters and was derived from the data of the Ecoinvent Centre as seen in Table A3.

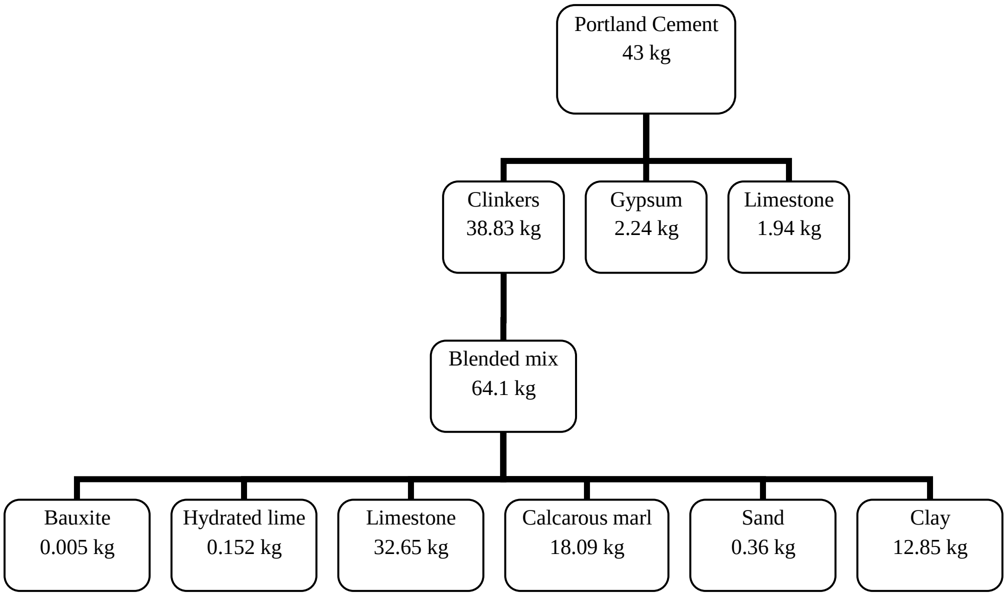

Figure A1. Flow diagram for production of 43 kg cement

b) System of lime and rice husk ash mixture

Similar calculation was implemented for the mixture of 80 kg of hydrated lime and 60 kg of rice husk ash. For hydrated lime, 1 kg of this material needs 0.769 kg of quick lime CaO, and 1 kg of quick lime needs 1.73 kg of limestone, so in total 106.43 kg of limestone is needed for the system. For rice husk ash, it accounts for about 20% or rice husk mass [22], so 60kg of rice husk ash can be collected from 300kg of rice husk. The material flow can be seen in Figure A2.

Emission of the production was calculated in Table A4. For the rice husk ash, the dust emission was assumed to be similar with the clinker production because there is not explicit date for this material. Due to its exothermic property, the consumed energy for the rice husk ash burning was neglected, so main emission from the rice husk ash was the dust.

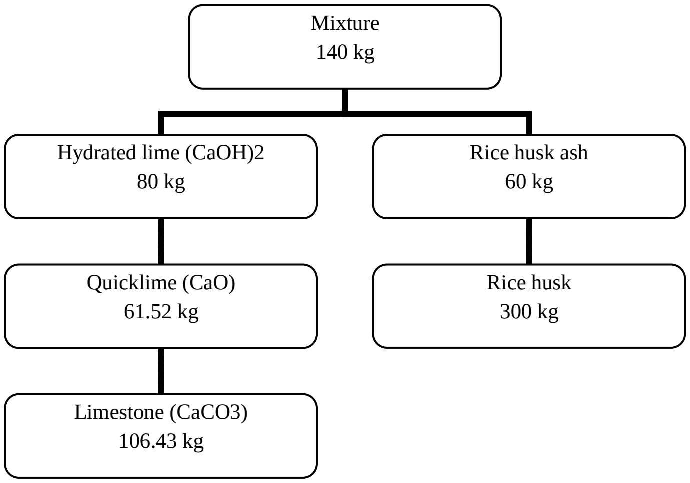

Figure A2. Flow diagram for production of the mixture of 80 kg lime and 60 kg RHA

A1.4. Comment on the result

The calculation shows that the production of the 43 kg cement consumes 140.5 MJ and releases 24.6 kg of CO2, while 140kg of the mixture consumes 9.4 MJ and releases 55.2 kg of CO2. In term of CO2 emission, the threaten from cement production is interestingly a half of the mixture production, but in term of consumed energy the cement production consumes 15 times of the mixture. The larger amount of released CO_2 from the rice husk ash – lime cement is due to the fact that more lime is needed in order to give a similar effectiveness. Nevertheless, the cement production consumes a huge amount of energy that the total amount still much higher than the lime based cement.

In conclusion, the mixture of lime and rice husk ash does not offer an interesting solution for the problem of CO_2 emission of cement production industry, but it has an optimistic ability for the industrial energy consumption. Final conclusion about the comparison needs a complete Life Cycle Analysis, but in such a crisis of energy in the present this advantage promises an attractive solution.

Table A3. ***Emission from production of 43 kg CEM I 42.5***

Out put	Remarks		Gypsum for		Clinker for		Limestone for		Total
		[kg]	0.65 kg*	2.236 kg	1kg*	38.83 kg	0.507 kg*	34.79 kg	
Waste heat	Same amount as electricity used	[MJ]	0.0033	0.011	3.620	140.561			140.572
Dust to air	particulate <2.5 µm	[53]	0.008	0.028	0.024	0.936	0.008	0.549	1.512
	particulate >2.5 µm and < 10 µm	[g]	0.04	0.138	0.008	0.308	0.040	2.745	3.190
	particulate >10 µm	[g]	0.112	0.385	0.006	0.220	0.112	7.686	8.291
CO2	from combustion of waste	[kg]			0.090	3.479			24.563
	from minerals	[kg]			0.543	21.084			

Table A4. Emission from production of 80 kg hydrated lime and 60 kg RHA for the mixture

Out put	Remarks		Limestone		quick lime		Hydrated lime		RHA		Total
		[kg]	0.507 kg*	106.43 kg	1 kg*	61.52 kg	1 kg*	80 kg	1 kg*	60 kg	
Waste heat	Same amount as electricity used	[MJ]			0.094	5.77	0.046	3.66			9.43
Dust to air	particulate <2.5µm	[g]	0.008	1.68	0.0136	0.84			0.024	1.45	3.96
	particulate >2.5µm and < 10µm	[g]	0.040	8.40	0.0273	1.68			0.008	0.48	10.55
	particulate >10µm	[g]	0.112	23.51	0.0273	1.68			0.006	0.34	25.53
CO2	from combustion of waste	[kg]			0.909	55.92					55.92

* Data from Ecoinvent Centre

APPENDIX 2 - RHA parameters

APPENDIX 2 - RHA parameters

A2.1. Particle density

A-RHA

Solid (g)			1.58	0.68	1.19	1.25	1.12	1.24	1.25	1.23	1.23	1.3
Bottle+liquid (g)			78.05	38.56	41.72	37.68	36.98	41.74	38.55	41.3	37.7	36.99
M'(total) (g)			78.98	38.95	42.49	38.46	37.72	42.5	39.31	42.08	38.47	37.79
Solid volume (cm^3)			0.824	0.368	0.532	0.596	0.482	0.608	0.621	0.570	0.583	0.634
Density	Mean	2.08	1.918	1.850	2.236	2.098	2.325	2.038	2.013	2.157	2.110	2.051
(g/cm^3)	Deviation of the mean	0.04										
	95% confidence interval	0.09										

Cr-RHA

Solid (g)			0.96	1.01	0.97	1.01	1.08	1.08	0.96	1.05	0.97	1.04
Bottle+liquid (g)			38.58	37.04	37.69	41.32	41.73	37.69	38.59	37.02	41.77	41.28
M'(total)	(g)		39.16	37.65	38.3	41.9	42.42	38.37	39.17	37.65	42.32	41.98
Solid volume (cm^3)			0.482	0.507	0.456	0.545	0.494	0.507	0.482	0.532	0.532	0.431
Density	Mean	2.05	1.993	1.992	2.126	1.853	2.185	2.130	1.993	1.972	1.822	2.413
(g/cm^3)	Deviation of the mean	0.06										
	95% confidence interval	0.11										

C-RHA

Solid (g)			1.13	1.19	1.12	1.04	1.2	1.06	1.47	1.5	1.48
Bottle+liquid (g)			37.04	41.31	37.71	38.57	41.77	37.04	41.33	37.71	38.61
M'(total)	(cm^3)		37.61	41.95	38.31	39.16	42.41	37.61	42.16	38.48	39.42
Solid volume (g)			0.710	0.697	0.659	0.570	0.710	0.621	0.811	0.925	0.849
Density	Mean	1.71	1.592	1.707	1.699	1.823	1.691	1.707	1.812	1.621	1.743
(g/cm^3)	Deviation of the mean	0.03									
	95% confidence interval	0.05									

A2.2. Elemenent Analysis

XRF results **24-May-12** **Instrument:** **Epsilon 3XL Panalytical Recycling Lab**

sample 1	A-RHA
sample 2	Cr-RHA
sample 3	C. RHA

normalised

sample 1		pellet
Compound	Conc	Unit
SiO2	94.525	%
K2O	2.18	%
CaO	0.883	%
Al2O3	0.612	%
P2O5	0.552	%
MgO	0.45	%
SO3	0.366	%
Fe2O3	0.16	%
MnO	0.126	%
ZnO	0.047	%
NiO	0.021	%
SnO2	0.02	%
CuO	0.018	%
Cl	0.017	%
PbO	0.01	%
TiO2	0.009	%
Cr2O3	0.003	%
As2O3	0.001	%
sum	100	

normalised

sample 2		pellet
Compound	Conc	Unit
SiO2	94.204	%
K2O	2.104	%
CaO	0.931	%
SO3	0.629	%
Al2O3	0.624	%
P2O5	0.597	%
MgO	0.439	%
Fe2O3	0.21	%
MnO	0.133	%
NiO	0.032	%
ZnO	0.029	%
CuO	0.02	%
SnO2	0.02	%
Cl	0.011	%
TiO2	0.011	%
Cr2O3	0.004	%
PbO	0.002	%
As2O3	0.001	%
sum	100.001	

not normalised

sample 3		pellet
Compound	Conc	Unit
SiO2	54.914	%
K2O	1.174	%
Al2O3	0.876	%
CaO	0.858	%
P2O5	0.557	%
SO3	0.474	%
Fe2O3	0.416	%
MgO	0.307	%
CuO	0.174	%
MnO	0.079	%
TiO2	0.037	%
ZnO	0.036	%
Cl	0.027	%
SnO2	0.019	%
NiO	0.018	%
PbO	0.01	%
Cr2O3	0.005	%
As2O3	0.001	%
sum	59.982	

A2.3. Crystal structure

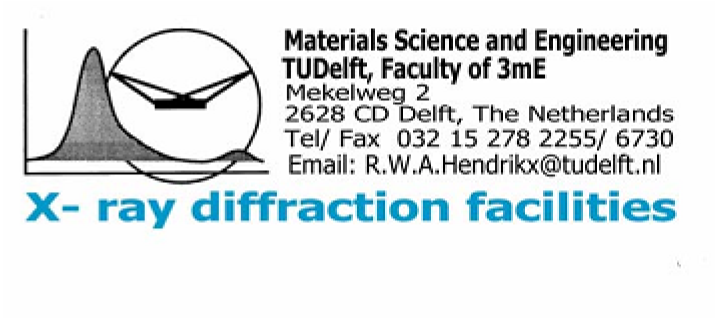

Materials Science and Engineering
TUDelft, Faculty of 3mE
Mekelweg 2
2628 CD Delft, The Netherlands
Tel/ Fax 032 15 278 2255/ 6730
Email: R.W.A.Hendrikx@tudelft.nl

X- ray diffraction facilities

XRD/XRF analysis of rice husk ash

Sample	rice husk ash burnt from different conditions, silica content
Client:	Vinh Pham
Date	04 jun 2012
Technician	Ruud Hendrikx

Experimental conditions XRD:

The measurements were performed with a Bruker- AXS D5005 diffractometer in Bragg-Brentano focusing geometry, equipped with a graphite monochromator in the diffracted beam. The sample powder was deposited as a thin layer on a Si{510} wafer. The θ-2θ scan was made in the range 10-60°2θ, using a step size of 0.02°2θ and a counting time per step of 5 s. The radiation is CuKa (0.15406 nm). Data evaluation was done with the Bruker program EVA.

All patterns are background-subtracted, meaning the contribution of air scatter and possible fluorescence radiation is subtracted.

Results:

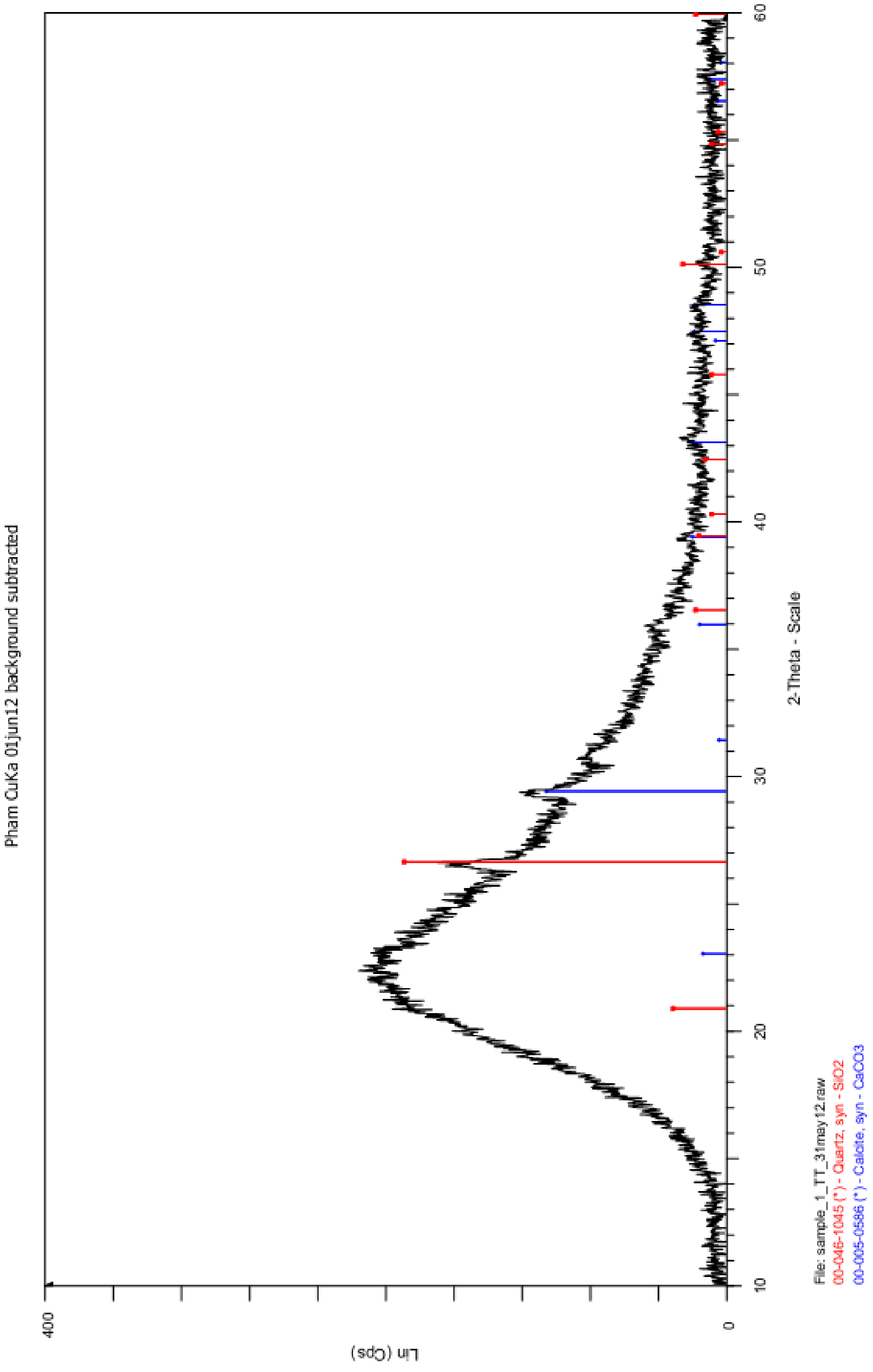

Figure 1 measured XRD pattern sample-1

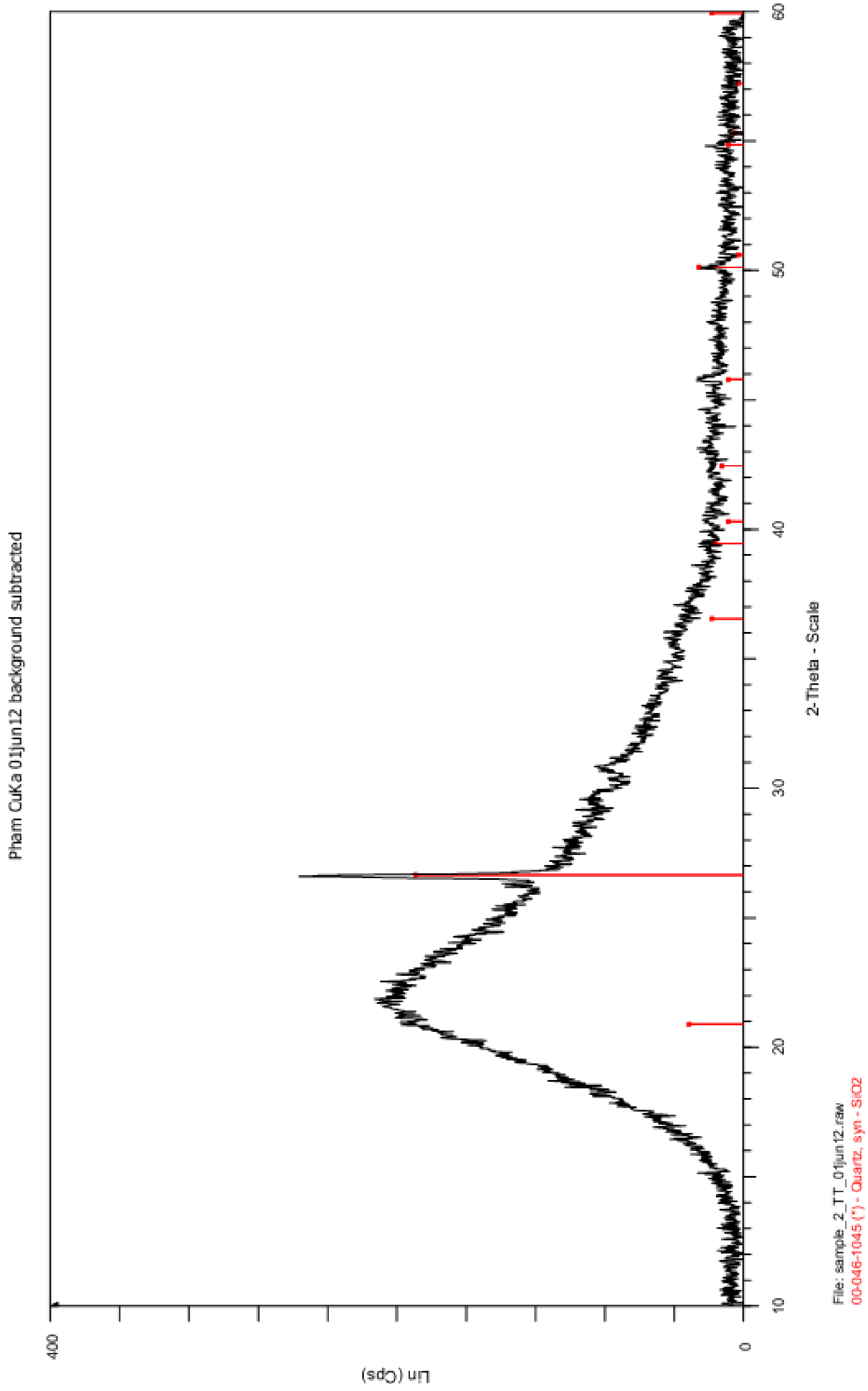

Figure 2 measured XRD pattern sample-2

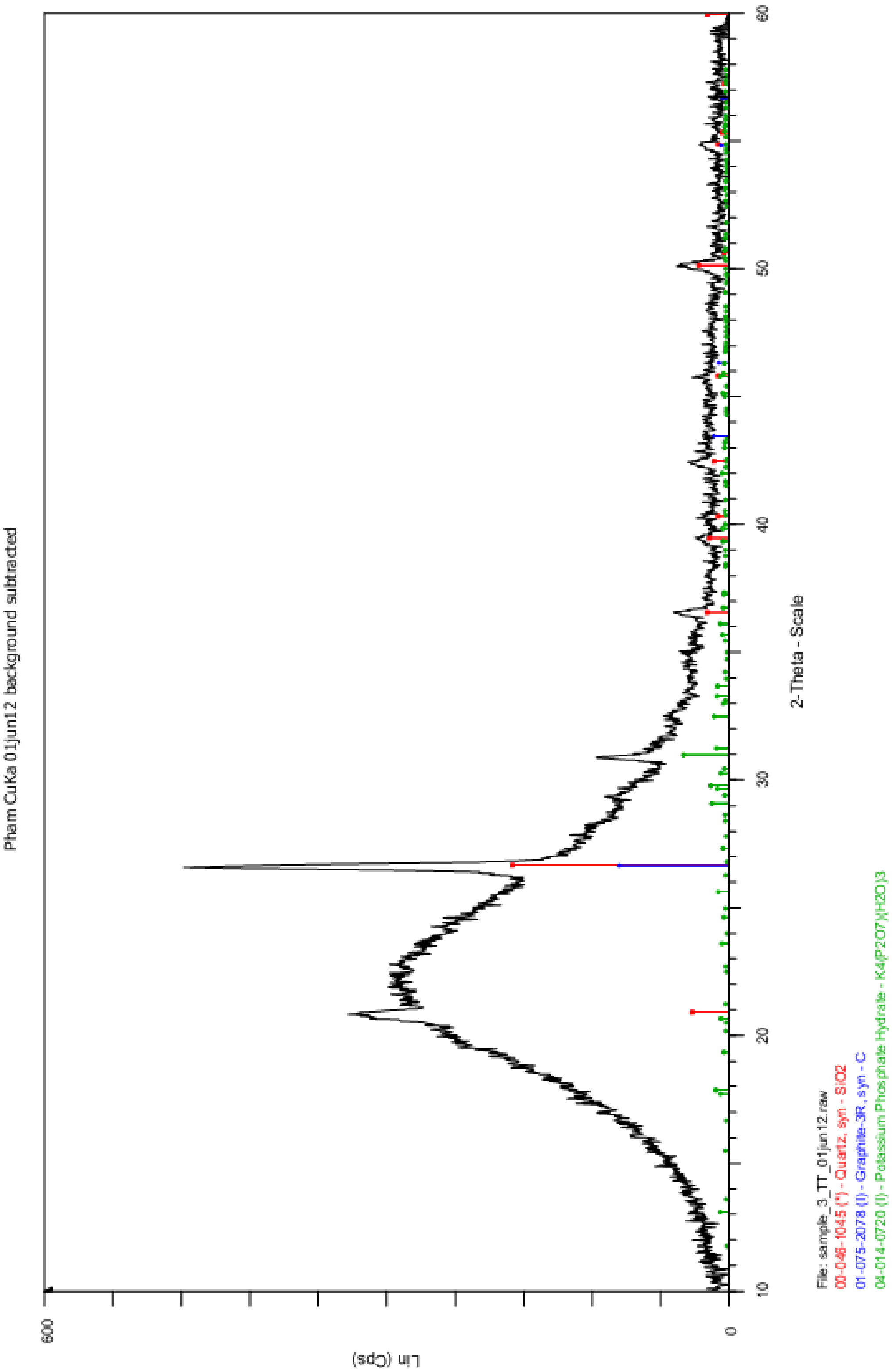

Figure 3 measured XRD pattern sample-3

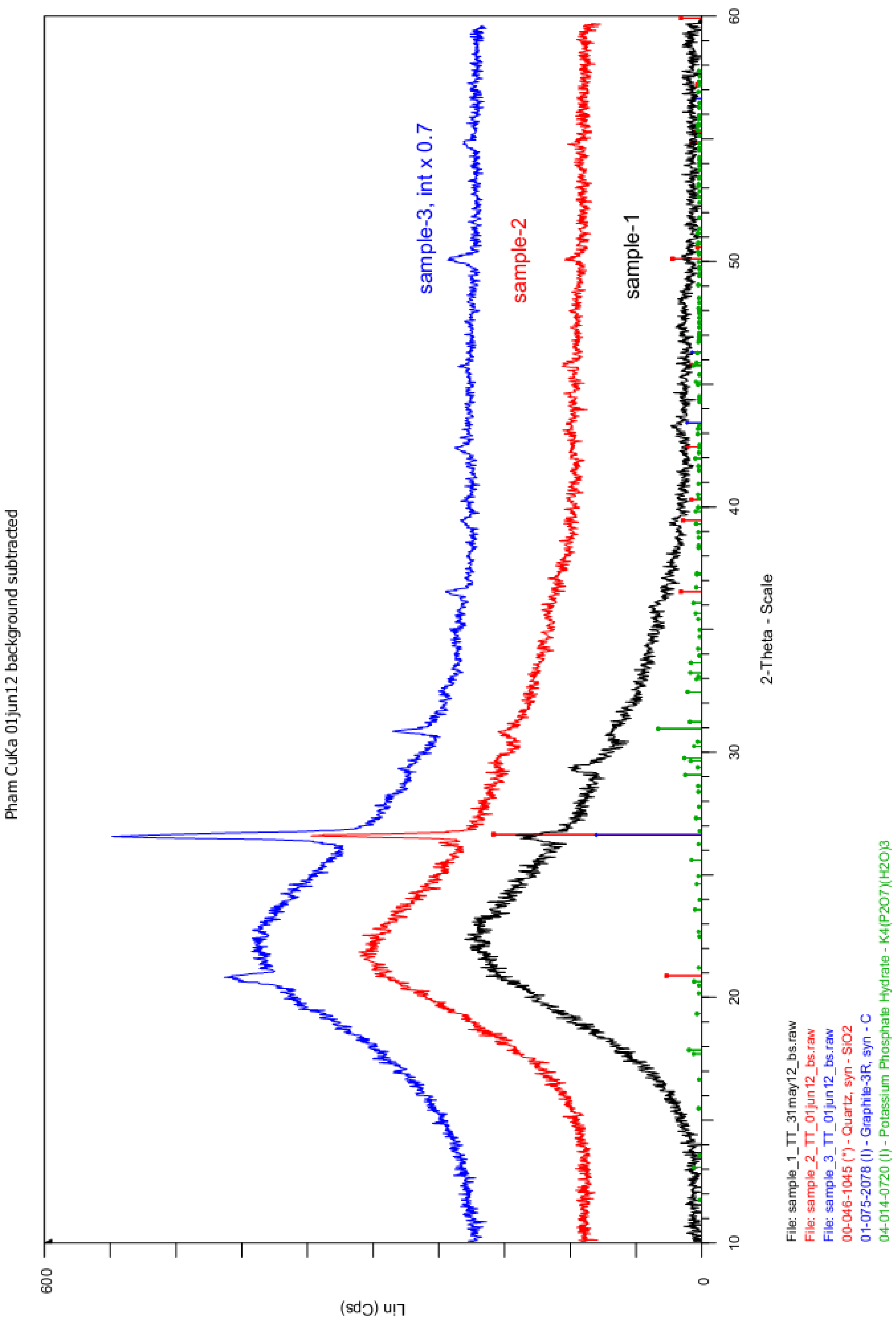

Figure 4 measured XRD pattern samples 1-3

APPENDIX 3 - Electrical conductivity and pH

APPENDIX 3 - Electrical conductivity and pH

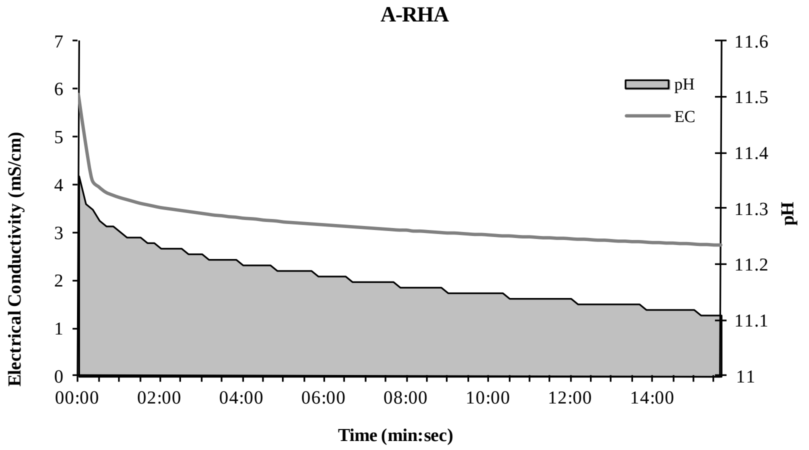

A-RHA

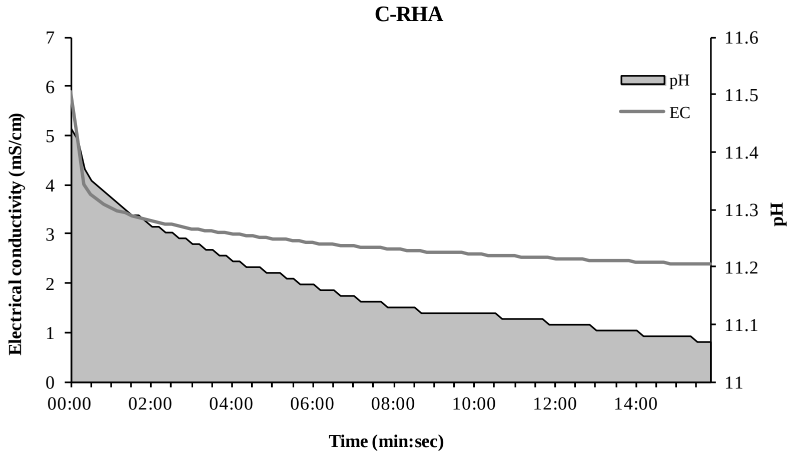

C-RHA

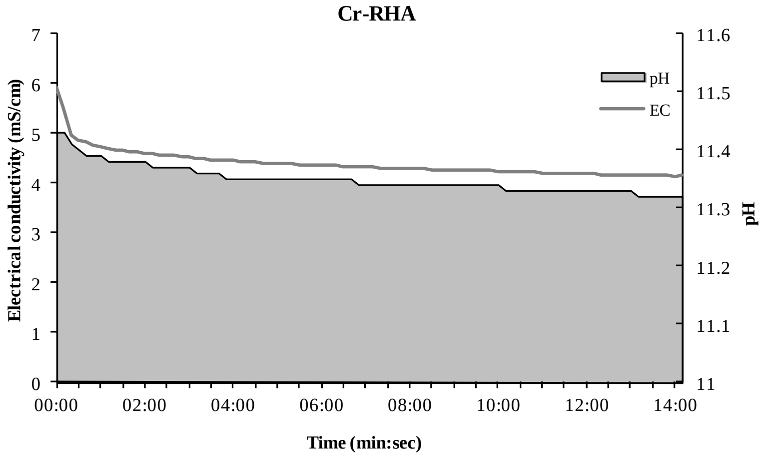

Cr-RHA

A-RHA

Time (min:sec)	**EC** (mS/c)	**pH**	**Temp.** (oC)
0:00:00	5.89	11.36	40.1
0:00:10	4.92	11.31	40.1
0:00:20	4.11	11.3	40.1
0:00:30	3.96	11.28	40.1
0:00:40	3.85	11.27	40
0:00:50	3.79	11.27	40
0:01:00	3.74	11.26	40
0:01:10	3.7	11.25	39.9
0:01:20	3.66	11.25	39.9
0:01:30	3.62	11.25	39.9
0:01:40	3.59	11.24	39.9
0:01:50	3.56	11.24	39.8
0:02:00	3.53	11.23	39.8
0:02:10	3.51	11.23	39.8
0:02:20	3.49	11.23	39.8
0:02:30	3.47	11.23	39.8
0:02:40	3.45	11.22	39.7
0:02:50	3.43	11.22	39.7
0:03:00	3.41	11.22	39.7
0:03:10	3.39	11.21	39.7
0:03:20	3.37	11.21	39.7
0:03:30	3.36	11.21	39.7
0:03:40	3.34	11.21	39.7
0:03:50	3.33	11.21	39.7
0:04:00	3.31	11.2	39.7
0:04:10	3.3	11.2	39.7
0:04:20	3.29	11.2	39.7
0:04:30	3.27	11.2	39.7
0:04:40	3.26	11.2	39.7
0:04:50	3.25	11.19	39.7
0:05:00	3.23	11.19	39.7
0:05:10	3.22	11.19	39.7
0:05:20	3.21	11.19	39.7
0:05:30	3.2	11.19	39.7
0:05:40	3.19	11.19	39.7
0:05:50	3.18	11.18	39.7
0:06:00	3.17	11.18	39.6
0:06:10	3.16	11.18	39.7
0:06:20	3.15	11.18	39.7
0:06:30	3.14	11.18	39.7
0:06:40	3.13	11.17	39.7
0:06:50	3.12	11.17	39.7
0:07:00	3.11	11.17	39.7
0:07:10	3.1	11.17	39.7
0:07:20	3.09	11.17	39.7
0:07:30	3.08	11.17	39.6
0:07:40	3.07	11.17	39.6
0:08:00	3.06	11.16	39.6
0:08:10	3.04	11.16	39.6
0:08:20	3.04	11.16	39.6
0:08:30	3.03	11.16	39.6
0:08:40	3.02	11.16	39.6
0:08:50	3.01	11.16	39.6
0:09:00	3	11.15	39.6
0:09:10	3	11.15	39.6
0:09:20	2.99	11.15	39.6
0:09:30	2.98	11.15	39.6
0:09:40	2.97	11.15	39.6
0:09:50	2.97	11.15	39.6
0:10:00	2.96	11.15	39.6
0:10:10	2.95	11.15	39.6
0:10:20	2.94	11.15	39.6
0:10:30	2.94	11.14	39.6
0:10:40	2.93	11.14	39.5
0:10:50	2.92	11.14	39.5
0:11:00	2.92	11.14	39.5
0:11:10	2.91	11.14	39.5
0:11:20	2.9	11.14	39.5
0:11:30	2.9	11.14	39.5
0:11:40	2.89	11.14	39.5
0:11:50	2.89	11.14	39.5
0:12:00	2.88	11.14	39.4

Time (min:sec)	**EC** (mS/c)	**pH**	**Temp.** (oC)
0:12:10	2.87	11.13	39.4
0:12:20	2.87	11.13	39.4
0:12:30	2.86	11.13	39.4
0:12:40	2.85	11.13	39.4
0:12:50	2.85	11.13	39.4
0:13:00	2.84	11.13	39.4
0:13:10	2.83	11.13	39.4
0:13:20	2.83	11.13	39.4
0:13:30	2.82	11.13	39.4
0:13:40	2.82	11.13	39.4
0:13:50	2.81	11.12	39.4
0:14:00	2.8	11.12	39.4
0:14:10	2.8	11.12	39.4
0:14:20	2.79	11.12	39.4
0:14:30	2.79	11.12	39.4
0:14:40	2.78	11.12	39.4
0:14:50	2.78	11.12	39.4
0:15:00	2.77	11.12	39.4
0:15:10	2.76	11.11	39.4
0:15:20	2.76	11.11	39.4
0:15:30	2.75	11.11	39.4
0:15:40	2.75	11.11	39.4

C-RHA

Time (min:sec)	**EC** (mS/c)	**pH**	**Temp.** (oC)
0:00:00	5.88	11.44	40.4
0:00:10	4.99	11.42	40.4
0:00:20	4	11.37	40.4
0:00:30	3.8	11.35	40.4
0:00:40	3.69	11.34	40.3
0:00:50	3.59	11.33	40.3
0:01:00	3.54	11.32	40.3
0:01:10	3.47	11.31	40.3
0:01:20	3.42	11.3	40.3
0:01:30	3.38	11.29	40.3
0:01:40	3.34	11.29	40.3
0:01:50	3.3	11.28	40.3
0:02:00	3.27	11.27	40.3
0:02:10	3.24	11.27	40.3
0:02:20	3.21	11.26	40.3
0:02:30	3.19	11.26	40.3
0:02:40	3.16	11.25	40.4
0:02:50	3.14	11.25	40.4
0:03:00	3.11	11.24	40.4
0:03:10	3.09	11.24	40.4
0:03:20	3.07	11.23	40.4
0:03:30	3.06	11.23	40.4
0:03:40	3.03	11.22	40.4
0:03:50	3.02	11.22	40.4
0:04:00	3	11.21	40.4
0:04:10	2.98	11.21	40.5
0:04:20	2.97	11.2	40.5
0:04:30	2.95	11.2	40.5
0:04:40	2.93	11.2	40.5
0:04:50	2.92	11.19	40.5
0:05:00	2.9	11.19	40.5
0:05:10	2.89	11.19	40.5
0:05:20	2.88	11.18	40.5
0:05:30	2.86	11.18	40.5
0:05:40	2.85	11.17	40.6
0:05:50	2.83	11.17	40.6
0:06:00	2.82	11.17	40.6
0:06:10	2.81	11.16	40.6
0:06:20	2.8	11.16	40.6
0:06:30	2.78	11.16	40.6
0:06:40	2.77	11.15	40.6
0:06:50	2.76	11.15	40.6
0:07:00	2.75	11.15	40.6
0:07:10	2.74	11.14	40.6
0:07:20	2.73	11.14	40.6
0:07:30	2.72	11.14	40.7
0:07:40	2.71	11.14	40.7
0:07:50	2.7	11.13	40.7
0:08:00	2.69	11.13	40.7
0:08:10	2.68	11.13	40.7

Time (min:sec)	EC (mS/c)	pH	Temp. (oC)
0:08:20	2.67	11.13	40.6
0:08:30	2.66	11.13	40.6
0:08:40	2.65	11.12	40.5
0:08:50	2.64	11.12	40.5
0:09:00	2.64	11.12	40.4
0:09:10	2.63	11.12	40.4
0:09:20	2.62	11.12	40.4
0:09:30	2.61	11.12	40.3
0:09:40	2.61	11.12	40.3
0:09:50	2.6	11.12	40.2
0:10:00	2.59	11.12	40.1
0:10:10	2.58	11.12	40.1
0:10:20	2.57	11.12	40.1
0:10:30	2.57	11.12	40.1
0:10:40	2.56	11.11	40
0:10:50	2.55	11.11	40
0:11:00	2.55	11.11	40
0:11:10	2.54	11.11	40
0:11:20	2.53	11.11	40
0:11:30	2.53	11.11	40
0:11:40	2.51	11.11	39.9
0:11:50	2.51	11.1	39.9
0:12:00	2.5	11.1	39.9
0:12:10	2.5	11.1	39.9
0:12:20	2.49	11.1	39.9
0:12:30	2.48	11.1	39.9
0:12:40	2.48	11.1	39.9
0:12:50	2.47	11.1	39.9
0:13:00	2.46	11.09	39.9
0:13:10	2.46	11.09	39.9
0:13:20	2.45	11.09	39.9
0:13:30	2.45	11.09	39.8
0:13:40	2.44	11.09	39.8
0:13:50	2.44	11.09	39.8
0:14:00	2.43	11.09	39.8
0:14:10	2.42	11.08	39.8
0:14:20	2.42	11.08	39.8
0:14:30	2.42	11.08	39.8
0:14:40	2.41	11.08	39.8
0:14:50	2.4	11.08	39.8
0:15:00	2.4	11.08	39.7
0:15:10	2.39	11.08	39.7
0:15:20	2.39	11.08	39.7
0:15:30	2.39	11.07	39.7
0:15:40	2.39	11.07	39.7
0:15:50	2.38	11.07	39.7

Cr-RHA

Time (min:sec)	EC (mS/c)	pH	Temp. (oC)
0:00:00	5.93	11.43	40.6
0:00:10	5.53	11.43	40.6
0:00:20	4.98	11.41	40.6
0:00:30	4.88	11.4	40.5
0:00:40	4.83	11.39	40.5
0:00:50	4.76	11.39	40.6
0:01:00	4.74	11.39	40.6
0:01:10	4.71	11.38	40.6
0:01:20	4.68	11.38	40.6
0:01:30	4.66	11.38	40.6
0:01:40	4.64	11.38	40.6
0:01:50	4.62	11.38	40.6
0:02:00	4.6	11.38	40.5
0:02:10	4.59	11.37	40.6
0:02:20	4.57	11.37	40.5
0:02:30	4.56	11.37	40.5
0:02:40	4.55	11.37	40.5
0:02:50	4.53	11.37	40.6
0:03:00	4.52	11.37	40.6
0:03:10	4.51	11.36	40.6
0:03:20	4.5	11.36	40.6
0:03:30	4.48	11.36	40.6
0:03:40	4.47	11.36	40.6
0:03:50	4.46	11.35	40.6
0:04:00	4.45	11.35	40.6
0:04:10	4.44	11.35	40.7

Time (min:sec)	**EC** (mS/c)	**pH**	**Temp.** (oC)
0:04:20	4.43	11.35	40.6
0:04:30	4.42	11.35	40.6
0:04:40	4.41	11.35	40.6
0:04:50	4.4	11.35	40.6
0:05:00	4.4	11.35	40.5
0:05:10	4.39	11.35	40.5
0:05:20	4.39	11.35	40.5
0:05:30	4.38	11.35	40.4
0:05:40	4.37	11.35	40.4
0:05:50	4.37	11.35	40.4
0:06:00	4.36	11.35	40.3
0:06:10	4.35	11.35	40.3
0:06:20	4.35	11.35	40.3
0:06:30	4.34	11.35	40.2
0:06:40	4.33	11.35	40.2
0:06:50	4.33	11.34	40.2
0:07:00	4.33	11.34	40.1
0:07:10	4.32	11.34	40.1
0:07:20	4.31	11.34	40.1
0:07:30	4.31	11.34	40.1
0:07:40	4.31	11.34	40.1
0:07:50	4.3	11.34	40
0:08:00	4.3	11.34	40
0:08:10	4.29	11.34	40
0:08:20	4.29	11.34	40
0:08:30	4.28	11.34	40
0:08:40	4.28	11.34	39.9
0:08:50	4.27	11.34	39.9
0:09:00	4.27	11.34	39.9
0:09:10	4.26	11.34	39.9
0:09:20	4.26	11.34	39.9
0:09:30	4.25	11.34	39.9
0:09:40	4.25	11.34	39.9
0:09:50	4.25	11.34	39.9
0:10:00	4.24	11.34	39.9
0:10:10	4.24	11.33	39.9
0:10:20	4.23	11.33	39.9
0:10:30	4.23	11.33	39.8
0:10:40	4.22	11.33	39.8
0:10:50	4.22	11.33	39.8
0:11:00	4.21	11.33	39.8
0:11:10	4.21	11.33	39.8
0:11:20	4.21	11.33	39.8
0:11:30	4.2	11.33	39.8
0:11:40	4.2	11.33	39.8
0:11:50	4.19	11.33	39.8
0:12:00	4.19	11.33	39.8
0:12:10	4.19	11.33	39.7
0:12:20	4.18	11.33	39.7
0:12:30	4.18	11.33	39.7
0:12:40	4.17	11.33	39.7
0:12:50	4.17	11.33	39.7
0:13:00	4.17	11.33	39.7
0:13:10	4.16	11.32	39.7
0:13:20	4.16	11.32	39.7
0:13:30	4.15	11.32	39.7
0:13:40	4.15	11.32	39.7
0:13:50	4.15	11.32	39.7
0:14:00	4.14	11.32	39.6
0:14:10	4.15	11.32	39.7

APPENDIX 4 - Plasticity modification

APPENDIX 4 – Plasticity modification

Plasticity modification by the additives

	i (mm×10)	cup (g)	cup+wet soil (g)	cup+dry soil (g)	w% %
Clay + 1% lime	PL	2.15	5.48	4.57	37.6
	PL	2.17	4.68	4.02	35.7
	39	2.17	13.85	10.14	46.5
	42	2.19	11.37	8.44	46.9
	74	2.2	16.93	11.77	53.9
	78	2.18	12.86	9.12	53.9
	109	2.17	12.05	8.43	57.8
	114	2.17	13.77	9.53	57.6
	138	2.16	16.69	11.02	64.0
	190	2.18	20.4	12.67	73.7
Clay + 2% lime	PL	2.15	4.96	4.1	44.1
	PL	2.15	6.04	4.85	44.1
	28	2.15	9.39	7.25	42.0
	29	2.16	9.5	7.16	46.8
	66	2.16	12.08	8.62	53.6
	65	2.17	11.63	8.3	54.3
	130	2.17	12.83	8.61	65.5
	127	2.17	16.54	10.85	65.6
	181	2.17	18.46	11.61	72.6
	208	2.17	20.71	12.69	76.2
Clay + 3% lime	PL	2.17	4.37	3.7	43.8
	PL	2.17	4.51	3.8	43.6
	40	2.18	14.88	10.76	48.0
	65	2.16	17.27	11.92	54.8
	116	2.18	17.21	11.5	61.3
	112	2.18	12.54	8.27	70.1
	141	2.17	18.65	11.6	74.8
	248	2.18	18.61	11.14	83.4
Clay + 6% lime	PL	2.17	5.08	4.21	42.6
	PL	2.17	5.06	4.19	43.1
	53	2.17	11.98	8.62	52.1
	56	2.17	10.55	7.69	51.8
	74	2.16	8.75	6.34	57.7
	77	2.16	9.7	6.93	58.1
	132	2.17	12.24	8.2	67.0
	186	2.17	19.22	11.77	77.6
	220	2.16	22.45	13.31	82.0

	i (mm×10)	**cup** (g)	**cup+wet soil** (g)	**cup+dry soil** (g)	**w%** %
Clay + 2% lime + 2% C-RHA	PL	2.17	5.15	4.28	41.2
	PL	2.17	5.18	4.28	42.7
	54	2.16	11.55	8.29	53.2
	56	2.16	7.77	5.84	52.4
	95	2.16	10.88	7.56	61.5
	96	2.17	10.14	7.1	61.7
	163	2.17	12.56	8.24	71.2
	158	2.17	12.56	8.24	71.2
	202	2.15	17.79	11.02	76.3
Clay + 3% lime + 3% C-RHA	PL	2.17	6.46	5.12	45.4
	PL	2.17	5.95	4.77	45.4
	57	2.17	12.34	8.76	54.3
	61	2.17	13.43	9.48	54.0
	84	2.16	14.6	9.98	59.1
	87	2.16	13.44	9.23	59.5
	111	2.17	10.99	7.54	64.2
	153	2.17	15.52	10.01	70.3
	209	2.17	17.07	10.56	77.6
Clay + 4% lime + 4% C-RHA	PL	2.17	5.58	4.61	39.8
	PL	2.16	5.05	4.19	42.4
	55	2.2	8.25	6.17	52.4
	53	2.18	9.02	6.68	52.0
	82	2.19	12.09	8.42	58.9
	84	2.17	13.37	9.23	58.6
	121	2.17	12.94	8.69	65.2
	121	2.2	12.26	8.3	64.9
	170	2.16	14.63	9.43	71.5
	190	2.18	19.39	12.02	74.9
	252	2.18	18.58	11.23	81.2
Clay + 3% lime + 3% A-RHA	PL	2.17	5.11	4.27	40.0
	PL	2.18	5.7	4.64	43.1
	50	2.17	14.27	10.18	51.1
	55	2.18	12.57	9.04	51.5
	77	2.21	11.66	8.2	57.8
	75	2.18	15.58	10.69	57.5
	129	2.17	12.99	8.69	66.0
	141	2.18	16.17	10.36	71.0
	208	2.18	22.97	13.86	78.0
Clay + 2% lime + 2% Cr-RHA	PL	2.18	5.06	4.18	44.0
	PL	2.18	4.9	4.1	41.7
	206	2.18	13.02	8.16	78.9
	206	2.2	12.66	7.98	78.6
Clay + 1% lime + 1% Cr-RHA	PL	2.18	5.48	4.6	36.4
	PL	2.19	5.42	4.53	38.0
	250	2.18	12.11	7.73	78.9
	250	2.18	13.27	8.37	79.2

Water content change within the clay mixed with lime and C-RHA

	Initial w% %	Time (minutes)	Cup (g)	Cup + mixed soil (g)	Cup + dry mixed soil (g)	Mixed soil (g)	Wet clay (g)	Initial water (g)	Current water (g)	Reduction ratio -
Clay + 1% lime + 1% C-RHA	48.06	5	2.14	17.58	12.78	15.44	15.14	4.91	4.80	0.98
		5	2.16	17.21	12.52	15.05	14.75	4.79	4.69	0.98
		15	2.19	15.79	11.56	13.6	13.33	4.33	4.23	0.98
		62	2.16	17.39	12.69	15.23	14.93	4.85	4.70	0.97
		62	2.16	18.96	13.77	16.8	16.47	5.35	5.19	0.97
		90	2.14	16.34	11.96	14.2	13.92	4.52	4.38	0.97
		90	2.15	15.56	11.42	13.41	13.15	4.27	4.14	0.97
Clay + 2% lime + 2% C-RHA	48.06	7	2.16	25.05	18.08	22.89	22.01	7.14	6.97	0.98
		7	2.18	27.91	20.07	25.73	24.74	8.03	7.84	0.98
		32	2.17	32.19	23.04	30.02	28.87	9.37	9.15	0.98
		32	2.16	33.3	23.86	31.14	29.94	9.72	9.44	0.97
		50	2.16	27.36	19.73	25.2	24.23	7.86	7.63	0.97
		50	2.14	19.4	14.17	17.26	16.60	5.39	5.23	0.97
		72	2.16	14.55	10.8	12.39	11.91	3.87	3.75	0.97
		72	2.15	13.19	9.84	11.04	10.62	3.45	3.35	0.97
Clay + 3% lime + 3% C-RHA	48.06	9	2.15	21.57	15.76	19.42	18.32	5.95	5.81	0.98
		9	2.17	24.15	17.6	21.98	20.74	6.73	6.55	0.97
		25	2.16	21.01	15.37	18.85	17.78	5.77	5.64	0.98
		25	2.17	39.02	28	36.85	34.76	11.28	11.02	0.98
		40	2.17	28.46	20.62	26.29	24.80	8.05	7.84	0.97
		40	2.16	24.63	17.94	22.47	21.20	6.88	6.69	0.97
		52	2.15	24.47	17.82	22.32	21.06	6.83	6.65	0.97
		52	2.15	27.05	19.64	24.9	23.49	7.62	7.41	0.97

	Initial w%	**Time**	**Cup**	**Cup + mixed soil**	**Cup + dry mixed soil**	**Mixed soil**	**Wet clay**	**Initial water**	**Current water**	**Reduction ratio**
	%	(minutes)	(g)	(g)	(g)	(g)	(g)	(g)	(g)	-
Clay + 4% lime + 4% C-RHA	47.37	10	2.18	25.26	18.54	23.08	21.37	6.87	6.72	0.98
		10	2.18	27.54	20.15	25.36	23.48	7.55	7.39	0.98
		40	2.18	25.11	18.47	22.93	21.23	6.82	6.64	0.97
		40	2.17	19.42	14.43	17.25	15.97	5.13	4.99	0.97
		70	2.16	27.19	19.92	25.03	23.18	7.45	7.27	0.98
		70	2.17	17.46	13.04	15.29	14.16	4.55	4.42	0.97
		115	2.17	11.45	8.77	9.28	8.59	2.76	2.68	0.97
		115	2.15	12.91	9.8	10.76	9.96	3.20	3.11	0.97
Clay being mixed continously	47.88	10	2.16	12.35	9.13	10.19	10.19	3.30	3.22	0.98
		10	2.17	19.48	13.95	17.31	17.31	5.60	5.53	0.99
		20	2.18	11.05	8.31	8.87	8.87	2.87	2.74	0.95
		20	2.19	13.38	9.9	11.19	11.19	3.62	3.48	0.96
		30	2.17	15.91	11.78	13.74	13.74	4.45	4.13	0.93
		30	2.16	10.53	8.02	8.37	8.37	2.71	2.51	0.93

APPENDIX 5 - c_u development

APPENDIX 5 - c_u development

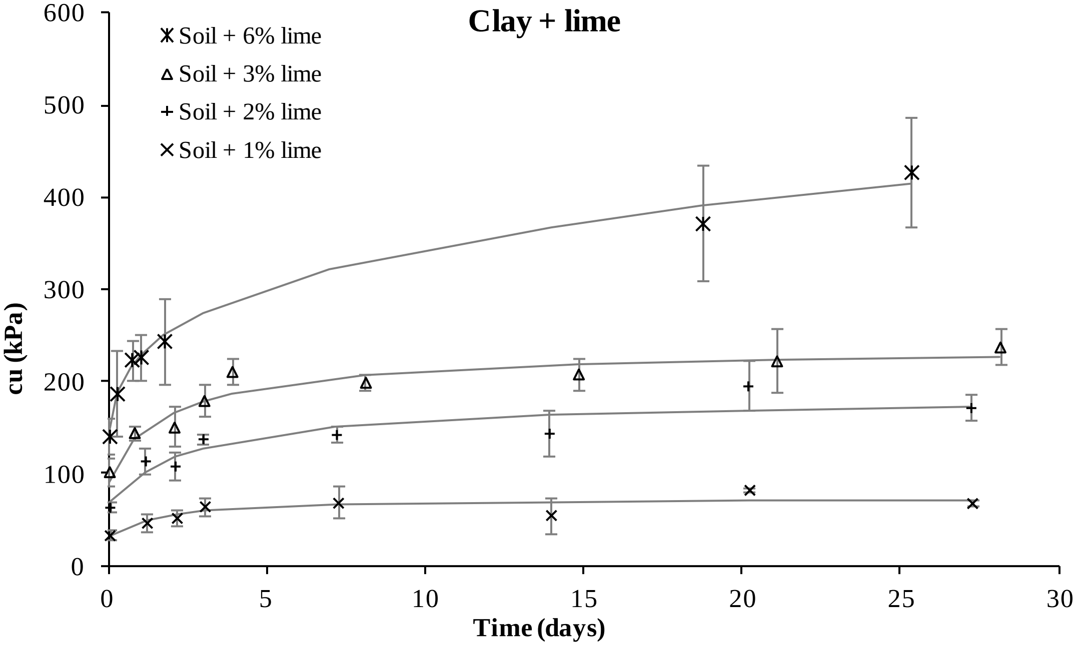

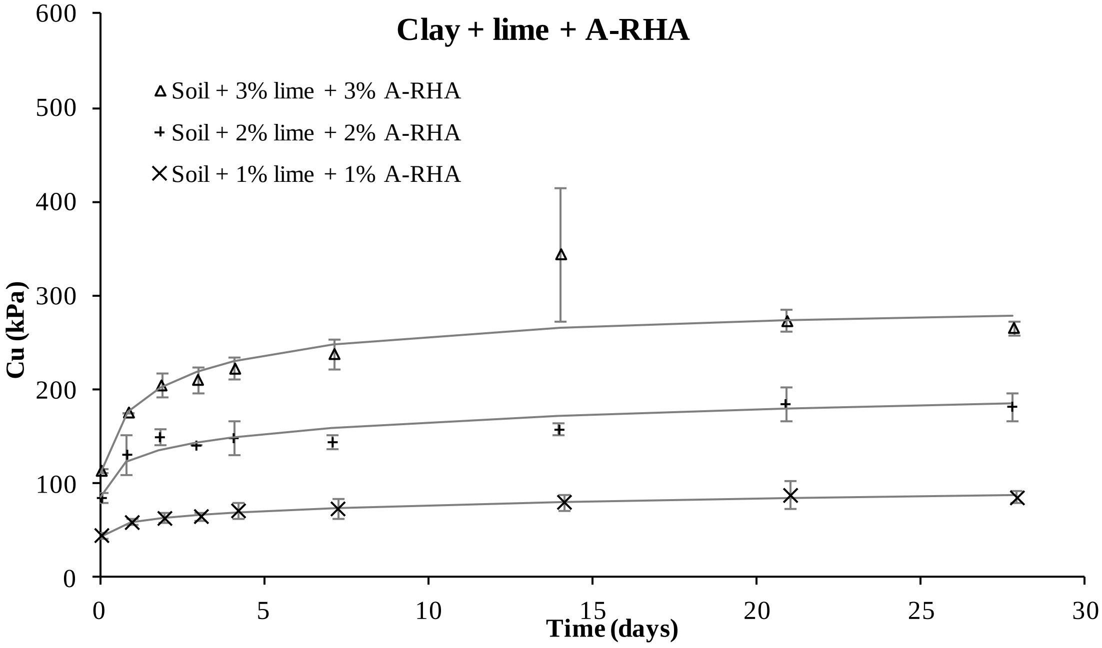

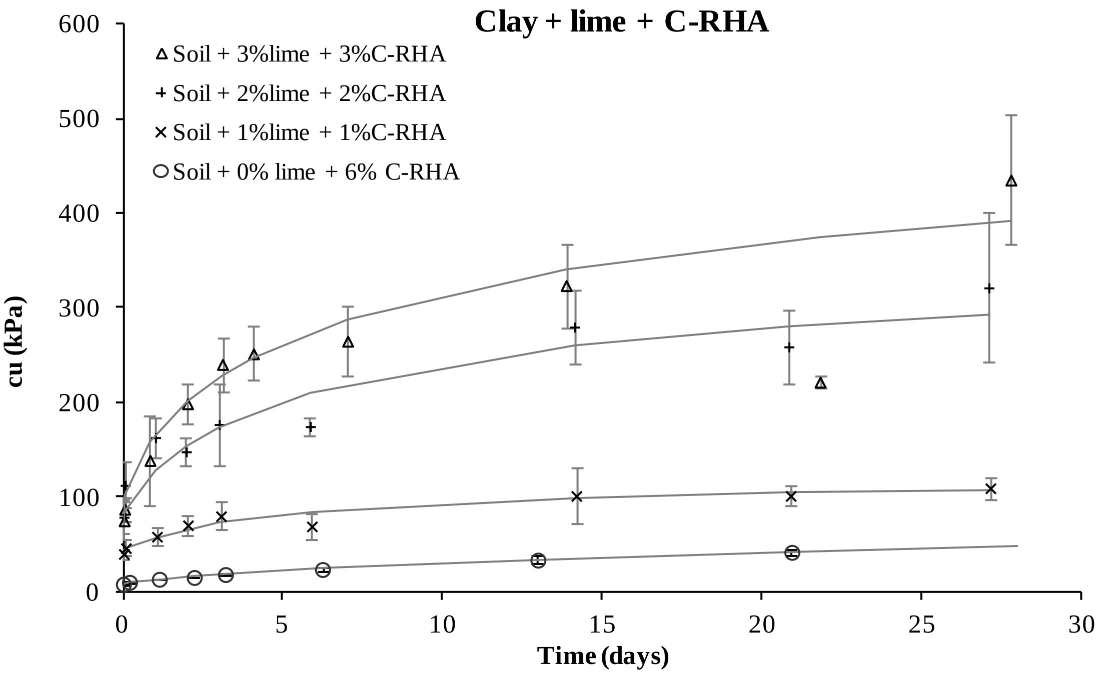
Clay + lime + C-RHA
Soil + 3%lime + 3%C-RHA
Soil + 2%lime + 2%C-RHA
Soil + 1%lime + 1%C-RHA
Soil + 0% lime + 6% C-RHA
cu (kPa)
Time (days)
0
100
200
300
400
500
600
0
5
10
15
20
25
30

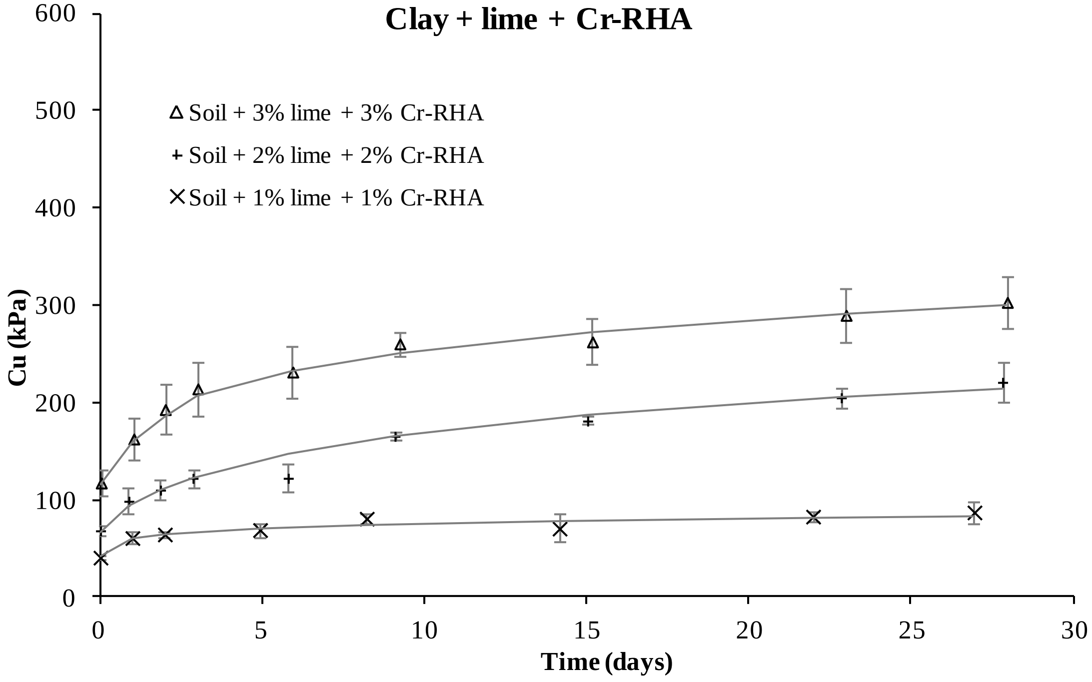
Clay + lime + Cr-RHA
Soil + 3% lime + 3% Cr-RHA
Soil + 2% lime + 2% Cr-RHA
Soil + 1% lime + 1% Cr-RHA
Cu (kPa)
Time (days)
0
100
200
300
400
500
600
0
5
10
15
20
25
30

A5.1. Clay + lime

Clay + 1% lime

Date	Time	Minutes	Days	Mass (g)	pi	i (mm)	cu (kPa)	Mean (kPa)	Deviation (kPa)
14-Feb	11:55	50	0	280	75	7.5	39.07	33.43	5.66
					89	8.9	27.74		
					81	8.1	33.49		
15-Feb	16:08	1743	1	280	65	6.5	52.01	46.96	10.21
					79	7.9	35.21		
					64	6.4	53.65		
16-Feb	14:48	3103	2	280	71	7.1	43.59	52.26	7.75
					73	7.3	41.24		
					62	6.2	57.17		
					63	6.3	55.37		
					62	6.2	57.17		
					61	6.1	59.06		
17-Feb	12:00	4375	3	280	55	5.5	72.64	64.84	9.40
					54	5.4	75.36		
					65	6.5	52.01		
					60	6.0	61.04		
					59	5.9	63.13		
21-Feb	16:57	10432	7	280	57	5.7	67.63	68.70	17.24
					50	5.0	87.90		
					59	5.9	63.13		
					52	5.2	81.27		
					71	7.1	43.59		
28-Feb	10:14	20109	14	585	87	8.7	60.66	55.34	19.61
					80	8.0	71.74		
					117	11.7	33.62		
5-Mar	16:35	29130	20	585	74	7.4	83.84	82.73	1.57
					75	7.5	81.62		
12-Mar	17:18	39253	27	585	81	8.1	69.98	68.34	2.83
					84	8.4	65.07		
					81	8.1	69.98		

Clay + 2% lime

Date	Time	Minutes	Days	Mass (g)	pi	i (mm)	cu (kPa)	Mean (kPa)	Deviation (kPa)
14-Feb	13:15	55	0	585	85	8.5	63.54	63.83	6.01
					81	8.1	69.98		
					89	8.9	57.96		
15-Feb	16:15	1675	1	585	68	6.8	99.29	114.16	14.18
					60	6.0	127.53		
					63	6.3	115.67		
16-Feb	14:45	3025	2	585	65	6.5	108.66	108.58	14.84
					61	6.1	123.38		
					70	7.0	93.70		
17-Feb	11:55	4295	3	585	57	5.7	141.31	138.17	5.44
					57	5.7	141.31		
					59	5.9	131.89		
21-Feb	16:55	10355	7	585	59	5.9	131.89	142.84	8.46
					55	5.5	151.77		
					56	5.6	146.40		
					57	5.7	141.31		
28-Feb	10:08	20028	14	585	65	6.5	108.66	144.21	25.89
					57	5.7	141.31		
					53	5.3	163.44		
					53	5.3	163.44		
5-Mar	16:38	29058	20	585	45	4.5	226.72	195.63	27.16
					50	5.0	183.64		
					51	5.1	176.51		
12-Mar	17:35	39195	27	585	49	4.9	191.22	172.06	14.03
					52	5.2	169.79		
					52	5.2	169.79		
					54	5.4	157.44		

Clay + 3% lime

Date	Time	Minutes	Days	Mass (g)	pi	i (mm)	cu (kPa)	Mean (kPa)	Deviation (kPa)
13-Feb	15:00	35	0	585	62	6.20	119.43	102.43	15.67
					72	7.20	88.56		
					68	6.80	99.29		
14-Feb	9:55	1170	1	585	56	5.60	146.40	144.88	7.76
					55	5.50	151.77		
					58	5.80	136.48		
15-Feb	16:03	2978	2	585	51	5.10	176.51	150.86	21.72
					55	5.50	151.77		
					61	6.10	123.38		
					55	5.50	151.77		
16-Feb	14:42	4337	3	585	51	5.10	176.51	179.74	18.13
					48	4.80	199.27		
					53	5.30	163.44		
17-Feb	11:55	5610	4	585	47	4.70	207.84	211.27	14.05
					45	4.50	226.72		
					48	4.80	199.27		
21-Feb	17:02	11677	8	585	47	4.70	207.84	199.53	9.60
					47	4.70	207.84		
					49	4.90	191.22		
					49	4.90	191.22		
28-Feb	10:19	21354	15	585	49	4.90	191.22	208.59	17.76
					47	4.70	207.84		
					45	4.50	226.72		
5-Mar	16:30	30365	21	585	46	4.60	216.97	222.82	34.89
					49	4.90	191.22		
					42	4.20	260.27		
12-Mar	17:43	40518	28	585	45	4.50	226.72	237.90	19.37
					45	4.50	226.72		
					42	4.20	260.27		

Clay + 6% lime

Date	Time	Minutes	Days	Mass (g)	pi	i (mm)	cu (kPa)	Mean (kPa)	Deviation (kPa)
21-Dec	11:10	40	0	580	56	5.6	145.15	140.97	19.12
					61	6.1	122.33		
					54	5.4	159.03		
					53	5.3	162.04		
					57	5.7	142.59		
					63	6.3	114.68		
21-Dec	16:53	383	0	580	55	5.5	153.25	187.31	45.73
					47	4.7	210.51		
					44	4.4	235.12		
					47	4.7	210.51		
					53	5.3	165.15		
					60	6.0	126.44		
					47	4.7	206.06		
22-Dec	10:30	1057	1	580	47	4.7	206.06	224.22	21.74
					43	4.3	246.18		
					43	4.3	246.18		
					47	4.7	206.06		
					44	4.4	235.12		
					46	4.6	215.12		
					46	4.6	215.12		
22-Dec	17:20	1467	1	580	44	4.4	235.12	227.04	25.36
					44	4.4	235.12		
					47	4.7	210.51		
					44	4.4	240.55		
					47	4.7	210.51		
					47	4.7	210.51		
					47	4.7	210.51		
23-Dec	11:10	2537	2	580	40	4.0	284.49	244.41	46.68
					41	4.1	270.78		
					49	4.9	189.58		
					39	3.9	299.27		
					45	4.5	224.78		
					48	4.8	197.56		
9-Jan	11:00	27007	19	580	37	3.7	332.49	372.17	63.40
					34	3.4	405.60		
					40	4.0	284.49		
					32	3.2	444.52		
					34	3.4	393.76		
16-Jan	14:00	36487	25	580	38	3.8	323.69	427.90	59.30
					33	3.3	417.98		
					32	3.2	444.52		
					32	3.2	444.52		
					30	3.0	505.76		
					33	3.3	430.94		

A5.2. Clay + lime + A-RHA

Clay + 1% lime + 1% A-RHA

Date	Time	Minutes	Days	Mass (g)	pi	i (mm)	cu (kPa)	Mean (kPa)	Deviation (kPa)
5-Mar	12:35	30	0	80	36	3.6	48.44	45.54	3.62
					97	9.7	48.79		
					105	10.5	41.64		
					103	10.3	43.28		
6-Mar	10:50	1365	1	585	87	8.7	60.66	59.39	3.49
					91	9.1	55.44		
					86	8.6	62.08		
7-Mar	10:43	2798	2	585	87	8.7	60.66	63.76	5.38
					87	8.7	60.66		
					81	8.1	69.98		
8-Mar	13:25	4400	3	585	81	8.1	69.98	65.76	4.72
					87	8.7	60.66		
					83	8.3	66.64		
9-Mar	16:37	6032	4	585	74	7.4	83.84	71.82	8.50
					83	8.3	66.64		
					80	8.0	71.74		
					84	8.4	65.07		
12-Mar	17:25	10400	7	585	84	8.4	65.07	73.90	10.24
					75	7.5	81.62		
					84	8.4	65.07		
					74	7.4	83.84		
19-Mar	15:05	20340	14	330	55	5.5	85.61	80.92	8.39
					79	7.9	72.93		
					71	7.1	90.30		
					78	7.8	74.82		
26-Mar	12:34	30269	21	580	78	7.8	74.82	88.24	15.04
					66	6.6	104.50		
					73	7.3	85.42		
2-Apr	10:30	40225	28	580	74	7.4	83.12	85.65	6.37
					70	7.0	92.89		
					75	7.5	80.92		

Clay + 2% lime + 2% A-RHA

Date	Time	Minutes	Days	Mass (g)	pi	i (mm)	cu (kPa)	Mean (kPa)	Deviation (kPa)
5-Mar	16:20	30	0	585	75	7.5	81.62	85.51	4.94
					71	7.1	91.07		
					74	7.4	83.84		
6-Mar	10:57	1147	1	585	56	5.6	146.40	131.57	20.82
					65	6.5	108.66		
					55	5.5	151.77		
					62	6.2	119.43		
7-Mar	10:48	2578	2	585	57	5.7	141.31	150.17	8.19
					54	5.4	157.44		
					55	5.5	151.77		
8-Mar	13:31	4181	3	585	57	5.7	141.31	141.31	0.00
					57	5.7	141.31		
					57	5.7	141.31		
9-Mar	16:47	5817	4	585	58	5.8	136.48	149.19	18.00
					57	5.7	141.31		
					52	5.2	169.79		
12-Mar	17:15	10165	7	585	55	5.5	151.77	144.88	7.76
					56	5.6	146.40		
					58	5.8	136.48		
19-Mar	15:09	20119	14	580	53	5.3	162.04	158.19	6.68
					53	5.3	162.04		
					55	5.5	150.47		
26-Mar	12:37	30047	21	580	51	5.1	175.00	185.36	17.93
					51	5.1	175.00		
					47	4.7	206.06		
2-Apr	10:30	40000	28	580	52	5.2	168.34	182.66	14.62
					50	5.0	182.07		
					48	4.8	197.56		

Clay + 3% lime + 3% A-RHA

Date	Time	Minutes	Days	Mass (g)	pi	i (mm)	cu (kPa)	Mean (kPa)	Deviation (kPa)
5-Mar	15:00	25	0	585	64.0	6.4	112.09	114.48	2.07
					63	6.3	115.67		
					63	6.3	115.67		
6-Mar	10:55	1220	1	585	51	5.1	176.51	176.51	0.00
					51	5.1	176.51		
					51	5.1	176.51		
7-Mar	10:45	2650	2	585	49	4.9	191.22	205.34	13.06
					47	4.7	207.84		
					46	4.6	216.97		
8-Mar	13:28	4253	3	585	47	4.7	207.84	211.27	14.05
					48	4.8	199.27		
					45	4.5	226.72		
9-Mar	16:40	5885	4	585	45	4.5	226.72	223.14	10.94
				585	44	4.4	237.14		
				585	45	4.5	226.72		
				1080	61	6.1	227.78		
				1080	63	6.3	213.55		
				1080	64	6.4	206.93		
12-Mar	17:20	10245	7	585	44	4.4	237.14	238.76	16.34
				585	42	4.2	260.27		
				585	44	4.4	237.14		
				1080	62	6.2	220.50		
19-Mar	15:12	20197	14	580	36	3.6	351.22	344.97	70.72
				580	34	3.4	393.76		
				580	40	4.0	284.49		
				1080	55	5.5	280.19		
				1080	43	4.3	458.40		
				1080	53	5.3	301.74		
26-Mar	12:40	30125	21	1080	55	5.5	280.19	273.75	11.15
				1080	55	5.5	280.19		
				1080	57	5.7	260.88		
2-Apr	10:30	40075	28	580	41	4.1	270.78	266.53	7.36
				580	41	4.1	270.78		
				580	42	4.2	258.04		

A5.3. Clay + lime + C-RHA

Clay + 1% lime + 1% C-RHA

Date	Time	Minutes	Days	Mass (g)	pi	i (mm)	cu (kPa)	Mean (kPa)	Deviation (kPa)
					117	11.7	33.54		
				585	105	10.5	41.64		
7/Feb	12:55	20	0	80	39	3.9	43.86	39.68	5.43
					95	9.5	50.87		
					113	11.3	35.95		
7/Feb	14:30	115	0	585	95	9.5	50.87	45.90	8.61
					99	9.9	46.84		
					86	8.6	62.08		
8/Feb	13:50	1515	1	585	84	8.4	65.07	57.99	9.77
					84	8.4	65.07		
					75	7.5	81.62		
9/Feb	13:10	2915	2	585	85	8.5	63.54	70.08	10.03
					51	5.1	84.48		
					59	5.9	63.13		
10/Feb	14:00	4405	3	280	49	4.9	91.52	79.71	14.79
					61	6.1	59.06		
					59	5.9	63.13		
13/Feb	10:20	8505	6	280	51	5.1	84.48	68.89	13.66
					43	4.3	118.84		
					54	5.4	75.36		
					39	3.9	144.47		
					54	5.4	75.36		
21/Feb	17:15	20440	14	280	49	4.9	91.52	101.11	30.05
					65	6.5	108.66		
28/Feb	10:28	30113	21	585	70	7.0	93.70	101.18	10.58
					65	6.5	108.66		
					69	6.9	96.43		
					65	6.5	108.66		
5/Mar	16:42	39127	27	585	61	6.1	123.38	109.29	11.03

Clay + 2% lime + 2% C-RHA

Date	Time	Minutes	Days	Mass (g)	pi	i (mm)	cu (kPa)	Mean (kPa)	Deviation (kPa)
					68	6.8	99.29		
					83	8.3	66.64		
7/Feb	14:15	25	0	585	81	8.1	69.98	78.64	17.96
					58	5.8	136.48		
					72	7.2	88.56		
7/Feb	15:10	80	0	585	64	6.4	112.09	112.38	23.96
					52	5.2	169.79		
					58	5.8	138.86		
8/Feb	14:00	1450	1	585	51	5.1	180.02	162.89	21.43
					57	5.7	143.82		
					58	5.8	136.48		
9/Feb	13:05	2835	2	585	53	5.3	163.44	147.91	13.94
					55	5.5	151.77		
					45	4.5	226.72		
10/Feb	13:50	4320	3	585	55	5.5	151.77	176.75	43.27
					53	5.3	163.44		
					51	5.1	176.51		
13/Feb	10:20	8430	6	585	50	5.0	183.64	174.53	10.25
					45	4.5	226.72		
					41	4.1	273.12		
					39	3.9	301.85		
21/Feb	17:08	20358	14	585	38	3.8	317.94	279.91	40.01
					43	4.3	248.30		
					45	4.5	226.72		
28/Feb	10:22	30032	21	585	39	3.9	301.85	258.96	38.68
					45	4.5	226.72		
					40	4.0	286.94		
					35	3.5	374.78		
5/Mar	16:45	39055	27	585	34	3.4	397.15	321.40	79.04

Clay + 3% lime + 3% C-RHA

Date	Time	Minutes	Days	Mass (g)	pi	i (mm)	cu (kPa)	Mean (kPa)	Deviation (kPa)
				80	44	4.4	0.00		
				80	27	2.7	86.12		
				580	79	7.9	72.93		
				580	70	7	92.89		
16/Jan	15:35	35	0	580	98	9.8	47.40	74.84	20.08
				580	67	6.7	101.40		
				580	74	7.4	83.12		
16/Jan	16:00	60	0	580	77	7.7	76.77	87.10	12.79
				580	48	4.8	197.56		
				580	55	5.5	150.47		
				580	53	5.3	162.04		
				580	66	6.6	104.50		
17/Jan	11:00	1200	1	580	76	7.6	78.81	138.68	47.18
				580	51	5.1	175.00		
				580	46	4.6	215.12		
18/Jan	15:15	2895	2	580	47	4.7	206.06	198.73	21.04
				580	46	4.6	215.12		
				580	41	4.1	270.78		
19/Jan	17:30	4470	3	580	44	4.4	235.12	240.34	28.20
				580	40	4	284.49		
				580	44	4.4	235.12		
20/Jan	16:50	5870	4	580	44	4.4	235.12	251.57	28.51
				580	39	3.9	299.27		
				580	45	4.5	224.78		
23/Jan	15:40	10120	7	580	41	4.1	270.78	264.94	37.58
				580	35	3.5	371.58		
				580	38	3.8	315.22		
30/Jan	12:00	19980	14	580	40	4	284.49	323.76	44.17
				580	46	4.6	215.12		
				580	45	4.5	224.78		
7/Feb	11:00	31440	22	580	45	4.5	224.78	221.56	5.58
				585	33	3.3	421.59		
				585	35	3.5	374.78		
13/Feb	10:30	40050	28	585	30	3	510.12	435.50	68.73

Soil + 0% lime + 6% C-RHA

Date	Time	Minutes	Days	Mass (g)	pi	i (mm)	cu (kPa)	Mean (kPa)	Deviation (kPa)
					87	8.7	8.29		
					96	9.6	6.81		
17/Jan	12:15	0	0	80	89	8.9	7.93	7.68	0.77
					83	8.3	9.11		
					78	7.8	10.45		
17/Jan	16:50	275	0	80	81	8.1	9.57	9.71	0.68
					70	7	12.81		
					70	7	12.81		
18/Jan	15:15	1620	1	80	69	6.9	13.19	12.94	0.22
					65	6.5	14.86		
19/Jan	17:30	3195	2	80	65	6.5	14.86	14.86	0.00
					60	6	17.44		
					59	5.9	18.04		
20/Jan	17:00	4605	3	80	58.5	5.85	18.35	17.94	0.46
					51	5.1	24.14		
					54	5.4	21.53		
23/Jan	18:00	8985	6	80	51	5.1	24.14	23.27	1.51
					42	4.2	35.59		
					47	4.7	28.42		
30/Jan	12:00	18705	13	80	42	4.2	35.59	33.20	4.14
					40	4	39.24		
					40	4	39.24		
7/Feb	11:00	30165	21	80	37	3.7	45.86	41.45	3.82

A5.4. Clay + lime + Cr-RHA

Soil + 1% lime + 1% Cr-RHA

Date	Time	Minutes	Days	Mass (g)	pi	i (mm)	cu (kPa)	Mean (kPa)	Deviation (kPa)
					80	8	40.47		
					81	8.1	39.47		
28/Mar	12:24	24	0	330	78	7.8	42.57	40.84	1.58
					68	6.8	56.01		
					62	6.2	67.37		
29/Mar	11:59	1439	1	330	66	6.6	59.45	60.95	5.83
					65	6.5	61.30		
					62	6.2	67.37		
30/Mar	12:00	2880	2	330	63	6.3	65.25	64.64	3.08
					59	5.9	74.40		
					65	6.5	61.30		
2/Apr	10:25	7105	5	330	60	6	71.94	69.21	6.96
					59	5.9	74.40		
					55	5.5	85.61		
5/Apr	17:18	11838	8	330	56	5.6	82.58	80.87	5.80
					65	6.5	61.30		
					57	5.7	79.71		
					55	5.5	85.61		
11/Apr	15:55	20395	14	330	68	6.8	56.01	70.66	14.23
				580	76	7.6	78.81		
				580	76	7.6	78.81		
				330	55	5.5	85.61		
19/Apr	11:25	31645	22	330	54	5.4	88.81	83.01	5.03
					56	5.6	82.58		
					57	5.7	79.71		
24/Apr	10:45	38805	27	330	51	5.1	99.57	87.29	10.73

Soil + 2% lime + 2% Cr-RHA

Date	Time	Minutes	Days	Mass (g)	pi	i (mm)	cu (kPa)	Mean (kPa)	Deviation (kPa)
					81	8.1	69.98		
					80	8.0	71.74		
27/Mar	15:35	25	0	585	85	8.5	63.54	68.42	4.31
					70	7.0	93.70		
					77	7.7	77.43		
					65	6.5	108.66		
					66	6.6	105.40		
28/Mar	12:33	1283	1	585	65	6.5	108.66	98.77	13.42
					62	6.2	119.43		
					64	6.4	112.09		
29/Mar	11:56	2686	2	585	68	6.8	99.29	110.27	10.20
					60	6.0	127.53		
					64	6.4	112.09		
30/Mar	12:00	4130	3	585	60	6.0	127.53	122.38	8.92
					58	5.8	136.48		
					60	6.0	127.53		
					61	6.1	123.38		
2/Apr	10:25	8355	6	585	67	6.7	102.27	122.42	14.50
					52	5.2	169.79		
					53	5.3	163.44		
5/Apr	17:22	13092	9	585	53	5.3	163.44	165.56	3.66
					51	5.1	176.51		
					50	5.0	183.64		
11/Apr	15:50	21640	15	585	50	5.0	183.64	181.27	4.12
					48	4.8	199.27		
					48	4.8	199.27		
19/Apr	11:25	32895	23	585	46	4.6	216.97	205.17	10.22
					48	4.8	199.27		
					45	4.5	226.72		
24/Apr	10:43	40053	28	585	44	4.4	237.14	221.04	19.57

Soil + 3% lime + 3% Cr-RHA

Date	**Time**	**Minutes**	**Days**	**Mass** (g)	**pi**	**i** (mm)	**cu** (kPa)	**Mean** (kPa)	**Deviation** (kPa)
					64	6.4	112.09		
					59	5.9	131.89		
27/Mar	12:33	58	0	585	65	6.5	108.66	117.55	12.54
					53	5.3	163.44		
					50	5.0	183.64		
28/Mar	12:38	1503	1	585	57	5.7	141.31	162.80	21.18
					47	4.7	207.84		
					47	4.7	207.84		
29/Mar	11:54	2899	2	585	53	5.3	163.44	193.04	25.63
					50	5.0	183.64		
					44	4.4	237.14		
					48	4.8	199.27		
30/Mar	12:00	4345	3	585	44	4.4	237.14	214.30	27.14
					45	4.5	226.72		
					47	4.7	207.84		
2/Apr	10:12	8557	6	585	42	4.2	260.27	231.61	26.55
					41	4.1	273.12		
					42	4.2	260.27		
5/Apr	17:25	13310	9	585	43	4.3	248.30	260.56	12.41
				585	41	4.1	273.12		
				585	41	4.1	273.12		
				585	40	4.0	286.94		
				1080	61	6.1	227.78		
11/Apr	15:50	21855	15	1080	58	5.8	251.96	262.58	23.13
				1080	58	5.8	251.96		
				1080	54	5.4	290.67		
				1080	53	5.3	301.74		
19/Apr	11:25	33110	23	580	38	3.8	315.22	289.90	27.21
				1080	54	5.4	290.67		
				1080	55	5.5	280.19		
				1080	55	5.5	280.19		
				580	37	3.7	332.49		
24/Apr	10:38	40263	28	580	37	3.7	332.49	303.21	27.07

APPENDIX 6 – Deformity modification

APPENDIX 6 – Deformity modification

SYMBOLS AND EQUATIONS

σ'	Effective vertical stress;
$\sigma'i$	The pressure applied in the previous load increment;
$\sigma'f$	the pressure applied in the load increment being considered;
di	Initial reading;
d_{fr}	First recored reading;
df	Final reading;
d(0%)	Start of the primary compression;
d(100%)	Theoretical 100% primary compression;
t50	Time to 50% consolidation ;
Cv	Coefficient of consolidation;
$C\alpha$	Coefficient of secondary compression;
Hi	Initial height at the start of an increment, and this is the height of the speciment at the end of the previous increment;
Hf	Height of the speciment at the end of an increment;
Hs	Equivalent height of solids;
ε_v	Vertical strain;
m_v	Coefficient of volume compressibility;
S_c	Compression stiffness index;
e	Void ratio;
$\sigma'p$	Apparent preconsolidation pressure;
Cc	Compression index;
Cr	Reloading Compression index;

$$C_v = T_{50}.\frac{D^2}{t_{50}} = 0.197 \times \frac{\frac{1}{4}\left(\frac{H_i + H_f}{2}\right)^2 .10^{-6}}{\frac{t_{50}}{365.24.3600}}$$

$$= 1.553 \times \frac{\left(\frac{H_i + H_f}{2}\right)^2}{t_{50}}$$

$$C_\alpha = \frac{\Delta H}{\Delta \lg t}.\frac{1}{H_i}$$

$$\varepsilon_v = \frac{H_o - H_f}{H_f}\%$$

$$m_v = \frac{H_i - H_f}{H_i} \times \frac{1000}{\sigma_i^{'} - \sigma_f^{'}}$$

$$S_c = \frac{\Delta \ln \sigma_v^{'}}{\Delta \varepsilon_v}$$

$$e = \frac{H_f - H_s}{H_s}$$

$$C_c = \left(\frac{-\Delta e}{\Delta \lg \sigma_v^{'}}\right)_{loading}$$

$$C_r = \left(\frac{-\Delta e}{\Delta \lg \sigma_v^{'}}\right)_{unloading}$$

A6.1. Clay

SPECIMEN:			
Dimensions:		Initial specimen	Final specimen
Diameter	(mm)	65.00	65.00
Height	(mm)	20.00	16.17
Area	(mm^2)	33.18	33.18
Volume	(cm^3)	66.37	53.65

Particle density (assumption)**:**	2.65

INITIAL STATE:

Water content:		Clay	
Cup	(g)	35.38	34.37
Cup + soil	(g)	42.02	47.86
Cup + dry soil	(g)	39.88	43.46
Water	(g)	2.14	4.40
Dry soil	(g)	4.50	9.09
Water content	%	47.56	48.40
Average	%	47.98	

Density:		
Ring	(g)	64.36
Ring+paper	(g)	64.98
Ring + soil+paper	(g)	177.12
Mixed soil	(g)	112.14
Bulk density	(g/cm^3)	1.69
Dry density	(g/cm^3)	1.14
Solid mass	(g)	75.78
Solid height	(mm)	8.62
Void ratio		1.32

FINAL STATE:

Water content:		
Plate	(g)	50.17
Plate + ring with soil	(g)	215.33
Plate + ring with dry soil	(g)	189.57
Water	(g)	25.76
Dry soil	(g)	75.04
Water content	%	34.33

Density:		
Wet soil	(g)	101.18
Bulk density	(g/cm^3)	1.80
Dry density	(g/cm^3)	1.40

Clay

SETTLEMENT

Settlement during loading:

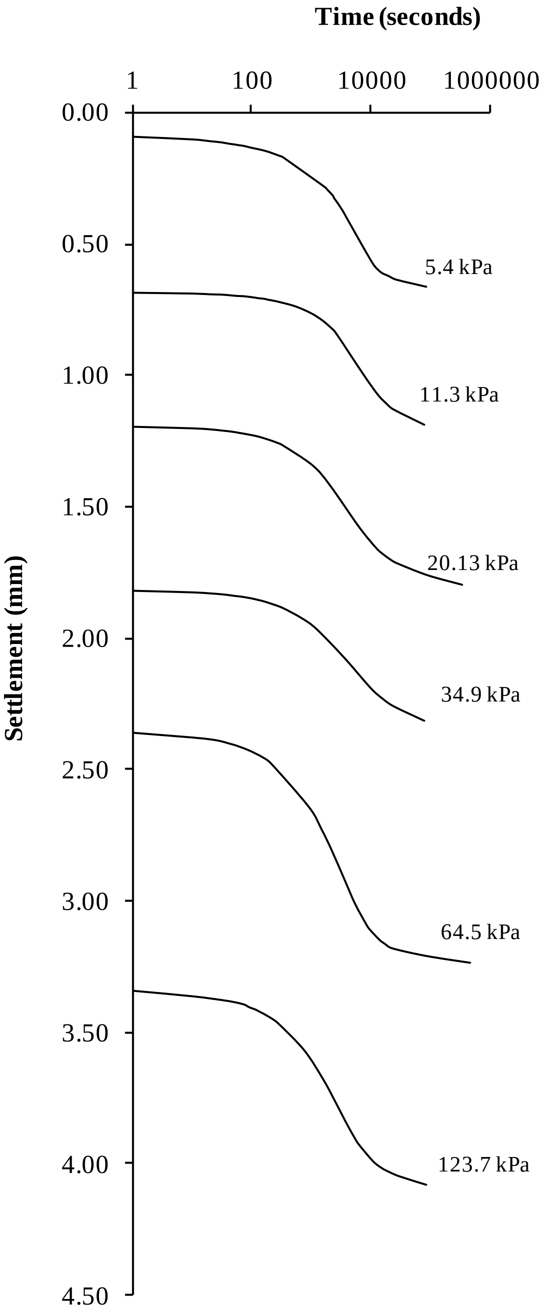

Settlement during unloading:

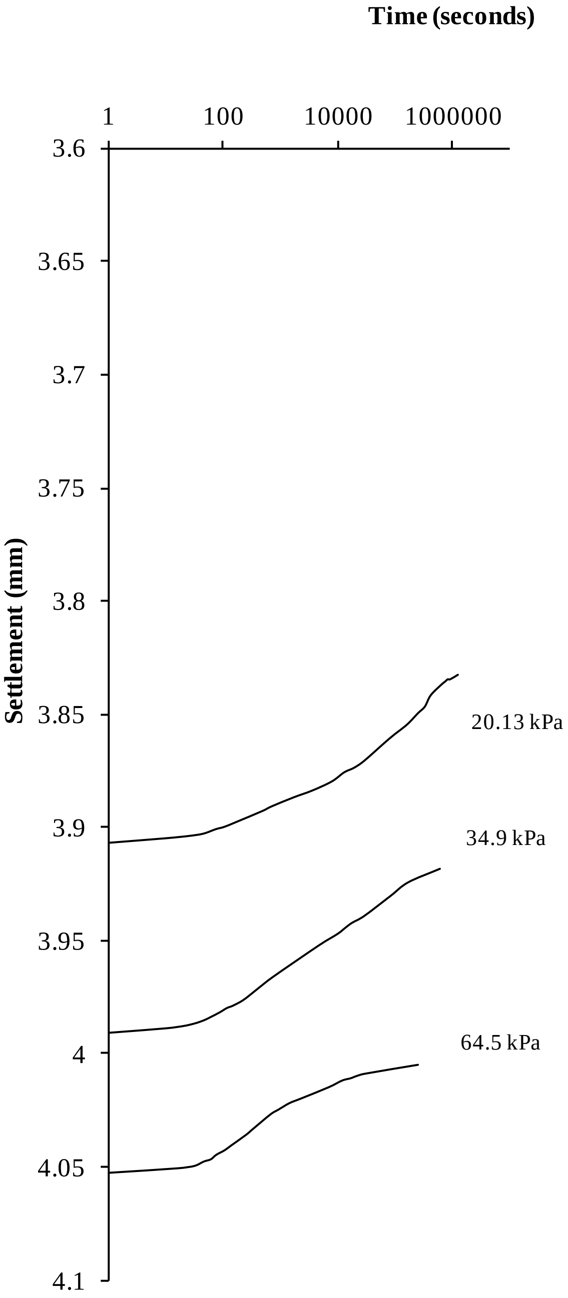

Clay

CALCULATION

	σ'	d_{fr}	df	d(0%)	d(100%)	t50	$Cv^{(*)}$	Cα	H	ε_v	m_v	S_c	e
	(kPa)	(mm)	(mm)	(mm)	(mm)	(s)	(m2/year)	×10-3	(mm)	%	(Mpa-1)	-	-
Loading									20.00	1.00			1.32
	5.35	0.096	0.663	0.10	0.621	3006	0.200	2.683	19.34	3.32	7.619	0.725	1.244
	11.26	0.685	1.188	0.674	1.11	3662	0.154	5.860	18.81	5.94	4.592	0.284	1.183
	20.13	1.196	1.764	1.173	1.719	2473	0.216	3.344	18.24	8.82	3.452	0.202	1.116
	34.91	1.822	2.314	1.804	2.238	2225	0.225	5.832	17.69	11.57	2.040	0.200	1.052
	64.48	2.361	3.207	2.344	3.177	1711	0.270	1.900	16.79	16.04	1.708	0.137	0.949
	123.69	3.340	4.078	3.322	4.009	1472	0.282	4.245	15.92	20.39	0.876	0.150	0.848
Unloading	64.48	4.078	4.005	-	-	-	-	-	16.00	20.03	-		0.856
	34.91	3.991	3.918	-	-	-	-	-	16.08	19.59	-		0.866
	20.13	3.907	3.833	-	-	-	-	-	16.17	19.17	-		0.876

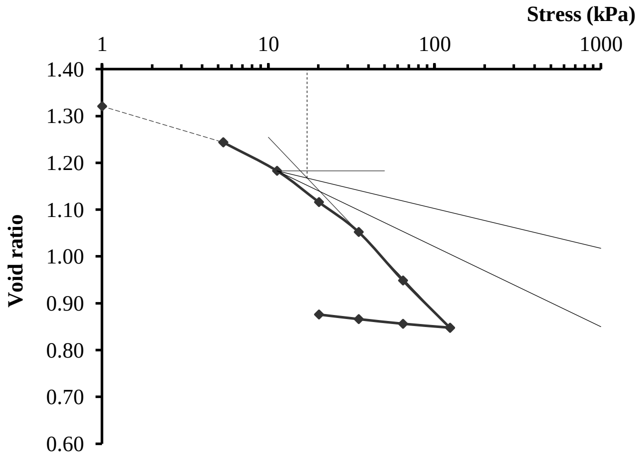

σ'p = 17.13 (kPa)(**)
Cc = 0.373 (***)
Cr = 0.036

(*) The coefficient of consolidation is identified by using the log time fitting method;
(**) The apparent preconsolidation pressure is identified by using Cassagrande method;
(***) The compression index is identified from the last two loading increment;

A6.2. Clay + 3% lime

PARAMETERS

SPECIMEN:

Dimensions:		Initial specimen	Final specimen
Diameter	(mm)	63.50	63.50
Height	(mm)	19.00	15.47
Area	(mm^2)	31.67	31.67
Volume	(cm^3)	60.17	48.99

Particle density:		(1)	(2)	(3)	(4)	Average
Solid	(g)	1.08	1.08	1.03	1.06	
(Bottle+liquid) at fixed volume	(g)	46.68	42.54	41.86	43.40	
(Bottle+liquid+solid) at fixed volume	(g)	47.31	43.17	42.46	44.03	
Solid volume	(cm3)	0.45	0.45	0.43	0.43	
Particle density	(g/cm^3)	2.40	2.40	2.40	2.47	2.42

INITIAL STATE:

Water content:		Clay		Clay mixed with the additives	
Cup	(g)	35.70	35.63	34.26	33.75
Cup + soil	(g)	41.02	39.69	40.83	44.05
Cup + dry soil	(g)	39.32	38.38	38.82	40.90
Water	(g)	1.70	1.31	2.01	3.15
Dry soil	(g)	3.62	2.75	4.56	7.15
Water content	%	46.96	47.64	44.08	44.06
Average	%	47.30		44.07	

Density:		
Ring	(g)	75.94
Ring + soil	(g)	178.04
Mixed soil	(g)	102.10
Bulk density	(g/cm^3)	1.70
Dry density	(g/cm^3)	1.18
Solid mass	(g)	70.87
Solid height	(mm)	9.27
Void ratio		1.05

FINAL STATE:

Water content:		
Plate	(g)	53.93
Plate + ring with soil	(g)	224.10
Plate + ring with dry soil	(g)	200.06
Water	(g)	24.04
Dry soil	(g)	70.19
Water content	%	34.25

Density:		
Wet soil	(g)	94.23
Bulk density	(g/cm^3)	1.92
Dry density	(g/cm^3)	1.43

Clay + 3% lime

SETTLEMENT

Settlement during loading:

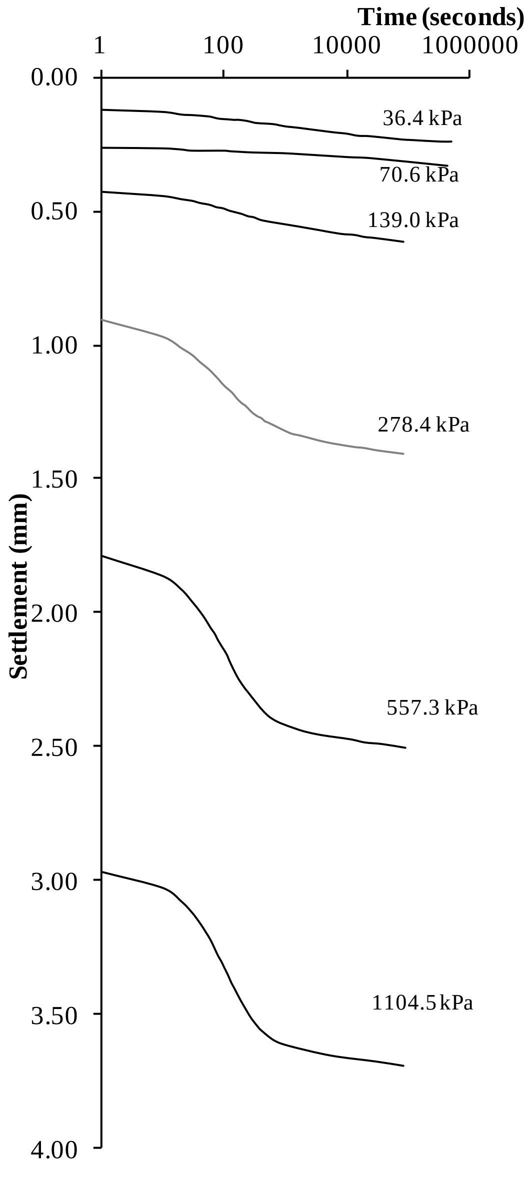

Settlement during unloading:

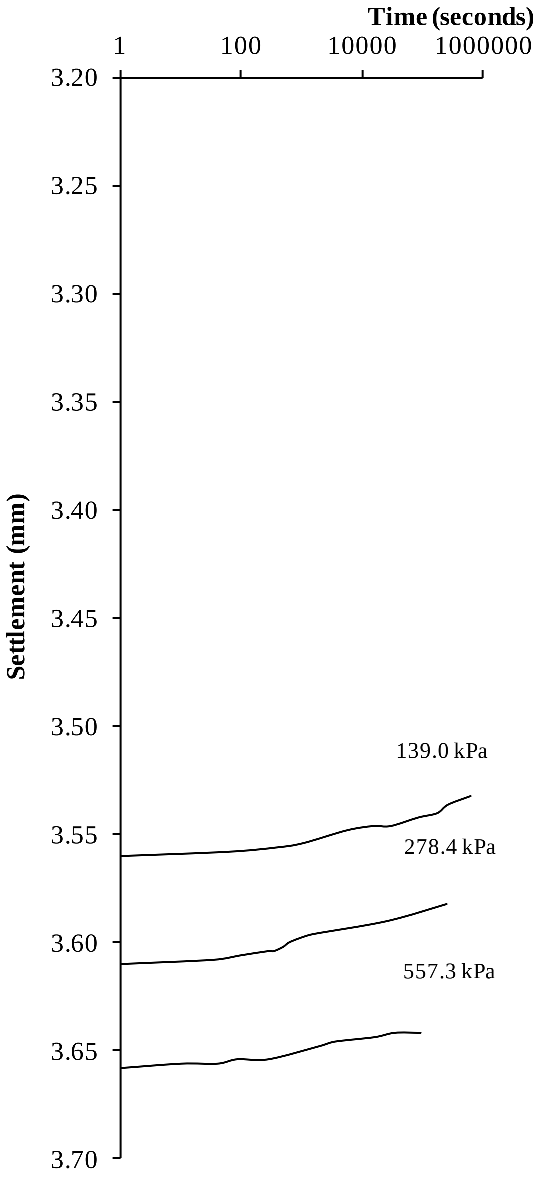

Clay + 3% lime

CALCULATION

	σ'	d_{fr}	df	d(0%)	d(100%)	t50	Cv$^{(*)}$	Cα	H	ε_v	m_v	S_c	e
	(kPa)	(mm)	(mm)	(mm)	(mm)	(s)	(m2/year)	×10-3	(mm)	%	(Mpa-1)	-	-
Loading									19.00	1.00			1.05
	36.37	0.12	0.242	0.12	0.234	658	0.841	0.708	18.76	1.27	0.360	13.131	1.024
	70.57	0.266	0.328	-	-	-	-	-	18.67	1.73	0.134	1.464	1.015
	138.96	0.426	0.614	0.423	0.552	94	5.673	1.655	18.39	3.23	0.224	0.450	0.984
	278.40	0.906	1.41	0.902	1.348	77	6.527	1.616	17.59	7.42	0.310	0.166	0.898
	557.29	1.786	2.506	1.725	2.422	68	6.634	2.102	16.49	13.19	0.223	0.120	0.780
	1104.45	2.97	3.692	2.888	3.609	67	5.861	2.164	15.31	19.43	0.131	0.110	0.652
Unloading	557.29	3.658	3.642	-	-	-	-	-	15.36	19.17	-		0.657
	278.40	3.61	3.582	-	-	-	-	-	15.42	18.85	-		0.664
	138.96	3.56	3.532	-	-	-	-	-	15.47	18.59	-		0.669

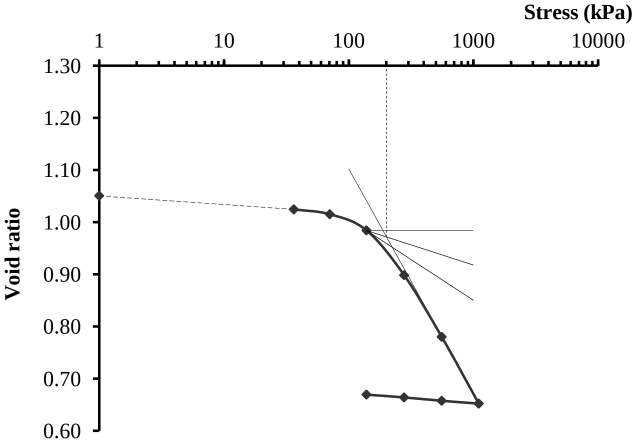

σ'p =	199.84	(kPa)(**)
Cc =	0.412	(***)
Cr =	0.019	

(*) The coefficient of consolidation is identified by using the log time fitting method;

(**) The apparent preconsolidation pressure is identified by using Cassagrande method;

(***) The compression index is identified from the last two loading increment;

A6.3. Clay + 3% lime + 3% A-RHA

PARAMETERS

SPECIMEN:

Dimensions:		Initial specimen	Final specimen
Diameter	(mm)	63.50	63.50
Height	(mm)	19.00	15.48
Area	(mm^2)	31.67	31.67
Volume	(cm^3)	60.17	49.02

Particle density:		(1)	(2)	(3)	(4)	Average
Solid	(g)	1.02	1.02	1.06	1.05	
(Bottle+liquid) at fixed volume	(g)	46.14	42.54	41.85	43.36	
(Bottle+liquid+solid) at fixed volume	(g)	46.75	43.13	42.47	43.98	
Solid volume	(cm3)	0.41	0.43	0.44	0.43	
Particle density	(g/cm^3)	2.49	2.37	2.41	2.44	2.43

INITIAL STATE:

Water content:		Clay		Clay mixed with the additives	
Cup	(g)	2.17	2.16	2.19	2.18
Cup + soil	(g)	6.39	8.59	11.35	8.42
Cup + dry soil	(g)	4.98	6.45	8.55	6.53
Water	(g)	1.41	2.14	2.8	1.89
Dry soil	(g)	2.81	4.29	6.36	4.35
Water content	%	50.18	49.88	44.03	43.45
Average	%	50.03		43.74	

Density:		
Ring	(g)	76.74
Ring+paper	(g)	77.14
Ring + soil+paper	(g)	177.76
Mixed soil	(g)	100.62
Bulk density	(g/cm^3)	1.67
Dry density	(g/cm^3)	1.16
Solid mass	(g)	70.00
Solid height	(mm)	9.11
Void ratio		1.09

FINAL STATE:

Water content:		
Plate	(g)	57.90
Plate + ring with soil	(g)	224.18
Plate + ring with dry soil	(g)	204.00
Water	(g)	20.18
Dry soil	(g)	69.36
Water content	%	29.09

Density:		
Wet soil	(g)	89.54
Bulk density	(g/cm^3)	1.83
Dry density	(g/cm^3)	1.41

Clay + 3% lime + 3% A-RHA

SETTLEMENT

Settlement during loading:

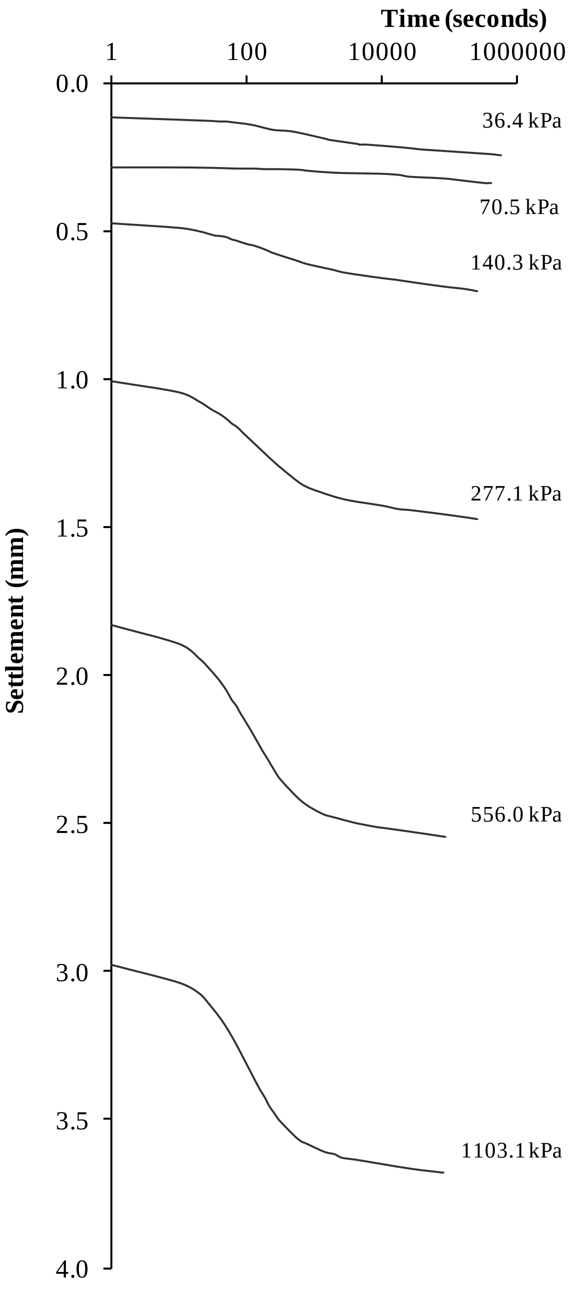

Settlement during unloading:

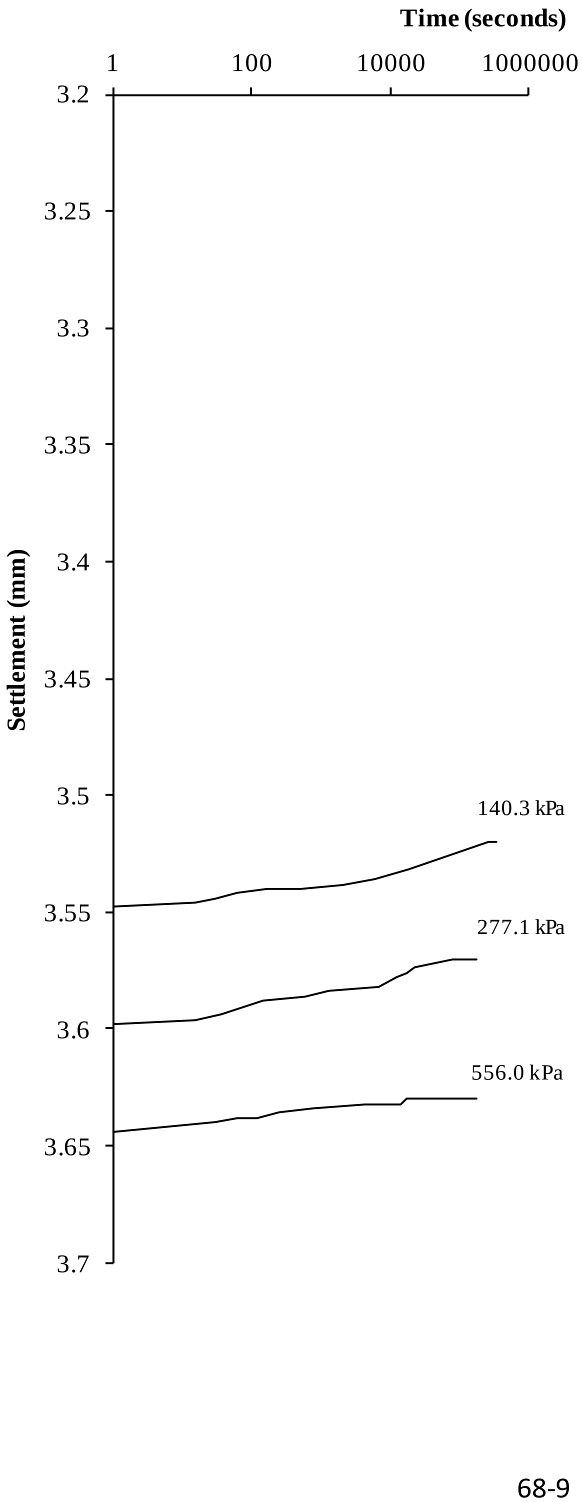

Clay + 3% lime + 3% A-RHA

CALCULATION

	σ'	d_{fr}	df	d(0%)	d(100%)	t50	Cv$^{(*)}$	Cα	H	ε_v	m_v	S_c	e
	(kPa)	(mm)	(mm)	(mm)	(mm)	(s)	(m2/year)	×10-3	(mm)	%	(Mpa-1)	-	-
Loading									19.00	1.00			1.09
	36.37	0.12	0.244	0.11	0.2	240	2.306	0.806	18.76	1.28	0.363	12.644	1.060
	70.57	0.284	0.338	-	-	-	-	-	18.66	1.78	0.147	1.340	1.050
	140.29	0.468	0.704	0.47	0.626	138	3.843	1.404	18.30	3.71	0.281	0.357	1.009
	277.08	1.004	1.474	0.973	1.41	98	5.084	1.487	17.53	7.76	0.308	0.168	0.925
	555.96	1.826	2.544	1.76	2.473	79	5.676	1.949	16.46	13.39	0.219	0.124	0.807
	1103.13	2.98	3.68	2.903	3.62	78	5.026	1.680	15.32	19.37	0.126	0.115	0.683
Unloading	555.96	3.644	3.63	-	-	-	-	-	15.37	19.11	-		0.688
	277.08	3.598	3.57	-	-	-	-	-	15.43	18.79	-		0.695
	140.29	3.548	3.52	-	-	-	-	-	15.48	18.53	-		0.700

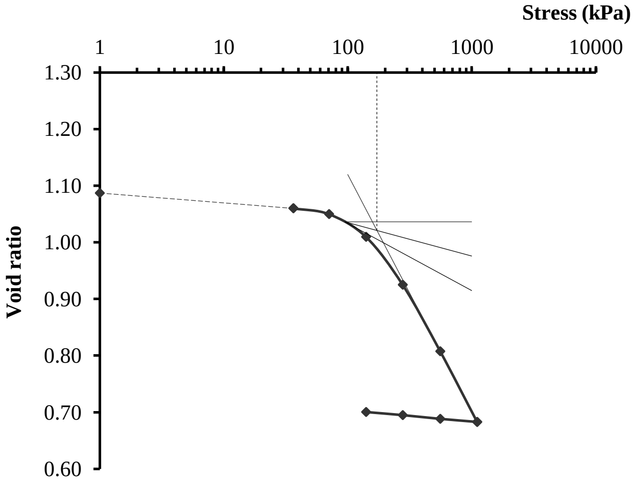

σ'p =	172.19	(kPa)(**)
Cc =	0.419	(***)
Cr =	0.020	

(*) The coefficient of consolidation is identified by using the log time fitting method;

(**) The apparent preconsolidation pressure is identified by using Cassagrande method;

(***) The compression index is identified from the last two loading increment;

A6.4. Clay + 3% lime + 3% C-RHA

PARAMETERS

SPECIMEN:

Dimensions:		Initial specimen	Final specimen
Diameter	(mm)	63.5	63.5
Height	(mm)	19.1	15.68
Area	(mm^2)	31.67	31.67
Volume	(cm^3)	60.49	49.66

Particle density:		(1)	(2)	(3)	(4)	Average
Solid	(g)	1	1.02	1.03	1.03	
(Bottle+liquid) at fixed volume	(g)	41.83	46.11	43.32	42.42	
(Bottle+liquid+solid) at fixed volume	(g)	42.39	46.71	43.92	43.06	
Solid volume	(cm3)	0.44	0.42	0.43	0.39	
Particle density	(g/cm^3)	2.27	2.43	2.40	2.64	2.43

INITIAL STATE:

Water content:		Clay		Clay mixed with the additives	
Cup	(g)	2.18	2.19	2.17	2.16
Cup + soil	(g)	9.8	8.45	9.14	10.6
Cup + dry soil	(g)	7.27	6.34	7.03	8.03
Water	(g)	2.53	2.11	2.11	2.57
Dry soil	(g)	5.09	4.15	4.86	5.87
Water content	%	49.71	50.84	43.42	43.78
Average	%	50.27		43.60	43.78

Density:		
Ring	(g)	75.93
Ring + soil	(g)	176.75
Mixed soil	(g)	100.82
Bulk density	(g/cm^3)	1.67
Dry density	(g/cm^3)	1.16
Solid mass	(g)	70.21
Solid height	(mm)	9.11
Void ratio		1.10

FINAL STATE:

Water content:		
Plate	(g)	52.99
Plate + ring with soil	(g)	217.32
Plate + ring with dry soil	(g)	198.45
Water	(g)	18.87
Dry soil	(g)	69.53
Water content	%	27.13

Density:		
Wet soil	(g)	88.40
Bulk density	(g/cm^3)	1.78
Dry density	(g/cm^3)	1.40

Clay + 3% lime + 3% C-RHA

SETTLEMENT

Settlement during loading:

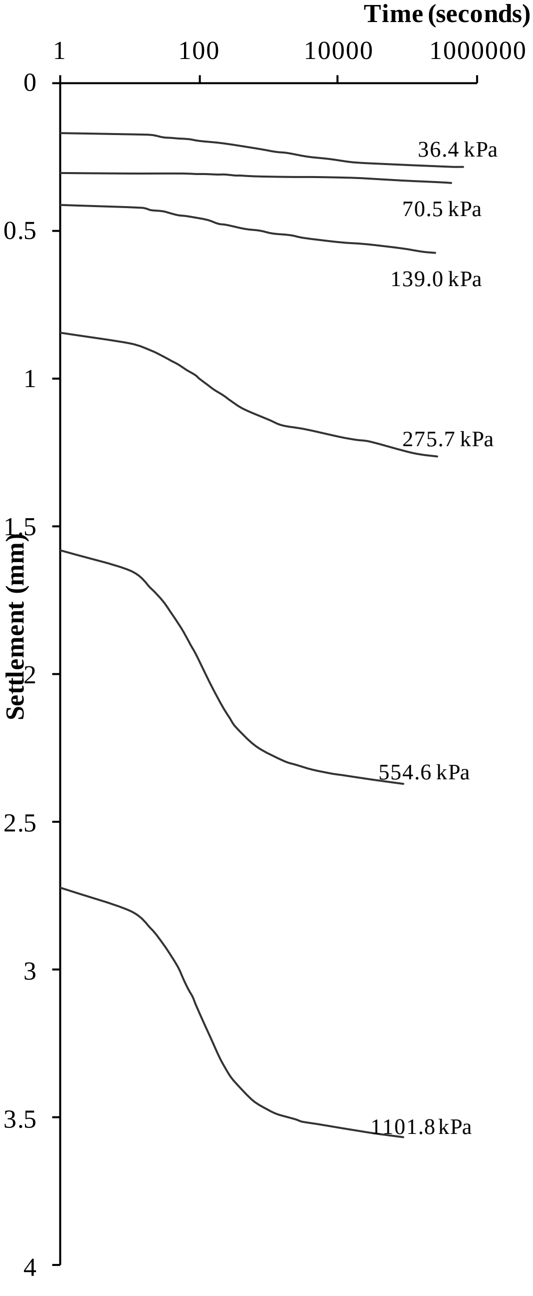

Settlement during unloading:

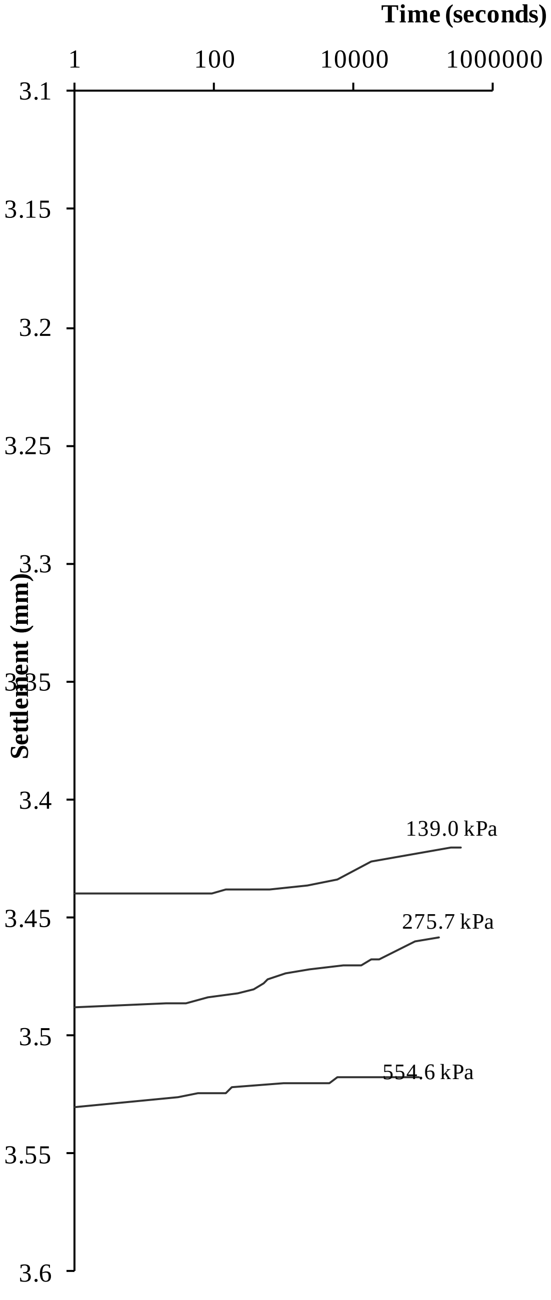

Clay + 3% lime + 3% C-RHA

CALCULATION

	σ'	d_{fr}	df	d(0%)	d(100%)	t50	$Cv^{(*)}$	Cα	H	ε_v	m_v	S_c	e
	(kPa)	(mm)	(mm)	(mm)	(mm)	(s)	(m2/year)	×10-3	(mm)	%	(Mpa-1)	-	-
Loading									19.10	1.00			1.10
	36.37	0.17	0.284	0.176	0.269	648	0.861	0.529	18.82	1.49	0.420	7.381	1.066
	70.57	0.30	0.342	-	-	-	-	-	18.76	1.79	0.090	2.183	1.060
	138.96	0.41	0.578	0.404	0.523	133	4.057	0.962	18.52	3.03	0.184	0.548	1.034
	275.75	0.85	1.264	0.83	1.131	73	7.031	1.985	17.84	6.62	0.271	0.191	0.959
	554.64	1.578	2.368	1.502	2.294	75	6.186	1.893	16.73	12.40	0.222	0.121	0.837
	1101.80	2.72	3.564	2.634	3.482	67	6.034	2.153	15.54	18.66	0.131	0.110	0.706
Unloading	554.64	3.53	3.518	-	-	-	-	-	15.58	18.42	-		0.711
	275.75	3.488	3.458	-	-	-	-	-	15.64	18.10	-		0.718
	138.96	3.44	3.42	-	-	-	-	-	15.68	17.91	-		0.722

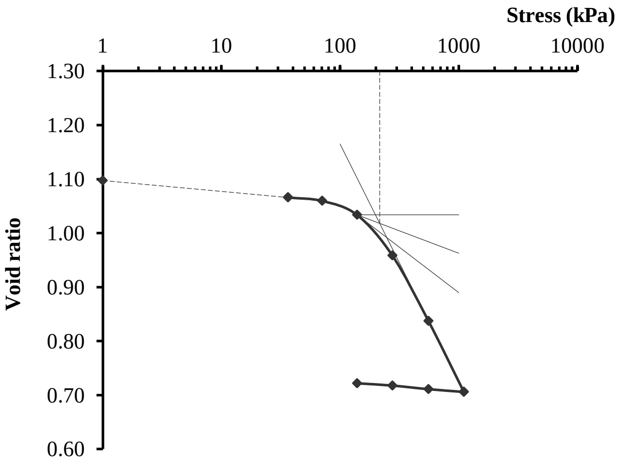

σ'p = 215.78 (kPa)(**)

Cc = 0.441 (***)

Cr = 0.018

(*) The coefficient of consolidation is identified by using the log time fitting method;

(**) The apparent preconsolidation pressure is identified by using Cassagrande method;

(***) The compression index is identified from the last two loading increment;

A6.5. Clay + 3% lime + 3% Cr-RHA

PARAMETERS

SPECIMEN:

Dimensions:		Initial specimen	Final specimen
Diameter	(mm)	63.50	63.50
Height	(mm)	19.00	15.69
Area	(mm^2)	31.67	31.67
Volume	(cm^3)	60.17	49.69

Particle density:		(1)	(2)	(3)	(4)	Average
Solid	(g)	1.06	1.01	1.04	1.00	
(Bottle+liquid) at fixed volume	(g)	43.40	46.19	41.81	42.53	
(Bottle+liquid+solid) at fixed volume	(g)	43.98	46.81	42.42	43.12	
Solid volume	(cm3)	0.48	0.39	0.43	0.41	
Particle density	(g/cm^3)	2.21	2.59	2.42	2.44	2.41

INITIAL STATE:

Water content:		Clay		Clay mixed with the additives	
Cup	(g)	2.17	2.17	2.17	2.21
Cup + soil	(g)	11.23	6.01	11.20	11.26
Cup + dry soil	(g)	8.31	4.74	8.51	8.57
Water	(g)	2.92	1.27	2.69	2.69
Dry soil	(g)	6.14	2.57	6.34	6.36
Water content	%	47.56	49.42	42.43	42.30
Average	%	48.49		42.36	

Density:		
Ring	(g)	76.71
Ring+paper	(g)	77.10
Ring + soil+paper	(g)	178.79
Mixed soil	(g)	101.69
Bulk density	(g/cm^3)	1.69
Dry density	(g/cm^3)	1.19
Solid mass	(g)	71.43
Solid height	(mm)	9.34
Void ratio		1.03

FINAL STATE:

Water content:		
Plate	(g)	61.36
Plate + ring with soil	(g)	228.02
Plate + ring with dry soil	(g)	208.83
Water	(g)	19.19
Dry soil	(g)	70.76
Water content	%	27.11

Density:		
Wet soil	(g)	89.95
Bulk density	(g/cm^3)	1.81
Dry density	(g/cm^3)	1.42

Clay + 3% lime + 3% Cr-RHA

SETTLEMENT

Settlement during loading:

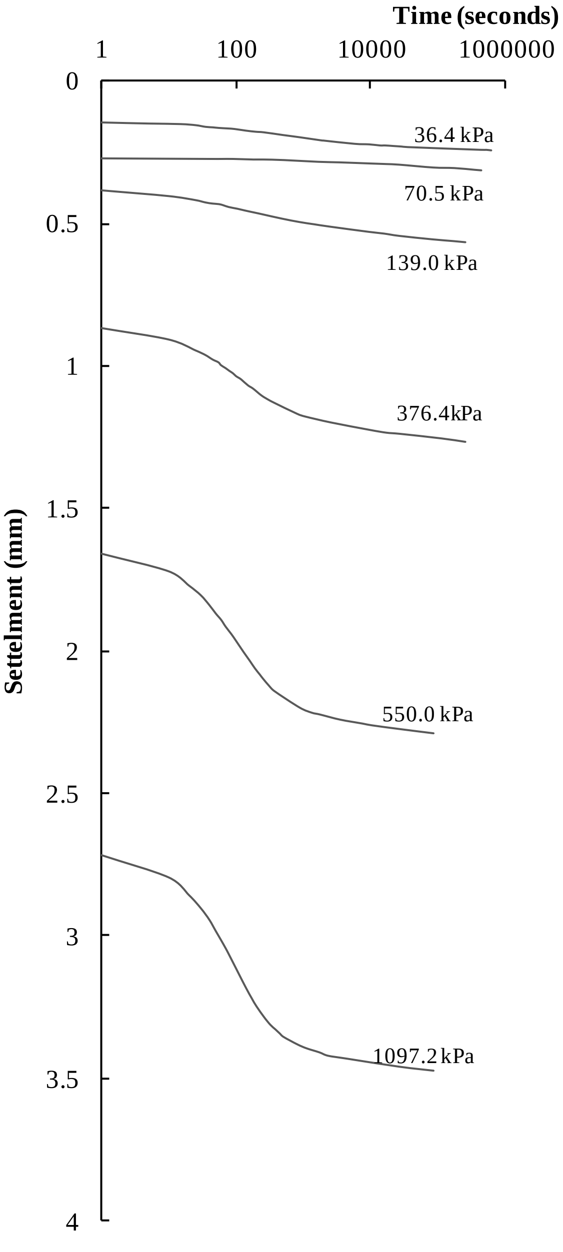

Settlement during unloading:

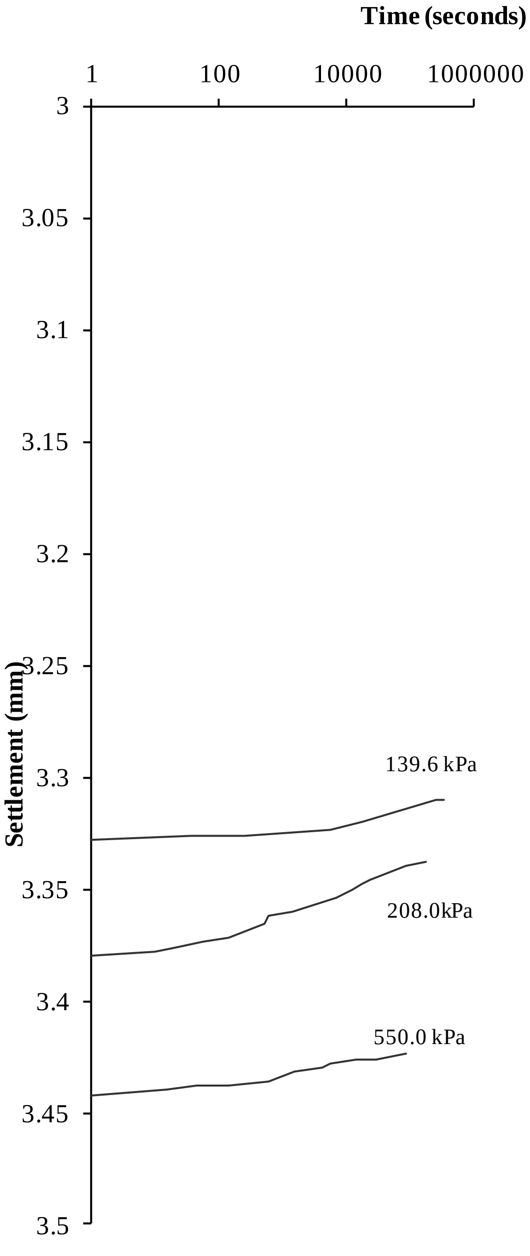

Clay + 3% lime + 3% Cr-RHA

CALCULATION

	σ'	d_{fr}	df	d(0%)	d(100%)	t50	Cv$^{(*)}$	Cα	H	ε_v	m_v	S_c	e
	(kPa)	(mm)	(mm)	(mm)	(mm)	(s)	(m2/year)	×10-3	(mm)	%	(Mpa-1)	-	-
Loading									19.00	1.00			1.03
	36.37	0.14	0.244	0.141	0.225	336	1.647	0.484	18.76	1.28	0.363	12.644	1.007
	70.57	0.27	0.312	-	-	-	-	-	18.69	1.64	0.106	1.852	1.000
	138.96	0.38	0.564	0.385	0.503	90	5.946	1.306	18.44	2.97	0.197	0.511	0.973
	276.42	0.87	1.264	0.849	1.197	86	5.907	1.413	17.74	6.65	0.276	0.187	0.898
	550.00	1.66	2.29	1.607	2.218	68	6.775	1.952	16.71	12.05	0.211	0.127	0.788
	1097.17	2.72	3.472	2.649	3.393	61	6.615	2.164	15.53	18.27	0.129	0.111	0.662
Unloading	550.00	3.442	3.424	-	-	-	-	-	15.58	18.02	-		0.667
	208.02	3.38	3.338	-	-	-	-	-	15.66	17.57	-		0.676
	139.62	3.328	3.31	-	-	-	-	-	15.69	17.42	-		0.679

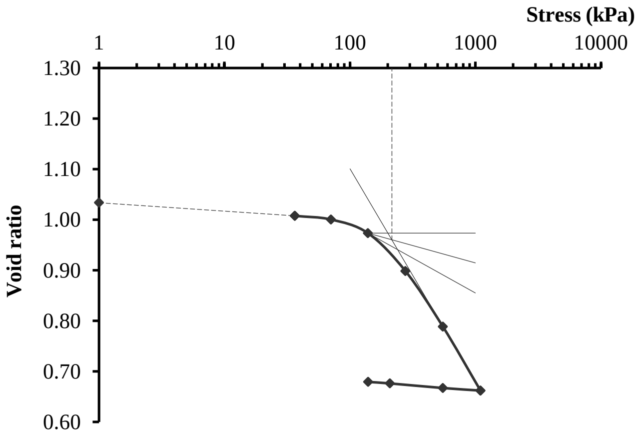

$\sigma'p$ = 216.25 (kPa)(**)

Cc = 0.422 (***)

Cr = 0.019

(*) The coefficient of consolidation is identified by using the log time fitting method;

(**) The apparent preconsolidation pressure is identified by using Cassagrande method;

(***) The compression index is identified from the last two loading increment;

A6.6. Clay + 6% lime

PARAMETERS

SPECIMEN:

Dimensions:		Initial specimen	Final specimen
Diameter	(mm)	50.00	50.00
Height	(mm)	19.10	15.95
Area	(mm^2)	19.63	19.63
Volume	(cm^3)	37.50	31.31

Particle density (assumption)**:**	2.42

INITIAL STATE:

Water content:		Clay		Clay mixed with the additives	
Cup	(g)	35.64	35.73	13.23	13.13
Cup + soil	(g)	43.03	43.55	22.95	19.73
Cup + dry soil	(g)	40.62	41.00	20.05	17.75
Water	(g)	2.41	2.55	2.90	1.98
Dry soil	(g)	4.98	5.27	6.82	4.62
Water content	%	48.39	48.39	42.52	42.86
Average	%	48.39		42.69	

Density:		
Ring	(g)	60.84
Ring + soil	(g)	124.39
Mixed soil	(g)	63.55
Bulk density	(g/cm^3)	1.69
Dry density	(g/cm^3)	1.19
Solid mass	(g)	44.54
Solid height	(mm)	9.37
Void ratio		1.04

FINAL STATE:

Water content:		
Plate	(g)	59.59
Plate + ring with soil	(g)	180.28
Plate + ring with dry soil	(g)	164.60
Water	(g)	15.68
Dry soil	(g)	44.17
Water content	%	35.50

Density:		
Wet soil	(g)	59.85
Bulk density	(g/cm^3)	1.91
Dry density	(g/cm^3)	1.41

Clay + 6% lime

SETTLEMENT

Settlement during loading:

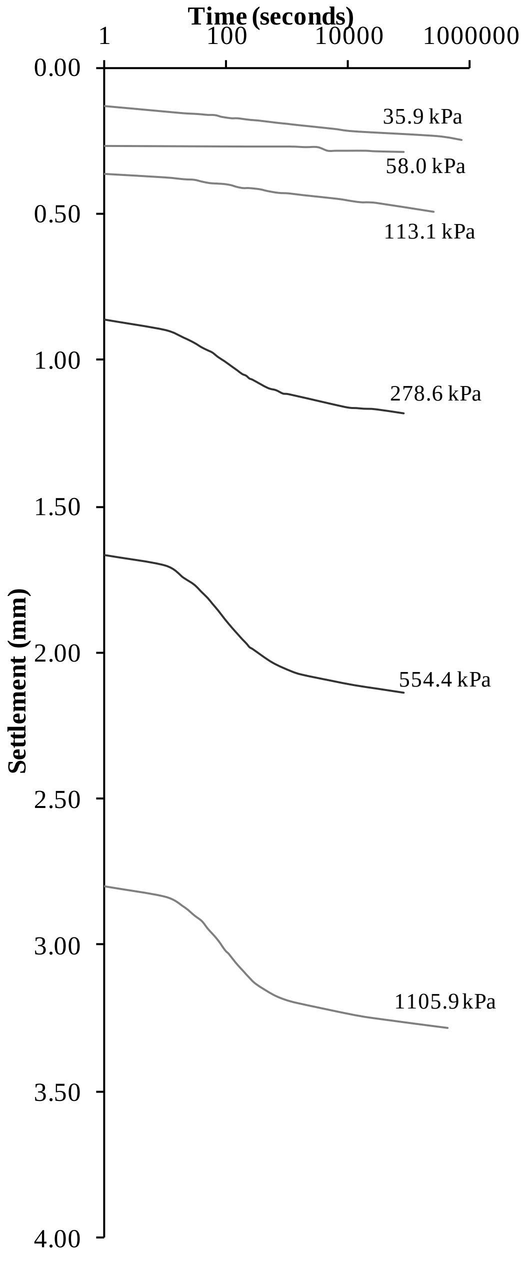

Settlement during unloading:

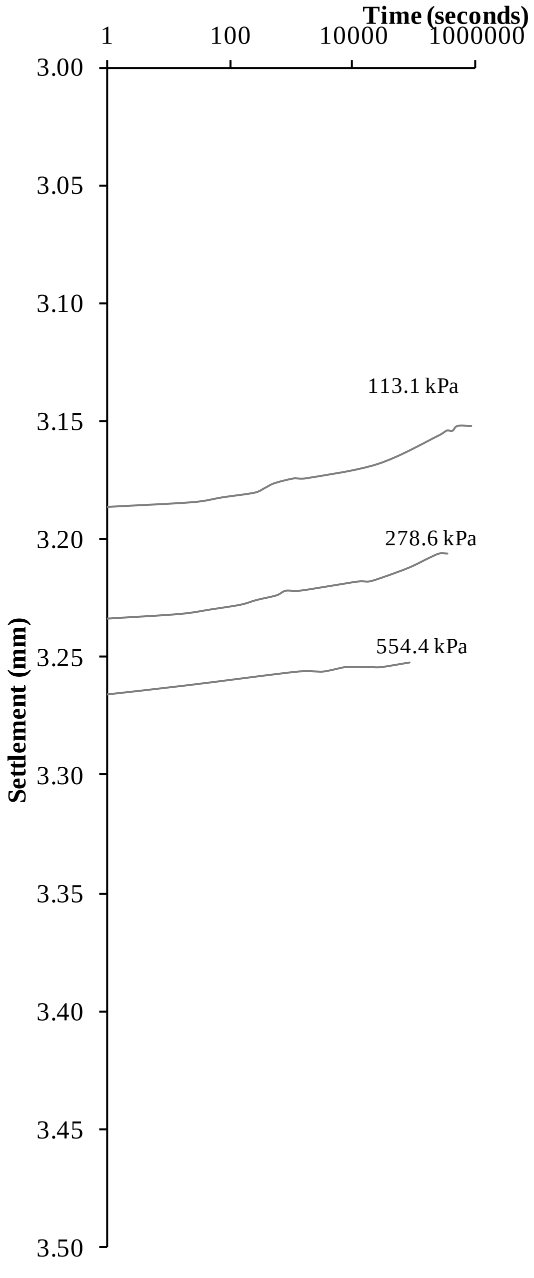

Clay + 6% lime

	σ'	d_{fr}	df	d(0%)	d(100%)	t50	Cv$^{(*)}$	Cα	H	ε_v	m_v	S_c	e
	(kPa)	(mm)	(mm)	(mm)	(mm)	(s)	(m2/year)	×10-3	(mm)	%	(Mpa-1)	-	-
Loading									19.10	1.00			1.04
	35.89	0.13	0.25	-	-	-	-	-	18.85	1.31	0.375	11.591	1.011
	57.96	0.27	0.288	-	-	-	-	-	18.81	1.51	0.091	2.408	1.007
	113.12	0.36	0.492	-	-	-	-	-	18.61	2.58	0.197	0.626	0.985
	278.59	0.86	1.184	0.845	1.138	77	6.727	1.256	17.92	6.20	0.225	0.249	0.911
	554.38	1.666	2.14	1.672	2.07	66	7.156	1.782	16.96	11.20	0.193	0.137	0.809
	1105.96	2.798	3.284	2.746	3.185	62	6.728	2.125	15.82	17.19	0.122	0.115	0.687
Unloading	554.38	3.266	3.252	-	-	-	-	-	15.85	17.03	-		0.691
	278.59	3.234	3.206	-	-	-	-	-	15.89	16.79	-		0.696
	113.12	3.186	3.152	-	-	-	-	-	15.95	16.50	-		0.701

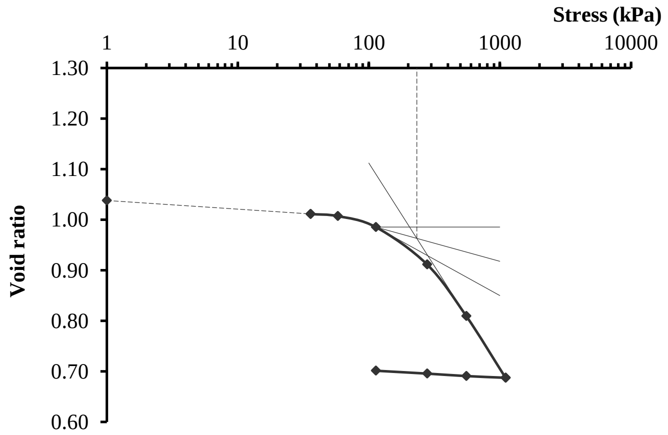

σ'p =	232.49	(kPa)(**)
Cc =	0.407	(***)
Cr =	0.014	

(*) The coefficient of consolidation is identified by using the log time fitting method;

(**) The apparent preconsolidation pressure is identified by using Cassagrande method;

(***) The compression index is identified from the last two loading increment;

A6.7. Data

A6.7.1. Clay

SETTLEMENT DURING LOADING

Stress		5.35	(kPa)
Date	**Time**	**Second**	**Read**
25-Apr	10:40:30	1	0.096
	10:40:40	10	0.106
	10:40:50	20	0.113
	10:41:00	30	0.117
	10:41:10	40	0.122
	10:41:20	50	0.125
	10:41:30	60	0.128
	10:41:40	70	0.130
	10:41:50	80	0.133
	10:42:00	90	0.136
	10:42:30	120	0.142
	10:43	150	0.147
	10:43:30	180	0.152
	10:44	210	0.157
	10:45:15	285	0.168
	10:46	330	0.174
	11:08:15	1665	0.287
	11:09	1710	0.289
	11:10	1770	0.293
	11:11	1830	0.297
	11:17:45	2235	0.318
	11:20	2370	0.329
	11:26	2730	0.348
	11:31	3030	0.364
	11:37	3390	0.381
	11:44	3810	0.402
	13:35	10470	0.575
	14:39	14310	0.608
	16:00	19170	0.622
	17:52	25890	0.636
26-Apr	9:35	82470	0.663

Stress		11.26	(kPa)
Date	**Time**	**second**	**read**
26-Apr	11:25:50	1	0.685
	11:26:00	10	0.688
	11:26:10	20	0.691
	11:26:20	30	0.692
	11:26:30	40	0.694
	11:26:45	55	0.697
	11:27:00	70	0.698
	11:27:15	85	0.700
	11:27:30	100	0.702
	11:27:45	115	0.704
	11:28:00	130	0.706
	11:28	160	0.708
	11:29:00	190	0.712
	11:30	250	0.717
	11:34:30	520	0.736
	11:42	980	0.763
	11:51:00	1510	0.790
	12:00	2080	0.817
	12:08	2530	0.837
	13:30	7450	0.997
	15:01:00	12910	1.073
	16:29	18190	1.108
	17:57	23470	1.129
27-Apr	9:03	77830	1.188

Clay

SETTLEMENT DURING LOADING

Stress		20.13	(kPa)
Date	**Time**	**Second**	**Read**
27-Apr	10:09:40	1	1.196
	10:09:50	10	1.202
	10:10:00	20	1.206
	10:10:10	30	1.210
	10:10:20	40	1.213
	10:10:30	50	1.216
	10:10:40	60	1.219
	10:11	80	1.224
	10:11:30	110	1.230
	10:12	140	1.236
	10:13	200	1.247
	10:14:05	265	1.257
	10:15:05	325	1.266
	10:27	1040	1.343
	10:44	2060	1.420
	11:56	6380	1.580
	13:37	12440	1.661
	14:36	15980	1.683
	16:10	21620	1.705
	17:45	27320	1.718
28-Apr	10:56	89180	1.764
1-May	10:07	345440	1.801

Stress		34.91	(kPa)
Date	**Time**	**Second**	**Read**
1-May	10:39:20	1	1.822
	10:39:30	10	1.828
	10:39:40	20	1.832
	10:39:50	30	1.835
	10:40:00	40	1.838
	10:40:10	50	1.841
	10:40:20	60	1.843
	10:40:30	70	1.845
	10:41	100	1.851
	10:41:30	130	1.857
	10:42	160	1.862
	10:43	220	1.872
	10:45	340	1.888
	10:51	700	1.926
	11:00	1240	1.967
	11:39	3580	2.074
	13:31	10300	2.192
	15:06	16000	2.230
	17:29	24580	2.259
2-May	9:07	80860	2.314

Clay

SETTLEMENT DURING LOADING

Stress		64.48	(kPa)
Date	**Time**	**Second**	**Read**
2-May	9:49:35	1	2.361
	9:49:45	10	2.379
	9:49:55	20	2.386
	9:50:05	30	2.393
	9:50:15	40	2.401
	9:50:25	50	2.407
	9:50:35	60	2.413
	9:51	85	2.426
	9:51:30	115	2.440
	9:52	145	2.452
	9:53	205	2.476
	10:04:45	910	2.644
	10:14	1465	2.727
	10:25:30	2155	2.805
	10:50	3625	2.922
	11:19	5365	3.010
	12:10	8425	3.091
	12:27	9445	3.107
	13:39	13765	3.146
	14:31	16885	3.161
	16:02	22345	3.178
3-May	9:00	83425	3.207
5-May	16:48	457105	3.233

Stress		123.69	(kPa)
Date	**Time**	**Second**	**Read**
10-May	9:57:25	1	3.340
	9:57:35	10	3.361
	9:58:00	35	3.377
	9:58:20	55	3.385
	9:58:40	75	3.393
	9:58:50	85	3.400
	9:59	95	3.405
	9:59:15	110	3.410
	9:59:30	125	3.416
	9:59	140	3.422
	10:00	155	3.427
	10:00:30	185	3.437
	10:01	215	3.446
	10:02	275	3.464
	10:10	755	3.567
	10:23:30	1565	3.677
	10:39:30	2525	3.764
	10:59:30	3725	3.838
	11:26	5315	3.901
	11:42	6275	3.926
	12:56	10715	3.988
	14:07	14975	4.014
	15:37	20375	4.030
	18:16	29915	4.046
11-May	9:19	84095	4.078

Clay

SETTLEMENT DURING UNLOADING

Stress		64.48	(kPa)
Date	**Time**	**Second**	**Read**
11-May	10:02:30	1	4.078
	10:02:45	1	4.053
	10:03:00	16	4.051
	10:03:15	31	4.050
	10:03:30	46	4.048
	10:03:45	61	4.047
	10:04	76	4.045
	10:04:30	106	4.043
	10:05	136	4.041
	10:07	256	4.036
	10:08	316	4.034
	10:14	676	4.027
	10:18	916	4.025
	10:41	2296	4.020
	11:59	6976	4.015
	13:24	12076	4.012
	14:45	16936	4.011
	16:01	21496	4.010
11-May	18:16	29596	4.009
14-May	8:58	255316	4.005

Stress		34.91	(kPa)
Date	**Time**	**Second**	**Read**
14-May	10:30:35	1	3.991
	10:30:45	10	3.989
	10:30:55	20	3.988
	10:31:05	30	3.987
	10:31:15	40	3.986
	10:31:25	50	3.985
	10:31:35	60	3.984
	10:32	85	3.982
	10:32:30	115	3.980
	10:33	145	3.979
	10:34	205	3.977
	10:35	265	3.975
	10:37:30	415	3.971
	10:43	745	3.966
	11:49	4705	3.952
	13:14	9805	3.947
	14:21	13825	3.944
	18:29	28705	3.939
15-May	9:39	83305	3.930
16-May	9:17	168385	3.924
21-May	9:05	599665	3.918

Stress		20.13	(kPa)
Date	**Time**	**Second**	**Read**
21-May	9:52:15	1	3.907
	9:52:25	10	3.905
	9:52:40	25	3.904
	9:53:00	45	3.903
	9:53:30	75	3.901
	9:54	105	3.900
	9:55	165	3.898
	10:00:25	490	3.893
	10:04	705	3.891
	10:21	1725	3.887
	10:53	3645	3.884
	12:06	8025	3.880
	13:32	13185	3.876
	15:18	19545	3.874
	18:01	29325	3.871
22-May	8:53	82845	3.861
23-May	7:50	165465	3.855
24-May	9:21	257325	3.850
25-May	8:56	342225	3.847
26-May	10:25	433965	3.842
29-May	9:10	688665	3.837
30-May	8:51	773925	3.836
31-May	8:57	860685	3.835
1-Jun	9:19	948405	3.835
1-Jun	9:19	948405	3.835
5-Jun	9:18	1293945	3.833

A6.7.2. Clay + 3% lime

SETTLEMENT DURING LOADING

Stress		36.37	(kPa)
Date	**Time**	**Second**	**Read**
10-May	11:22:35	1	0.122
	11:22:45	10	0.130
	11:22:55	20	0.140
	11:23:05	30	0.142
	11:23:15	40	0.144
	11:23:25	50	0.146
	11:23:35	60	0.148
	11:23:45	70	0.152
	11:24	85	0.156
	11:24:30	115	0.158
	11:25	145	0.160
	11:25:30	175	0.160
	11:26:30	235	0.164
	11:27:15	280	0.168
	11:28:15	340	0.172
	11:33	625	0.176
	11:37	865	0.182
	11:41	1105	0.186
	11:50	1645	0.190
	12:56	5605	0.206
	14:08	9925	0.212
	15:37	15265	0.220
	18:16	24805	0.222
11-May	9:19	78985	0.234
11-May	18:16	111205	0.236
14-May	8:58	336925	0.242
16-May	9:58	513325	0.242

Stress		70.57	(kPa)
Date	**Time**	**second**	**read**
16-May	11:39:25	1	0.266
	11:39:35	10	0.268
	11:39:45	20	0.272
	11:39:55	30	0.276
	11:41:05	100	0.276
	11:41:30	125	0.278
	11:42:30	185	0.280
	11:44	275	0.282
	11:51	695	0.284
	12:00	1235	0.286
	14:26	9995	0.298
16-May	18:33	24815	0.302
21-May	9:05	422735	0.328

Clay + 3% lime

SETTLEMENT DURING LOADING

Stress		138.96	(kPa)
Date	**Time**	**Second**	**Read**
21-May	9:55:55	1	0.426
	9:56:05	10	0.442
	9:56:15	20	0.454
	9:56:25	30	0.460
	9:56:35	40	0.468
	9:56:45	50	0.472
	9:56:55	60	0.476
	9:57:10	75	0.484
	9:57:30	95	0.488
	9:58	125	0.498
	9:59	185	0.508
	10:00	245	0.518
	10:01	305	0.522
	10:03	425	0.534
	10:22	1565	0.556
	10:54	3485	0.570
	12:06	7805	0.584
	13:33	13025	0.588
	15:18	19325	0.596
	18:01	29105	0.600
22-May	8:53	82625	0.614

Stress		278.40	(kPa)
Date	**Time**	**Second**	**Read**
22-May	9:31:15	1	0.906
	9:31:25	10	0.970
	9:31:35	20	1.012
	9:31:45	30	1.038
	9:31:55	40	1.064
	9:32:05	50	1.082
	9:32:15	60	1.098
	9:32:25	70	1.114
	9:32:35	80	1.128
	9:32:45	90	1.142
	9:33	105	1.158
	9:33:30	135	1.180
	9:34	165	1.204
	9:34:30	195	1.220
	9:35	225	1.230
	9:36	285	1.254
	9:37	345	1.268
	9:38	405	1.276
	9:39	465	1.288
	9:40:15	540	1.294
	9:51	1185	1.332
	10:01	1785	1.342
	10:47	4545	1.366
	13:06	12885	1.384
	14:47	18945	1.388
	18:43	33105	1.398
23-May	8:50	83925	1.410

Clay + 3% lime

SETTLEMENT DURING LOADING

Stress		557.29	(kPa)
Date	**Time**	**Second**	**Read**
23 may	8:30:55	1	1.786
	8:31:05	10	1.862
	8:31:15	20	1.912
	8:31:25	30	1.958
	8:31:35	40	1.994
	8:31:45	50	2.026
	8:31:55	60	2.056
	8:32:05	70	2.078
	8:32:15	80	2.104
	8:32:30	95	2.132
	8:32:45	110	2.156
	8:33	125	2.186
	8:33:30	155	2.230
	8:34	185	2.260
	8:35	245	2.298
	8:40	545	2.390
	8:55	1445	2.434
	9:27	3365	2.456
	11:39	11285	2.474
	13:57	19565	2.486
	18:54	37385	2.492
24-May	9:21	89405	2.506

Stress		1104.45	(kPa)
Date	**Time**	**Second**	**Read**
24-May	9:56:35	1	2.970
	9:56:45	10	3.030
	9:56:55	20	3.080
	9:57:05	30	3.122
	9:57:15	40	3.160
	9:57:25	50	3.194
	9:57:35	60	3.224
	9:57:45	70	3.256
	9:57:55	80	3.284
	9:58:05	90	3.304
	9:58:15	100	3.326
	9:58:30	115	3.354
	9:58:45	130	3.382
	9:59	145	3.402
	9:59:30	175	3.438
	10:00	205	3.466
	10:01:05	270	3.512
	10:02:15	340	3.542
	10:03:15	400	3.560
	10:07:30	655	3.598
	10:15:30	1135	3.618
	11:28:00	5485	3.654
	18:08	29485	3.676
25-May	8:56	82765	3.692

Clay + 3% lime

SETTLEMENT DURING UNLOADING

Stress		557.29	(kPa)
Date	**Time**	**Second**	**Read**
25-May	9:25:20	1	3.658
	9:25:30	10	3.656
	9:26:00	40	3.656
	9:26:45	85	3.654
	9:30:00	280	3.654
	9:58:00	1960	3.648
	10:23	3460	3.646
	13:44	15520	3.644
	18:47	33700	3.642
26-May	10:25	89980	3.642

Stress		138.96	(kPa)
Date	**Time**	**Second**	**Read**
29-May	9:44:45	1	3.560
	9:45:45	60	3.558
	9:51:00	375	3.556
	10:02:00	1035	3.554
	11:16:00	5475	3.548
	13:54	14955	3.546
	17:47	28935	3.546
30-May	8:51	83175	3.542
31-May	8:57	169935	3.540
1-Jun	9:19	257655	3.536
5-Jun	10:19	606855	3.532

Stress		278.40	(kPa)
Date	**Time**	**Second**	**Read**
26-May	10:26:45	1	3.610
	10:27:20	35	3.608
	10:28:20	95	3.606
	10:31:20	275	3.604
	10:32:30	345	3.604
	10:35	495	3.602
	10:37	615	3.600
	10:42	915	3.598
	10:53	1575	3.596
26-May	17:36	25755	3.590
29-May	9:10	254595	3.582

A6.7.3. Clay + 3% lime + 3% A-RHA

SETTLEMENT DURING LOADING

Stress		36.37	(kPa)
Date	**Time**	**Second**	**Read**
5-Apr	11:49:15	1	0.116
	11:49:25	10	0.124
	11:49:45	30	0.128
	11:49:55	40	0.130
	11:50:05	50	0.130
	11:50:15	60	0.132
	11:51:15	120	0.141
	11:53:25	250	0.158
	11:57:30	495	0.164
	12:14	1485	0.188
	12:18	1725	0.192
	13:06	4605	0.206
	13:07	4665	0.208
	13:32	6165	0.208
	16:45	17745	0.216
	20:50	32445	0.222
5-Apr	22:35	38745	0.224
10-Apr	11:11	429705	0.240
11-Apr	8:54	507885	0.242
12-Apr	10:45	600945	0.244

Stress		70.57	(kPa)
Date	**Time**	**second**	**read**
12-Apr	10:45:50	1	0.284
	10:46:00	10	0.284
	10:46:30	40	0.286
	10:47:00	70	0.288
	10:48	130	0.288
	10:49	190	0.290
	10:51	310	0.290
	10:56	610	0.292
	11:00	850	0.296
	11:18	1930	0.302
	11:48	3730	0.304
	13:37	10270	0.306
	15:58	18730	0.310
12-Apr	18:02	26170	0.316
13-Apr	9:40	82450	0.322
14-Apr	10:03	170230	0.330
16-Apr	9:07	339670	0.338
17-Apr	9:12	426370	0.338

Clay + 3% lime + 3% A-RHA

SETTLEMENT DURING LOADING

Stress		140.29	(kPa)
Date	**Time**	**Second**	**Read**
17-Apr	10:55:50	1	0.468
	10:56:00	10	0.484
	10:56:10	20	0.496
	10:56:23	33	0.510
	10:56:30	40	0.512
	10:56:40	50	0.516
	10:56:50	60	0.524
	10:57	70	0.528
	10:57	100	0.540
	10:58	130	0.546
	10:59	190	0.560
	11:00	250	0.572
	11:04:30	520	0.596
	11:09	790	0.610
	11:25:10	1760	0.628
	11:44	2890	0.640
	13:36	9610	0.658
	15:21	15910	0.664
17-Apr	18:21	26710	0.672
18-Apr	9:47	82270	0.688
19-Apr	9:06	166210	0.696
20-Apr	9:12	252970	0.704

Stress		277.08	(kPa)
Date	**Time**	**Second**	**Read**
20-Apr	10:15:30	1	1.004
	10:15:40	10	1.042
	10:15:50	20	1.074
	10:16:00	30	1.100
	10:16:10	40	1.116
	10:16:20	50	1.132
	10:16:30	60	1.148
	10:16:40	70	1.158
	10:16:50	80	1.170
	10:17:00	90	1.182
	10:18	150	1.230
	10:19	210	1.262
	10:20:10	280	1.288
	10:21	330	1.302
	10:26:30	660	1.356
	10:36	1230	1.382
	11:04:30	2940	1.408
	13:02	9990	1.428
	15:08	17550	1.440
20-Apr	17:58	27750	1.444
21-Apr	17:37	112890	1.462
23-Apr	9:11	255330	1.474

Clay + 3% lime + 3% A-RHA

SETTLEMENT DURING LOADING

Stress		555.96	(kPa)
Date	**Time**	**Second**	**Read**
23-Apr	9:39:40	1	1.826
	9:39:50	10	1.890
	9:40:00	20	1.940
	9:40:10	30	1.982
	9:40:20	40	2.016
	9:40:30	50	2.048
	9:40:40	60	2.080
	9:40:50	70	2.100
	9:41:00	80	2.124
	9:41	110	2.176
	9:42	140	2.218
	9:42:30	170	2.252
	9:43	200	2.278
	9:44	260	2.322
	9:45	320	2.352
	9:50:30	650	2.424
	10:00:30	1250	2.464
	10:09	1803	2.476
	10:15	2120	2.480
	10:44	3860	2.496
	11:52	7940	2.510
	12:38	10700	2.514
	17:43	29000	2.528
24-Apr	9:21	85280	2.544

Stress		1103.13	(kPa)
Date	**Time**	**Second**	**Read**
24-Apr	10:00:50	1	2.980
	10:01:00	10	3.040
	10:01:10	20	3.076
	10:01:20	30	3.120
	10:01:30	40	3.156
	10:01:40	50	3.188
	10:01:50	60	3.218
	10:02:02	72	3.250
	10:02:30	100	3.312
	10:03:00	130	3.362
	10:03:30	160	3.400
	10:04:00	190	3.428
	10:04:30	220	3.456
	10:05:00	250	3.474
	10:05:30	280	3.490
	10:06:00	310	3.504
	10:10	580	3.566
	10:15	850	3.586
	10:25	1450	3.610
	10:35	2050	3.618
	10:45	2650	3.630
	11:19	4690	3.638
	17:17	26170	3.666
25-Apr	9:21	84010	3.680

Clay + 3% lime + 3% A-RHA

SETTLEMENT DURING UNLOADING

Stress		555.96	(kPa)
Date	**Time**	**Second**	**Read**
25-Apr	9:45:00	1	3.644
	9:45:30	30	3.640
	9:46:00	60	3.638
	9:47:00	120	3.638
	9:49:00	240	3.636
	9:57:30	750	3.634
	10:55	4200	3.632
	13:36	13860	3.632
	14:39	17640	3.630
	17:53	29280	3.630
26-Apr	9:00	83700	3.630
27-Apr	9:35	172200	3.630

Stress		140.29	(kPa)
Date	**Time**	**Second**	**Read**
28-Apr	11:00:30	1	3.548
	11:00:45	15	3.546
	11:01:00	30	3.544
	11:01:30	60	3.542
	11:03:15	165	3.540
	11:04	240	3.540
	11:09	510	3.540
	11:34	2010	3.538
	12:38	5850	3.536
28-Apr	16:00	17970	3.532
1-May	10:00	255570	3.520
2-May	9:07	338790	3.520

Stress		277.08	(kPa)
Date	**Time**	**Second**	**Read**
26-Apr	11:37:30	1	3.598
	11:37:45	15	3.596
	11:38:05	35	3.594
	11:38:25	55	3.592
	11:38:50	80	3.590
	11:40	150	3.588
	11:47:30	600	3.586
	11:58:30	1260	3.584
	13:31	6810	3.582
	15:01	12210	3.578
	16:29	17490	3.576
	17:57	22770	3.574
27-Apr	9:03	77130	3.570
28-Apr	10:56	170310	3.570

A6.7.4. Clay + 3% lime + 3% C-RHA

SETTLEMENT DURING LOADING

Stress		36.37	(kPa)
Date	**Time**	**Second**	**Read**
5-Apr	10:24:25	1	0.172
	10:24:35	10	0.176
	10:24:45	20	0.178
	10:24:55	30	0.186
	10:25:05	40	0.188
	10:25:15	50	0.190
	10:25:35	70	0.192
	10:26:05	100	0.198
	10:28:05	220	0.206
	10:36:05	700	0.224
	10:45	1235	0.234
	10:55	1835	0.238
	11:23:40	3555	0.250
	12:28	7415	0.258
	14:34	14975	0.268
5-Apr	17:55	27035	0.272
10-Apr	11:11	434795	0.284
11-Apr	8:54	512975	0.284
12-Apr	10:34	605375	0.284

Stress		70.57	(kPa)
Date	**Time**	**second**	**read**
12-Apr	10:36:30	1	0.302
	10:36:40	10	0.304
	10:36:50	20	0.304
	10:37:30	60	0.304
	10:38	90	0.306
	10:38:30	120	0.306
	10:39:30	180	0.308
	10:40:30	240	0.308
	10:42	330	0.312
	10:43	390	0.312
	10:45	510	0.314
	10:50	810	0.316
	11:15	2310	0.318
	11:48	4290	0.318
	13:37	10830	0.320
	15:58	19290	0.322
12-Apr	18:02	26730	0.324
13-Apr	9:40	83010	0.332
14-Apr	10:03	170790	0.336
16-Apr	11:00	347010	0.340
17-Apr	9:12	426930	0.342

Clay + 3% lime + 3% C-RHA

SETTLEMENT DURING LOADING

Stress		138.96	(kPa)
Date	**Time**	**Second**	**Read**
17-Apr	10:50:50	1	0.410
	10:51:05	15	0.420
	10:51:10	20	0.428
	10:51:20	30	0.432
	10:51:30	40	0.440
	10:51:40	50	0.446
	10:51:50	60	0.448
	10:52:00	70	0.450
	10:53	130	0.462
	10:54	190	0.476
	10:55	250	0.480
	10:58:30	460	0.494
	11:03:20	750	0.500
	11:10	1150	0.510
	11:25:20	2070	0.516
	11:46	3310	0.526
	13:36	9910	0.540
	15:21	16210	0.544
17-Apr	18:21	27010	0.548
18-Apr	9:47	82570	0.562
19-Apr	9:06	166510	0.574
20-Apr	9:12	253270	0.578

Stress		275.75	(kPa)
Date	**Time**	**Second**	**Read**
20-Apr	10:10:20	1	0.846
	10:10:30	10	0.882
	10:10:40	20	0.906
	10:10:50	30	0.926
	10:11:00	40	0.942
	10:11:10	50	0.954
	10:11:25	65	0.972
	10:11:40	80	0.984
	10:11:50	90	0.992
	10:12	100	1.002
	10:12:30	130	1.022
	10:13	160	1.038
	10:14	220	1.058
	10:15	280	1.076
	10:17:30	430	1.104
	10:26:45	985	1.140
	10:36	1540	1.159
	11:05	3280	1.172
	13:02	10300	1.198
	15:08	17860	1.208
20-Apr	17:58	28060	1.214
21-Apr	17:37	113200	1.252
23-Apr	9:11	255640	1.264

Clay + 3% lime + 3% C-RHA

SETTLEMENT DURING LOADING

Stress		554.64	(kPa)
Date	**Time**	**Second**	**Read**
23-Apr	9:33:25	1	1.578
	9:33:35	10	1.646
	9:33:45	20	1.706
	9:33:55	30	1.750
	9:34:05	40	1.792
	9:34:15	50	1.826
	9:34:25	60	1.856
	9:34:40	75	1.898
	9:34:50	85	1.920
	9:35:00	95	1.942
	9:35	125	2.000
	9:36:00	155	2.044
	9:36:30	185	2.078
	9:37	215	2.106
	9:37:30	245	2.128
	9:38	275	2.146
	9:39	335	2.176
	9:44:30	665	2.242
	10:00:30	1625	2.290
	10:15	2495	2.304
	10:44	4235	2.320
	11:52	8315	2.334
	12:38	11075	2.338
	17:43	29375	2.353
24-Apr	9:21	85655	2.368

Stress		1101.80	(kPa)
Date	**Time**	**Second**	**Read**
24-Apr	9:54:30	1	2.720
	9:54:40	10	2.798
	9:54:50	20	2.858
	9:55:00	30	2.910
	9:55:10	40	2.954
	9:55:20	50	2.992
	9:55:30	60	3.034
	9:55:40	70	3.066
	9:55:50	80	3.090
	9:56:00	90	3.120
	9:56:30	120	3.186
	9:57	150	3.236
	9:57:30	180	3.278
	9:58	210	3.310
	9:59	270	3.354
	10:00	330	3.380
	10:04:15	585	3.440
	10:10:45	975	3.472
	10:16:15	1305	3.486
	10:25	1830	3.496
	10:35	2430	3.504
	10:45	3030	3.512
	11:19	5070	3.520
	17:17	26550	3.548
25-Apr	9:21	84390	3.564

Clay + 3% lime + 3% C-RHA

SETTLEMENT DURING UNLOADING

Stress		554.64	(kPa)
Date	**Time**	**Second**	**Read**
25-Apr	9:41:30	1	3.530
	9:42:00	30	3.526
	9:42:30	60	3.524
	9:43:00	90	3.524
	9:44:00	150	3.524
	9:44:30	180	3.522
	9:57:30	960	3.520
	10:55	4410	3.520
	11:19	5850	3.518
	13:36	14070	3.518
	17:53	29490	3.518
26-Apr	9:00	83910	3.518
27-Apr	9:35	86010	3.518

Stress		138.96	(kPa)
Date	**Time**	**Second**	**Read**
28-Apr	10:57	1	3.440
	10:58:00	30	3.440
	10:59:00	90	3.440
	11:00:00	150	3.438
	11:08:00	630	3.438
	11:34:00	2190	3.436
	12:38	6030	3.434
28-Apr	16:00	18150	3.426
1-May	10:00	255750	3.420
2-May	9:07	338970	3.420

Stress		275.75	(kPa)
Date	**Time**	**Second**	**Read**
26-Apr	11:31	1	3.488
	11:31:40	20	3.486
	11:32:00	40	3.486
	11:32:40	80	3.484
	11:35:00	220	3.482
	11:37:30	370	3.480
	11:40	520	3.478
	11:41	580	3.476
	11:48:30	1030	3.474
	12:09	2260	3.472
	13:30	7120	3.470
	15:01	12580	3.470
	16:29	17860	3.468
	17:57	23140	3.468
27-Apr	9:03	77500	3.460
28-Apr	10:56	170680	3.458

A6.7.5. Clay + 3% lime + 3% Cr-RHA

SETTLEMENT DURING LOADING

Stress		36.37	(kPa)
Date	**Time**	**Second**	**Read**
5-Apr	13:00:50	1	0.142
	13:00:55	5	0.146
	13:01:05	15	0.148
	13:01:15	25	0.152
	13:01:25	35	0.158
	13:01:35	45	0.16
	13:01:45	55	0.162
	13:02:05	75	0.164
	13:02:25	95	0.166
	13:03:10	140	0.172
	13:04:05	195	0.176
	13:05:05	255	0.178
	13:09:05	495	0.188
	13:15:15	865	0.196
	13:32	1870	0.208
	13:33	1930	0.208
	14:35	5650	0.22
	15:36	9310	0.222
	16:45	13450	0.226
	17:30	16150	0.226
	18:55	21250	0.228
	20:50	28150	0.23
5-Apr	22:35	34450	0.232
10-Apr	10:00	421150	0.242
11-Apr	8:54	503590	0.242
12-Apr	10:51	597010	0.244

Stress		70.57	(kPa)
Date	**Time**	**second**	**read**
12-Apr	10:51:30	1	0.27
	10:52:10	40	0.272
	10:52:30	60	0.272
	10:53	90	0.272
	10:54:30	180	0.274
	10:55:45	255	0.274
	11:00	510	0.276
	11:19	1650	0.282
	11:48	3390	0.284
	13:37	9930	0.288
	15:36	17070	0.29
12-Apr	18:02	25830	0.292
13-Apr	9:40	82110	0.302
14-Apr	10:03	169890	0.304
16-Apr	9:07	339330	0.31
17-Apr	9:12	426030	0.312

Clay + 3% lime + 3% Cr-RHA

SETTLEMENT DURING LOADING

Stress		138.96	(kPa)
Date	**Time**	**Second**	**Read**
17-Apr	11:00:45	1	0.384
	11:00:55	10	0.404
	11:01:10	25	0.418
	11:01:20	35	0.426
	11:01:30	45	0.43
	11:01:41	56	0.432
	11:01:50	65	0.436
	11:02:03	78	0.442
	11:02:30	105	0.448
	11:03:00	135	0.454
	11:04:00	195	0.462
	11:05:00	255	0.468
	11:08:40	475	0.482
	11:15:20	875	0.494
	11:25	1455	0.502
	11:42	2475	0.51
	13:36	9315	0.528
	15:21	15615	0.534
17-Apr	18:21	26415	0.542
18-Apr	9:47	81975	0.554
19-Apr	9:06	165915	0.56
20-Apr	9:12	252675	0.564

Stress		276.42	(kPa)
Date	**Time**	**Second**	**Read**
20-Apr	10:22:00	1	0.866
	10:22:10	10	0.906
	10:22:25	25	0.944
	10:22:35	35	0.96
	10:22:45	45	0.976
	10:22:55	55	0.986
	10:23	60	0.996
	10:23:10	70	1.006
	10:23:20	80	1.016
	10:23:30	90	1.024
	10:23:40	100	1.034
	10:23:50	110	1.04
	10:24	120	1.046
	10:24:30	150	1.066
	10:25	180	1.078
	10:26	240	1.102
	10:27:10	310	1.118
	10:28	360	1.126
	10:35:30	810	1.166
	10:40:10	1090	1.176
	11:04:30	2550	1.196
	13:02	9600	1.222
	15:08	17160	1.232
20-Apr	17:58	27360	1.236
21-Apr	17:37	112500	1.252
23-Apr	9:11	254940	1.264

Clay + 3% lime + 3% Cr-RHA

SETTLEMENT DURING LOADING

Stress		550.00	(kPa)
Date	**Time**	**Second**	**Read**
23-Apr	9:45:50	1	1.66
	9:46:00	10	1.722
	9:46:10	20	1.772
	9:46:20	30	1.806
	9:46:30	40	1.84
	9:46:40	50	1.87
	9:46:50	60	1.892
	9:47:00	70	1.916
	9:47:15	85	1.942
	9:47:30	100	1.966
	9:48:00	130	2.006
	9:48:30	160	2.036
	9:49	190	2.062
	9:49:35	225	2.084
	9:50	250	2.098
	9:51	310	2.124
	9:52	370	2.142
	10:00:30	880	2.2
	10:08:10	1340	2.218
	10:15	1750	2.224
	10:44	3490	2.242
	11:52	7570	2.256
	12:38	10330	2.262
	17:43	28630	2.276
24-Apr	9:21	84910	2.29

Stress		1097.17	(kPa)
Date	**Time**	**Second**	**Read**
24-Apr	10:06:40	1	2.72
	10:06:50	10	2.798
	10:07:00	20	2.86
	10:07:10	30	2.906
	10:07:20	40	2.946
	10:07:30	50	2.986
	10:07:40	60	3.018
	10:07:50	70	3.046
	10:08:00	80	3.072
	10:08:30	110	3.136
	10:09	140	3.184
	10:09	170	3.22
	10:10	200	3.248
	10:11	260	3.286
	10:12	320	3.312
	10:13	380	3.328
	10:14	440	3.342
	10:15	500	3.354
	10:20	800	3.38
	10:25	1100	3.394
	10:35	1700	3.408
	10:45	2300	3.42
	11:19	4340	3.43
	17:17	25820	3.458
25-Apr	9:21	83660	3.472

Clay + 3% lime + 3% Cr-RHA

SETTLEMENT DURING UNLOADING

Stress		550.00	(kPa)
Date	**Time**	**Second**	**Read**
25-Apr	9:47:45	1	3.442
	9:48:00	15	3.44
	9:48:30	45	3.438
	9:49:00	75	3.438
	9:50:00	135	3.438
	9:57:30	585	3.436
	10:13	1515	3.432
	10:55	4035	3.43
	11:19	5475	3.428
	13:36	13695	3.426
	14:39	17475	3.426
	17:53	29115	3.426
	9:35	85635	3.424

Stress		139.62	(kPa)
Date	**Time**	**Second**	**Read**
28-Apr	11:04:55	1	3.328
	11:05:30	35	3.326
	11:06:30	95	3.326
	11:09:00	245	3.326
	12:38	5585	3.324
28-Apr	16:00	17705	3.32
1-May	10:07	255725	3.31
2-May	9:07	338525	3.31

Stress		208.02	(kPa)
Date	**Time**	**Second**	**Read**
26 kPa	11:38:50	1	3.38
	11:39:00	10	3.378
	11:39:10	20	3.376
	11:39:45	55	3.374
	11:41:10	140	3.372
	11:47:30	520	3.366
	11:48:05	555	3.364
	11:48:45	595	3.362
	12:03	1450	3.36
	13:31	6730	3.354
	15:01	12130	3.35
	16:29	17410	3.348
	17:57	22690	3.346
27-Apr	11:03	84250	3.34
28-Apr	10:56	170230	3.338

A6.7.6. Clay + 6% lime

SETTLEMENT DURING LOADING

Stress		35.89	(kPa)
Date	**Time**	**Second**	**Read**
2-May	12:03:30	1	0.128
	12:03:40	10	0.148
	12:03:50	20	0.154
	12:04:00	30	0.156
	12:04:10	40	0.158
	12:04:20	50	0.160
	12:04:30	60	0.160
	12:04:40	70	0.162
	12:04:50	80	0.166
	12:05	90	0.168
	12:05:30	120	0.172
	12:06	150	0.172
	12:06:30	180	0.174
	12:07:40	250	0.178
	12:09	330	0.180
	12:14:30	660	0.188
	12:20	990	0.192
	12:27	1410	0.196
	13:39	5730	0.210
	14:31	8850	0.216
2-May	16:02	14310	0.220
5-May	16:48	276270	0.236
10-May	17:48	711870	0.250

Stress		57.96	(kPa)
Date	**Time**	**second**	**read**
10-May	10:05	1	0.268
	10:09:00	210	0.270
	10:24:00	1110	0.270
	10:39:00	2010	0.272
	10:59:00	3210	0.272
	11:24:00	4710	0.284
	11:54	6510	0.284
	12:56	10230	0.284
	13:08	10950	0.284
	15:37	19890	0.284
	18:16	29430	0.286
11-May	9:19	83610	0.288

Clay + 6% lime

SETTLEMENT DURING LOADING

Stress		113.12	(kPa)
Date	**Time**	**Second**	**Read**
11-May	10:09	1	0.364
	10:09:10	10	0.376
	10:09:20	20	0.382
	10:09:30	30	0.384
	10:09:40	40	0.390
	10:09:50	50	0.394
	10:10:00	60	0.396
	10:10:30	90	0.398
	10:11	120	0.402
	10:11:30	150	0.408
	10:12:10	190	0.412
	10:13	240	0.412
	10:15	360	0.416
	10:17	480	0.422
	10:21	720	0.428
	10:27	1080	0.430
	10:40:15	1875	0.436
	11:59	6600	0.448
	13:24	11700	0.456
	14:45	16560	0.460
	16:01	21120	0.460
11-May	18:16	29220	0.462
14-May	8:58	254940	0.492

Stress		278.59	(kPa)
Date	**Time**	**Second**	**Read**
14-May	10:25	1	0.860
	10:25:35	10	0.896
	10:25	20	0.922
	10:25:55	30	0.940
	10:26:05	40	0.956
	10:26:15	50	0.966
	10:26:25	60	0.974
	10:26:40	75	0.990
	10:27	95	1.004
	10:27:30	125	1.022
	10:28	155	1.036
	10:28:30	185	1.048
	10:29	215	1.054
	10:29:30	245	1.064
	10:30	275	1.068
	10:33:30	485	1.096
	10:36:30	665	1.104
	10:40	875	1.116
	10:43:30	1085	1.118
	11:49	5015	1.150
	13:15	10175	1.164
	14:22	14195	1.166
	15:32	18395	1.168
	18:29	29015	1.170
15-May	9:39	83615	1.184

Clay + 6% lime

SETTLEMENT DURING LOADING

Stress		554.38	(kPa)
Date	**Time**	**Second**	**Read**
15-May	10:20	1	1.666
	10:20	10	1.702
	10:20	20	1.744
	10:20	30	1.768
	10:21	40	1.794
	10:21	50	1.814
	10:21	60	1.834
	10:21	75	1.858
	10:22	95	1.886
	10:22	125	1.916
	10:23	155	1.938
	10:23	185	1.956
	10:24	215	1.970
	10:24	245	1.984
	10:25	275	1.990
	10:30	575	2.036
	10:40	1175	2.066
	10:50	1775	2.078
	11:46	5135	2.098
	13:52	12695	2.114
	18:42	30095	2.126
16-May	9:17	82595	2.140

Stress		1105.96	(kPa)
Date	**Time**	**Second**	**Read**
16-May	11:35:10	1	2.798
	11:35:20	10	2.834
	11:35:30	20	2.868
	11:35:40	30	2.898
	11:35:50	40	2.918
	11:36:00	50	2.944
	11:36:10	60	2.962
	11:36:20	70	2.978
	11:36:30	80	2.994
	11:36:40	90	3.010
	11:36:50	100	3.022
	11:37:00	110	3.030
	11:37:30	140	3.058
	11:38:00	170	3.078
	11:38:30	200	3.094
	11:39:00	230	3.108
	11:40:20	310	3.134
	11:45:00	590	3.170
	11:51:00	950	3.188
	12:00:00	1490	3.199
	14:26	10250	3.236
16-May	18:33	25070	3.250
21-May	9:05	422990	3.284

Clay + 6% lime

SETTLEMENT DURING UNLOADING

Stress		554.38	(kPa)
Date	**Time**	**Second**	**Read**
21-May	10:01	1	3.266
	10:01:40	20	3.262
	10:22	1240	3.256
	10:54:00	3160	3.256
	12:06	7480	3.254
	13:33	12700	3.254
	15:18	19000	3.254
	18:01	28780	3.254
	8:53	82300	3.252

Stress		278.59	(kPa)
Date	**Time**	**Second**	**Read**
22-May	9:37	1	3.234
	9:37:45	15	3.232
	9:38	50	3.230
	9:40:00	150	3.228
	9:42	270	3.226
	9:47	570	3.224
	9:51	810	3.222
	10:00	1350	3.222
	10:47	4170	3.220
	13:06	12510	3.218
	14:47	18570	3.218
	18:43	32730	3.216
23-May	8:50	83550	3.212
24-May	9:21	171810	3.208
25-May	8:56	256710	3.206
26-May	10:25	348450	3.206

Stress		113.12	(kPa)
Date	**Time**	**Second**	**Read**
26-May	10:28	1	3.186
	10:28:40	25	3.184
	10:29	75	3.182
	10:32:30	255	3.180
	10:34	375	3.178
	10:37	540	3.176
	10:47	1125	3.174
	10:57	1725	3.174
26-May	17:36	25665	3.168
29-May	9:10	254505	3.156
30-May	8:51	339765	3.154
31-May	8:57	426525	3.154
1-Jun	9:19	514245	3.152
5-Jun	9:18	859785	3.152